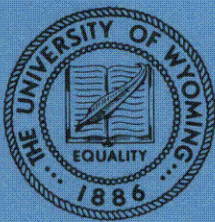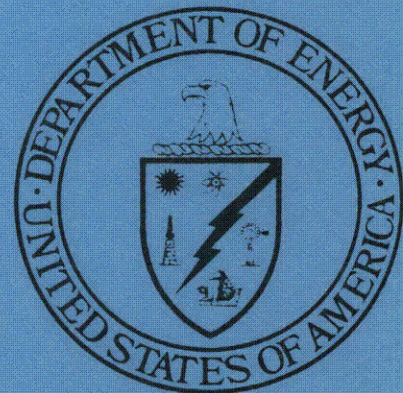National Uranium Resource Evaluation

VOLUME 3
URANIUM ASSESSMENT FOR THE PRECAMBRIAN PEBBLE CONGLOMERATES IN SOUTHEASTERN WYOMING

By: Leon E. Borgman
Cassandra K. Sever
William F. Quimby
Michael E. Andrew
Robert S. Houston
Karl E. Karlstrom

UNIVERSITY OF WYOMING
Laramie, Wyoming
February, 1981

**PREPARED FOR U.S. DEPARTMENT OF ENERGY
GRAND JUNCTION OFFICE, COLORADO**

VOLUME 3

URANIUM ASSESSMENT FOR THE PRECAMBRIAN PEBBLE
CONGLOMERATES IN SOUTHEASTERN WYOMING

By: Leon E. Borgman
      Cassandra Sever
      William F. Quimby
      Michael E. Andrew
      Karl E. Karlstrom
      Robert S. Houston

UNIVERSITY OF WYOMING
MARCH, 1981

CONTENTS

ILLUSTRATIONS

INTRODUCTION

Uranium and thorium occur in Precambrian pebble conglomerate meta-sediments in the Sierra Madre and Medicine Bow Mountains of southeastern Wyoming as shown on Figure 1. The Geology Department of the University of Wyoming was asked to make a geostatistical assessment of the uranium endowment of these deposits as a part of the World Class core drilling operations of the Bendix Field Engineering Corporation. This study was to include (a) the development of optimum geostatistical methodology for assessing uranium endowment in areas of close drill control (1 mile or less centers) as well as in areas of distant drill control (5 mile centers or more), (b) the implementation of this methodology in assessing the uranium resources of the pebble conglomerates in southeastern Wyoming, and (c) the determination of the overall geostatistical uncertainty of the resource estimates. In addition, methods were to be studied for projecting the assessments into new areas, including prediction of estimate uncertainty.

The resource assessment consisted of four phases of activity. These were (a) a detailed geological study of the configuration, genesis, and structure of the deposits, (b) the statistical design of a sampling plan and the collection of rock samples from drill core and outcrops, (c) the geostatistical analysis of the assays of these samples, and (d) the integrated geological and statistical interpretation of these results to produce resource estimates and error predictions.

7

Legend:
- Libby Creek Group
- Deep Lake Group
- Archean Granite
- Phantom Lake Suite
- Archean Gneiss
- Principal Radioactive Units

0   5   10 miles

Onemile Creek

Threemile Creek

Arrastre Lake

Carrico Ranch

Dexter Peak

CHEYENNE BELT

Medicine Bow Mountains

Sierra Madre
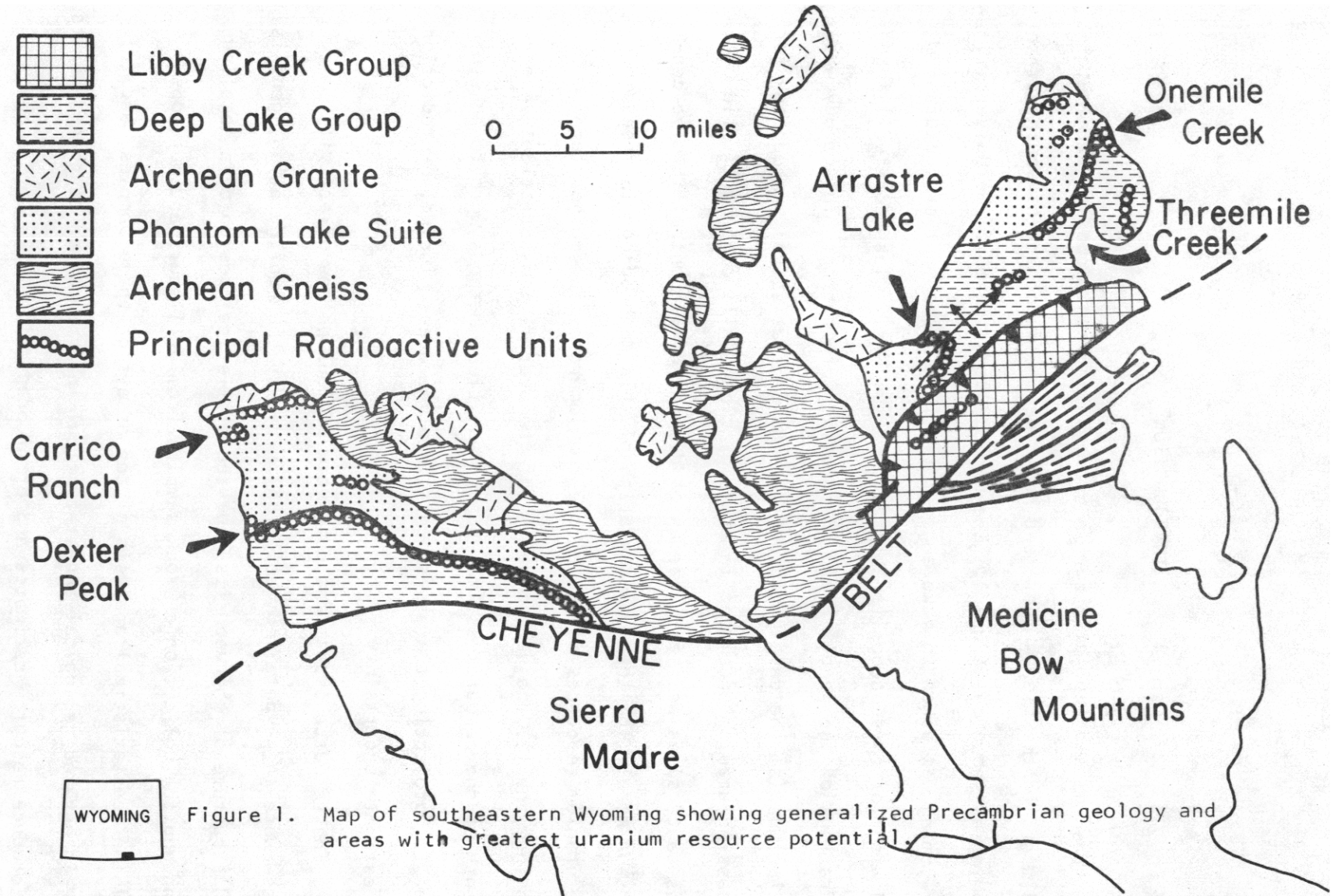
WYOMING

Figure 1. Map of southeastern Wyoming showing generalized Precambrian geology and areas with greatest uranium resource potential.

8

Geostatistical sampling and analysis is somewhat different depending on whether the mineral resource is in the reconnaissance, exploration, development, or production phase of operations. Closely spaced drilling and sampling is characteristic of development and production operations. The sampling can be strongly controlled by statistical considerations with geological interpretations having reduced importance. In reconnaissance and early exploration effort, the geological interpretation is all important and statistics plays a supporting role. Actual data measurements may be quite sparse over large areas and, in the extreme situation of very sparse data, methods based on subjective probability and geological judgment may be the only available procedures.

In the assessment of the uranium endowment in southeastern Wyoming, enough data has been accumulated to form the basis for estimation with a modified version of optimal averaging called "kriging." This method takes into account spatial persistence of enrichment within the deposit and provides systematic procedures for predicting the errors in the resource estimates. In general, the kriging method assumes statistical stationarity over the zone for which the estimates are being prepared. In practical applications where trends are present, the analysis proceeds in three steps. These are (a) trend removal and various transformations to produce an approximate stationarity, at least, over sub-portions of the ore deposit, (b) the production of kriged estimates for the transformed endowment, and (c) the reverse transformation to estimate the resource in terms of the actual "in-place" endowment. Because the data available from outcrop and drill core is relatively sparse, modifications of the geostatistical procedures are required to remove trends and other

types of spatial changes in statistical behavior so that data from one area of the deposit can be used to make predictions for other portions of the deposit.

In the southeastern Wyoming study, the principal trend present was that associated with near-surface leaching of uranium by ground water. This varies with depth and possibly, with other mineralogical and physical properties of the host rock; hence, the adjusted values allow the use of surface and near-surface samples to estimate uranium endowment at depths below leaching horizons. The deposit was divided into small enough subzones so that horizontal spatial trends did not appear important. Thus, the analysis procedure consisted of an adjustment for leaching, the computation of kriged estimates, and the reverse transformation to predict the actual leached tonnages present in each depth interval.

If a large amount of data had been available from each depth interval (such as would be obtained from closely spaced production drilling on a tight grid), the entire leaching correction and reverse transformation process would be unnecessary. The unadjusted data from each depth interval would be used to predict the tonnage within that interval. In the present situation, the data consists of assays from a large number of outcrop transects perpendicular to formation strike, plus assays from as many drill holes as time and budget would permit. The drill hole data makes a significant and essential contribution to the assessment, particularly in evaluating leaching and geological continuity with depth, but the down-hole encounters of the enriched beds are much too widely spaced both in vertical and horizontal position to allow a simple average of data over each depth interval. Consequently, the three-step procedure of leaching adjustment, kriging, and reverse transformation appears to provide the most efficient use of the data in the resource assessment.

The uranium enrichment occurs in pebble conglomerate lenses (probably deposited as alluvial fans) scattered through a roughly tabular zone which crops out with an essentially linear strike and which dips fairly steeply (40 to 60 degrees). A convenient geometric model for such tabular deposits is that of a "mineable surface". That is, the thickness of the bed is temporarily ignored and attention is focused on a single bedding plane (i.e. mineable surface) of the formation.

This whole procedure of reducing the three-dimensional ore deposit to a two-dimensional mineable surface is sometimes called the "method of accumulation". It was originally developed for gold deposits in South Africa. It substantially simplifies the geostatistical computations without the loss of essential information.

The areas of the mineable surface within each depth interval provide basic input for the tonnage calculations for that depth interval. All data are projected onto the mineable surface. The total thickness of the beds with U_3O_8 exceeding 100 ppm along a given drill hole or surface transect is assigned to the point on the mineable surface where the drill hole or transect encounters the surface. The thickness must, of course, be corrected to true thickness as measured along a perpendicular to the mineable surface at that location.

The average ore grade is similarly projected along a perpendicular to the mineable surface, using bed thickness as weights.

$$\text{Average grade} = \frac{\Sigma(\text{bed thickness} \times \text{ppm } U_3O_8)}{\Sigma \text{ bed thickness}} \tag{1}$$

The sum is restricted to those beds exceeding a U_3O_8 grade of 100 ppm.

Hence, relative to the mineable surface, the basic data can be reduced to an average thickness and an average grade at each piercement

11

of the mineable surface by drill hole or surface outcrop transect. In addition, the areas of the mineable surface are calculated for each depth interval for which resource estimates are required. The basic relation for resource tonnage is, then, of the general form:

$$\text{resource} = \text{mineable surface area} \times \text{average thickness} \times \text{average grade.} \tag{2}$$

The actual implementation of this relation is quite a bit more complicated, but the basic concept remains correct.

In order for the concept to remain valid, the sampling must be controlled so that the assays along a given transect or drill hole can be regarded as representing a channel sample through the tabular ore zone along a perpendicular to the mineable surface. In the case of uranium and other radioactive elements, the measured radioactivity provides a convenient method to guarantee that all zones with U_3O_8 exceeding 100 ppm have been completely sampled.

SUMMARY OF THE GEOLOGICAL DESCRIPTION OF THE DEPOSITS

The uranium-bearing quartz pebble conglomerate in southeastern
Wyoming occur in two separate areas. One area lies on the Carrico Ranch
in the northwestern Sierra Madre, while the other is in the northeastern
Medicine Bow Mountains at the Onemile Creek and Threemile Creek localities.
The two areas and some regional details are shown in Figure 1. The geology
for each will be summarized separately.

Geology of the Sierra Madre Deposits

The Sierra Madre region of the Late Archean (greater than 2600 m.y.)
and Early Proterozoic (2500-2000 m.y.) metasediments was evaluated for
syngenetic fossil placer uranium deposits. The metasediments in the area
fall into two major groups: (1) the Phantom Lake Metamorphic Suite, and
(2) the Deep Lake Group (Graff, 1979; Houston and Karlstrom, 1980).
These metasediments were deposited in epicontinental and miogeoclinal
environments, near the southern margin of the Wyoming Archean Province.

Radioactive rocks have been identified near the base of each meta-
sediment group. The Deep Gulch Formation is believed to be near the
base of the Phantom Lake Suite and the Magnolia Formation is the base of
the Deep Lake Group. The Magnolia Formation was found to be low-grade
(less than 10-20 ppm U) over most of the Sierra Madre, so resource
evaluation concentrated on the Deep Gulch Formation.

The Deep Gulch Formation is composed of four distinct lithologic
units as follows:

13

(lowest)   Unit 1 - Arkosic conglomerate - slightly radioactive

Unit 2 - Trough cross-bedded, subarkosic quartzite -
slightly radioactive

Unit 3 - Interbedded radioactive, pyritic, quartz-pebble
conglomerate and subarkosic granular quartzite

Unit 4 - Planar cross-bedded, subarkosic quartzites -
nonradioactive.

Unit 3 is the major target for uranium resource evaluations in the
Sierra Madre region. Unit 3 crops out in the northwestern Sierra Madre
(see Figure 2) and the area of the unit (see Appendix B) was used as a
basis for the calculation of uranium resources in the Sierra Madre.

Unit 3 varies in thickness, but in general, it averages 60-70 feet
thick in the western area and gradually thickens to 100-110 feet in the
eastern exposures.

It consists of 5-15 conglomerate "reefs" (coalesced conglomerate
lenses forming mappable stratigraphic beds) which vary in thickness from
2 inches to 3 feet and in length from 50 feet to over a mile. The
thickest "reef" may be continuous for up to four miles.

Radioactive units of the Deep Gulch Formation in the northwest
Sierra Madre strike northeast, dip northwest and are overturned. The
beds are part of the overturned limb of a large reclined isoclinal fold
system plunging west. This structure is further complicated by intra-
limb reverse faults of unknown displacement.

Because of the complex structure, the subsurface extent of the
Deep Gulch Formation is conjectural. For the present resource evaluation

14

Figure 2.
NW Sierra Madre
Surface Trace of Unit 3

Scale 1:24000

·········· Area underlain by endowment

JP-1 ⊙ Drill holes intersecting Unit 3

16 ╱ Transects on Unit 3

▢ Unit 3 outcrop boundary*

--- Unit 3 contact, inferred

N

WYOMING

*outcrop width slightly exaggerated
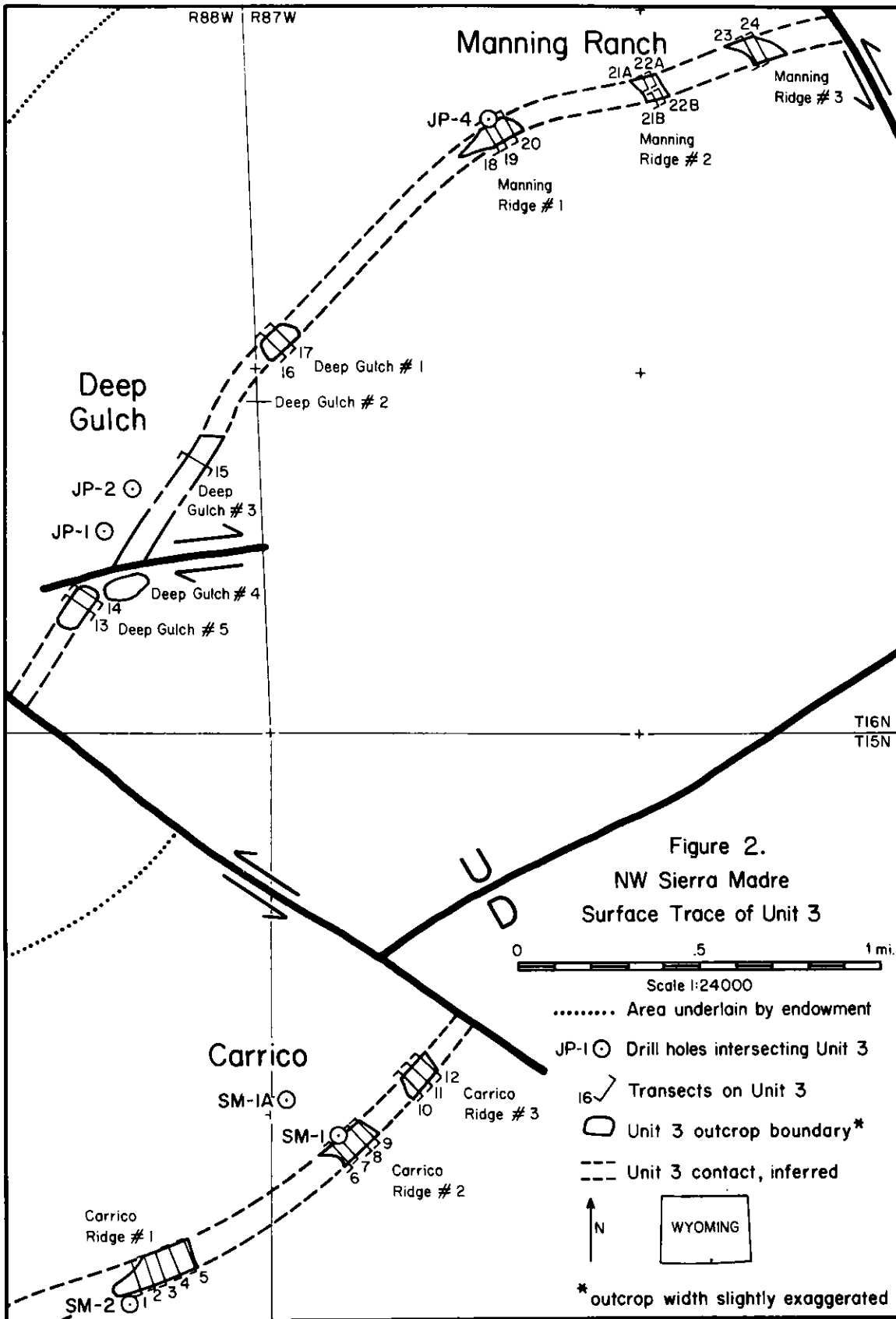
the beds were projected to the depth of 5000 feet for the following

reasons.

1. Long outcrop trace suggests significant lateral continuity in a
    down-dip direction.

2. Drill holes indicate uniform dips to depths of at least 500-1000
    feet.

3. Information on the depth to the hinge of the syncline is not
    available and the uniform projection down dip is the most simple
    interpretation and perhaps the most reasonable guess, given the
    existing data.

Geology of the Medicine Bow Deposits

Although the depositional and structural history of the middle

Precambrian metasedimentary sequences in the Sierra Madre and Medicine

Bow Mountains are very similar, there are minor but important differ-

ences between the two areas.

In the Medicine Bows, the Phantom Lake Suite is metavolcanic in

the lower part, with more typical quartzite and arkosic conglomerates

occurring in the upper part of the suite. Reconnaissance and subse-

quent work (Karlstrom and Houston, 1979) indicates that although some

weakly radioactive zones occur, quartz-pebble conglomerates are absent

in the Phantom Lake Suite of the Medicine Bow Mountains. The Magnolia

Formation of the Deep Lake Group, however, contains numerous quartz-

pebble conglomerates, and those in the Onemile Creek and the Threemile

Creek areas exhibit substantial radioactivity.

The Magnolia Formation is about 500 m (1600 feet) thick in the

Onemile Creek area and consists mainly of radioactive, muscovitic, granu-

lar quartzite and pyritic conglomerates, having much the same character

16

as those in the Sierra Madre, i.e. individual lenses which coalesce into a body of mappable proportions. Individual outcrops of these units are variable in thickness and radioactivity, but may be mapped as essentially continuous beds. Three of these units are significantly more radioactive than the others and were the targets for uranium resource evaluation. The extent of these units, designated as unit 1 (which is near the base of the Magnolia Formation) and units 5a and 5b (which are in the upper portion of the formation) is shown on Figure 3.

The major structure in the Onemile Creek area is a faulted and intruded overturned syncline in the Magnolia Formation. This syncline is documented by top and bottom criteria in the Magnolia quartzites (personal communication, Karlstrom, 1980). Uncertainties still exist in this interpretation. The plunge of the syncline is poorly known and evidence can support either an inclined or a reclined structure. These problems bear on the resource evaluation because a geometry based on the reclined synclinal model will have more extensive conglomerage units than one based on the inclined model. The geometries shown in Appendix B, have been based on a simple isoclinal, inclined fold system and the areas calculated are therefore conservative estimates of the area of radioactive zones in the Onemile Creek area.

The Threemile Creek area shown in Figure 4 is located about 1 1/2 miles south of the Onemile Creek area. Paraconglomerates rather than quartz-pebble conglomerates comprise most of the radioactive units in this area, and correlation with metasedimentary units to the north is difficult because of the less conglomeratic nature of the lithologies and because of the complex structure which separates the two areas. Additionally,

Figure 3. Generalized geologic map of the Onemile Creek area, northern Medicine Bow Mountains, showing drill holes and surface transects.

EXPLANATION

m — MAFIC INTRUSIVE ROCK: Amphibolized gabbro and pyroxenite.

Cq — CASCADE QUARTZITE: Pebbly quartzite and non-radioactive quartz-pebble conglomerate.

UNCONFORMITY

MAGNOLIA FORMATION: Arkose, subarkose, arkosic paraconglomerate, and biotite chlorite schist in lower part; muscovitic subarkose, quartzite, and quartz-pebble conglomerate in upper part. -Principal radioactive zones, labeled 1, 5a and 5b.

UNCONFORMITY

gg — Granite and granitic gneiss

q — Fine-grained quartzite

mb — Metabasalt

sc — STAGE CROSSING GNEISS

MAP SYMBOLS

Faults, dotted where invaded by igneous rocks; bar and ball on downtrown side, arrows show relative horizontal movement.

Overturned syncline.

Approximate or inferred contact.

EMB-9 (50°) — Drill hole, shows name, bearing, plunge, and total length.

Surface transect, showing location of analyzed samples.

SEC. 7 | SEC. 8

the contacts in the Threemile area are gradational. Karlstrom, Houston and others (Vol. 1, this report) conclude that the radioactive units here are basal Magnolia units rather than a facies of the typically paraconglomeratic Phantom Lake Suite but do not extend Onemile Creek stratigraphy into the Threemile Creek area.

Surface mapping and information from a single drillhole indicate that the principal radioactive zone occurs in beds which form the overturned limb of the Sand Lake Syncline. The geometry used as a basis for the resource estimation is similar to the overturned structures in the Onemile Creek area. (See Karlstrom, Houston and others, 1981, Vol. 1, this report for detailed discussion of geology).

Figure 4.

Generalized geologic map of the Three-
mile Creek area, northern Medicine
Bow Mountains, showing drill hole EMB-11.

EXPLANATION

MAFIC INTRUSIVE ROCK

MAGNOLIA FORMATION: Arkosic
paraconglomerate, quartz-granule
conglomerate and quartz-pebble
conglomerate.

Principal radioactive zone

UNCONFORMITY

ROCKS OF PHANTOM LAKE SUITE:
Metabasalt, fine-grained quartzite
and paraconglomerate

Inferred fault, bar on downthrown
side.

Inferred formation contact.

Overturned anticline.

Drill hole showing bearing, plunge
and total extent.

OUTCROP AND DRILL CORE SAMPLING PROCEDURES

Since the sampling procedures had to be designed early in the project when very little data was available, several weeks of intensive field measurement and mapping of surface radioactivity was initiated to provide a data base adequate to plan further sampling. The geostatistical characteristics needed were the variance, σ^2, of the uranium endowment, the zone of influence, h_o, (defined as the distance of separation along the strike in a radioactive bed at which two uranium assays become uncorrelated), and the nugget effect, a^2, (defined as the expected-square-difference between uranium assays taken from spatial locations near each other). The variance measures the dispersion of the uranium values, h_o characterizes spatial persistence, and a^2 indicates the amount of local discontinuities present; more detailed definitions and discussion of their importance in the technique of geostatistical kriging will be given in the next section. These three parameters, together with sample size, control the estimation error and are, therefore, needed in planning the number and placement of the samples to be collected.

Spectrometer readings with various separations in distance along radioactive conglomerate layers were used to make preliminary judgments concerning geostatistical characteristics of the radioactive beds. The sequences of readings were taken at 6-inch, 1-foot, and 6-foot spacings along a number of conglomerate layers. The measurement site was on

21

ridge 1 and 2 in the Sierra Madre on the Carrico Ranch. The spectrometers were calibrated at the Bendix offices in Grand Junction, Colorado.

The median zone of influence, h_o, was found to be 10 feet. The nugget-effect-to-variance quotient, a^2/σ^2, had a median of 0.62. Finally, the average of the standard deviation-to-mean value quotient, $\sigma/\bar{V}$ was 0.9. All these characteristics were determined for the uranium accumulation defined as

$$U \text{ accumulation} = (\text{estimates ppm U}) \times (\text{bed thickness in inches}). \quad (3)$$

Outcrop Sampling Plan

These geostatistical characteristics provided a basis for the design of an outcrop sampling plan. A variety of possible sampling plans were studied. The method which appeared most appropriate consisted of the collection of samples for assay along transects perpendicular to the strike of the conglomerate beds, supplemented with certain radiometric readings to monitor the geostatistical character of the beds from area to area. The transect procedure for various spacings between lines of samples was studied by two methods. One method was by direct analysis via geostatistical formulas. The other method utilized digital simulation on the SIGMA 7 as based on a statistical model incorporating many of the geological characteristics of the formations. The two methods produced similar results.

The target in a resource evaluation is to produce estimates of the ore reserve with controlled accuracy. One measure of this accuracy is the probable error (PE). The probable error is defined as the median of the absolute value of the error. Fifty percent of the time the error

22

magnitude will be less than PE and fifty percent of the time it will be larger. Thus, the probable error is a measure of what the error actually is.

In practice, it is more convenient to work with the relative probable error (PE%) as compared to the mean value of the deposit. If $\overline{V}$ is the average grade of deposit and PE is the probable error of the estimate of grade, then

$$PE\% = \frac{PE}{\overline{V}} \times 100. \tag{4}$$

The PE% value is related to h_o, a^2/σ^2, and $\sigma/\overline{V}$ the geostatistical characteristics listed in the introduction. The following assumptions are made in the development of the formula.

1. A linear deposit of length L requires a reserve estimate with relative probable error PE%.

2. The transect values are separated by more than a zone of influence h_o, from one another. They need not be exactly equally spaced but should be roughly equidistant.

3. The transect locations are not selected so as to "high-grade" the deposit.

4. There is geological continuity between transects in a statistical sense.

5. The average of the variograms along a transect remains about the same along the deposit.

6. The ore block averages being estimated are approximately normally distributed. Generally this will be true by a central limit theorem if the blocks are large, even if the local ore values have some other probability law (e.g., lognormal).

23

The formula then is, (with n = number of transects along L)

$$PE\% = 67.45 \ (\sigma/\overline{V}) \sqrt{\frac{1}{n} - (1 - \frac{a^2}{\sigma^2})\left[\frac{h_o}{L} + \frac{1}{3}\left(\frac{h_o}{L}\right)^2\right]} \ .$$

(5)

When h_o = 10 feet, $\sigma/\overline{V}$ = 0.9, and a^2/σ^2 = 0.62 are substituted into the formula, the equation reduces to

$$PE\% = 60.7 \ \sqrt{\frac{1}{n} - 3.8\left[\frac{1}{L} + \frac{10}{3L^2}\right]} \ .$$

(6)

This relation is presented graphically in Figure 5. The basic question remains as to what PE% represents the best balance of accuracy and effort.

As an examination of the graph shows, greater accuracy requires more transects. For example, a 100-foot long deposit attains a PE% of 15% with 10 transects, but 15 transects are required if the PE% is to be reduced to 10%. Seven transects would give a 20% probable error for the same length.

For most regional resource valuations, a relative probable error of about 18 to 20% is usually acceptable. In development-type reserve estimates, at a mine site for example, a smaller PE% of 5% would be desirable. The more marginal the deposit is, the greater will be the accuracy needed to guarantee against loss if the property is mined. Everything considered, it appeared reasonable to design the Sierra Madre-Medicine Bow uranium estimates for a PE% = 20%.

The value of the length L depends on whether an estimate for the local area is desired, or a regional estimate is being made. For this study we looked only at the three favorable sites which contained the high-

24

Based on Sierra Madre measurements Ridges # I and 2 Carrico Ranch.

$$h_o = 10 \text{ ft.}, \quad \frac{a^2}{\sigma^2} = .62, \quad \frac{\sigma}{V} = 0.9$$

(Geological Continuity assumed between Transects)

PE %

5%

10%

15%

20%

25%

Number of Transects in Region (use nearest integer larger than scale reading)

Length of Region (ft)
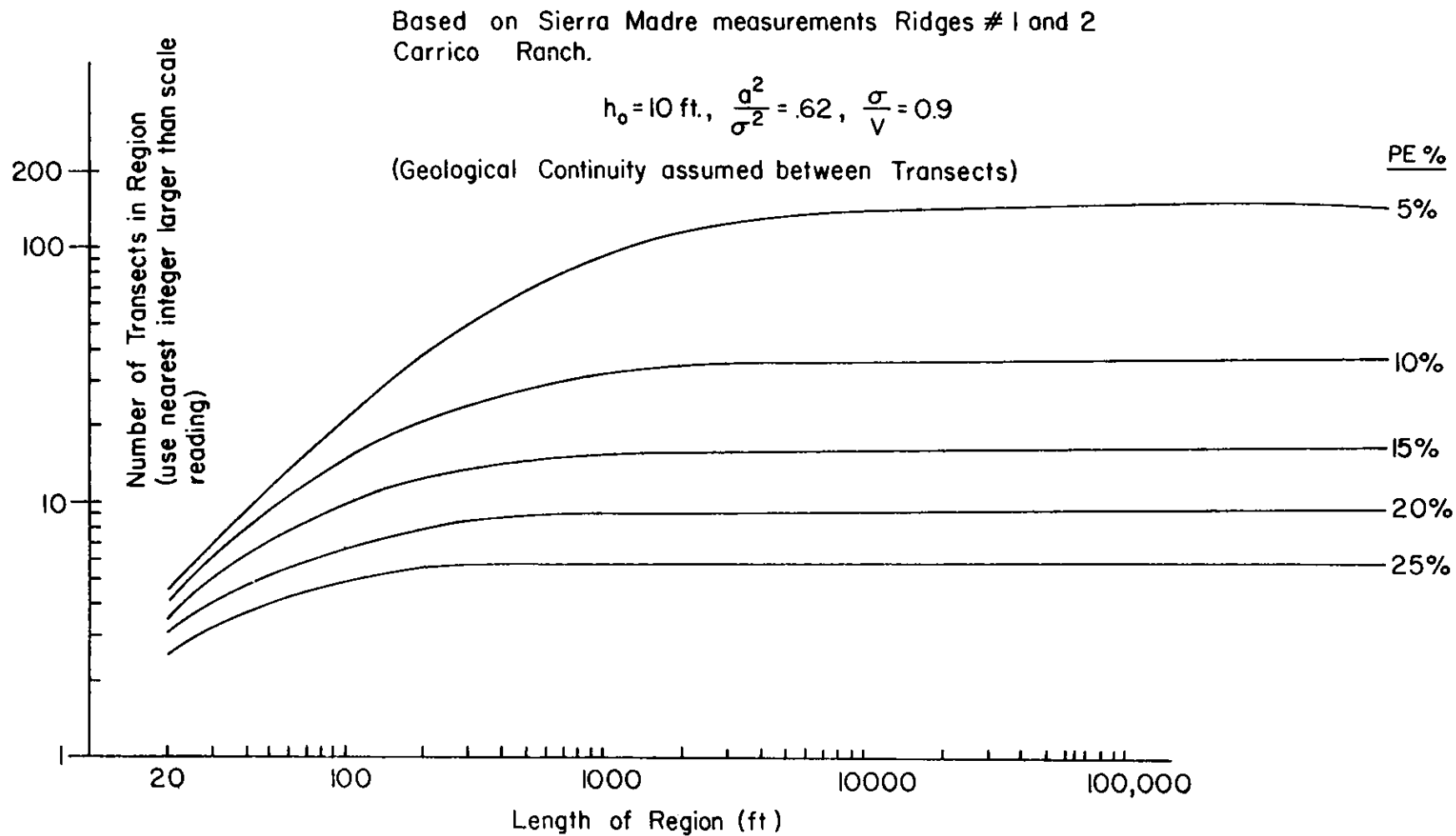
Figure 5. Relationship between length of bed, number of transects and percent probable error.

est grade materials (Onemile Creek, Threemile Creek, and Carrico Ranch areas). Outcrops in high grade material will use an L of approximately 400 feet as the length of the outcrop, although several nearby outcrops may be linked if the outcrops are too short. The number of transects needed to give a PE% = 20% for that L is then 9, as read from the graph.

Transect sampling was carried out as follows. Spectrometer readings of total gamma radiation were made more or less continuously along the transect, to locate "hot" layers. These readings were not recorded individually, although an overall summary was written for general and special features present. Readings were recorded for extra-hot zones.

Attempts were made to sample all hot layers encountered. Thin layers, less than 8 inches, were sampled with one or two chunks of rock. Thicker layers were sampled at 3 or 4 places through the bed. The intent here was to approximate a channel sample of the "hot" bed as closely as possible. The samples for a single "hot" bed were bagged together and analyzed as a single combined sample which yielded an estimate of the average uranium in that bed at that location. Country rock, with radioactivity fairly uniform, was sampled at 2 or 3 locations along the transect.

Drill Core Sampling Plan

Assays of samples taken from drill core serve two important purposes. The assay values may be used to estimate reserves and they may be studied to lead to a more complete understanding of the geological processes present in the deposit. The sampling plan designed here was primarily directed to the first purpose - that of estimating reserves.

26

However, modifications have been introduced to allow the sampling plan to satisfy the second purpose reasonably well.

The accumulation for a core is defined as the integral of the ore value along the core. Let $V(\bar{z})$ be the uranium concentration at vertical position $\bar{z}$.

$$\text{Accumulation} = \int_{\bar{z}_{top}}^{\bar{z}_{bottom}} V(\bar{z})d\bar{z}. \qquad (7)$$

Then the integral of the accumulation over the horizontal area of the deposit, after division by the volume of the deposit, gives the average value of the deposit.

Various elaborations, such as making the computations in zones or introducing statistical techniques like kriging, may be incorporated into the analysis. The procedure outlined above, however, illustrates the essential aspects of the method. To achieve this target, a three step procedure was used.

1. The core was scanned continuously with a spectrometer to locate "hot" zones accurately. The spectrometer scan was done in such a way as to give a continuous run of readings. This scan was confirmed by down-hole spectrometer measurements in the drill hole. As an operational definition, it appeared reasonable to define a "hot" zone as an interval of readings where the total gamma count is 20% greater than the nearby country rock average count. The location and length of the "hot" zones were carefully recorded for the collection of assay samples.

27

2. The "hot" zones were sampled for assay in intervals not exceed-
   ing one foot or the length of the "hot" zone, whichever was less.
   A lengthwise cut of the core, of uniform cross-section, running the
   full length of the interval, was crushed and split for the assay.
   If the "hot" zone was longer than one foot, several intervals were
   needed to cover the whole zone. The essential point is that the entire
   "hot" zone interval was covered by these interval samples.

   In addition it was desirable to collect "point" samples at the
   bottom, middle, and top of the hot zones if the zones were of sub-
   stantial thickness. As guided by geological judgment, it was desir-
   able to sample any additional locations along the core where signi-
   ficant changes appeared to be present. These samples were largely in-
   tended to assist in geological interpretation, rather than reserve
   estimation.

3. The "warm" country rock surrounding the hot zones was sampled approxi-
   mately every twenty-five feet. The root-mean-square percentage error
   in using a 25 foot sampling interval to estimate the country rock
   accumulation was found to be about 1%. Sampling at 80 foot intervals
   led to a 2.4% R.M.S. error. The 25-foot interval was suggested be-
   cause it also offered some protection against unforeseen trends or
   variations in the uranium content of the country rock. It also has
   a quite acceptable accuracy. Since the overall accuracy of reserve
   estimation was planned for about 20%, the 1% error in vertical accumu-
   lation is quite satisfactory in not interfering with the horizontal
   (areal) outcrop sampling directed at achieving the 20% accuracy.

   The samples for assay taken every 25 feet were point samples

(not interval or channel samples). In addition, extra samples were collected at locations along the core where the geologist believed that significant changes occur in the country rock.

OUTLINE OF GEOSTATISTICAL METHODOLOGY AND THE

STATISTICAL PARAMETERS OF THE DEPOSIT

The Variogram

The basic characterization of spatial persistence used in mining geostatistics is the variogram function, sometimes called the semi-variogram. It is a function of distance and direction of the separation or "lag" between two ore grades in the deposit. More specifically, the variogram, $\gamma(\underline{h})$, is defined as one-half of the average of the squared-difference between ore grades separated by the vector $\underline{h}$. The difference between grades for each pair is squared. One-half of the average of these squared-differences would give an estimate of the variogram at lag $\underline{h}$. This would have to be repeated at a number of different lag values to develop a clear delineation of $\gamma(\underline{h})$ for all $\underline{h}$ values. If the ore assays are established on some regular grid, the variogram can be estimated using neighboring pairs of grades for the shortest lag. Pairs separated by two grid spacing can be used for the next larger lag of averaging. Then 3 grid separations can be used, and so forth.

If the variogram does not vary with direction of lag but only depends on the distance of separation, the random field of data is said to be "isotropic." The variogram is then a function of the length, h, not the vector, $\underline{h}$.

For the uranium-bearing pebble conglomerates, the radioactivity appears to be isotropic within the mineable surface. Hence, the further

discussion will be restricted to this case. The theorems derived in

Appendix A, however, are more general and are based on an anisotropic

variogram with elliptical zone of influence over the mineable surface.

A typical isotropic variogram might have the shape shown in Figure

6. As the value of h becomes small, spatial persistence makes the

grades increasingly similar to each other, and the $\gamma(h)$ value approaches

zero. The squared difference between grades of samples close together

is small. As h gets large, the grade at one end of the separation

becomes more and more unrelated to the grade at the other end. The

squared difference gets larger. At some distance, called the zone of

influence, h_o, the two grades are uncorrelated with each other and the

average squared distance stays at about the same value for all larger h.

It can be shown that for statistically stationary random fields of ore

grade, the variogram will level off at a value equal to the variance, σ^2, of

the grade. Finally, one often encounters variograms with the appearance of

Figure 7. If the $\gamma(h)$ values at the shorter lags are extrapolated to

zero, the line of extrapolation does not pass through zero, but gives

$a^2 > 0$ where

$$a^2 = \lim_{h \to 0} \gamma(h). \tag{8}$$

This means that there are abrupt changes in grade on a local scale

(fractures, rich veins in waste, etc.). Thus, the average squared dif-

ference stays large even for spatial separations very small.

The variogram often motivates interesting geological conjectures

concerning the deposit. Some other typical cases are given in Figure 8.

32
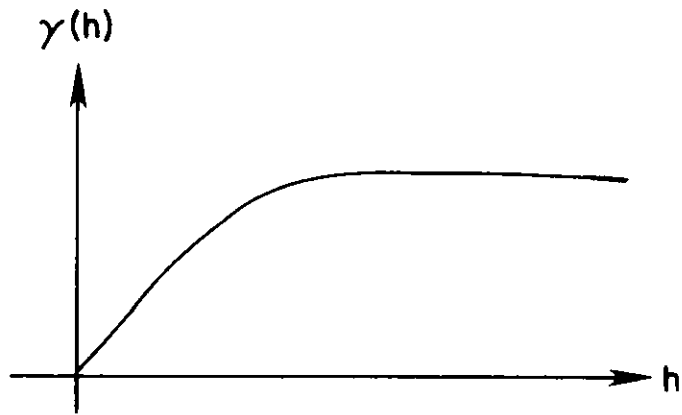
Figure 6.   A typical isotropic variogram.
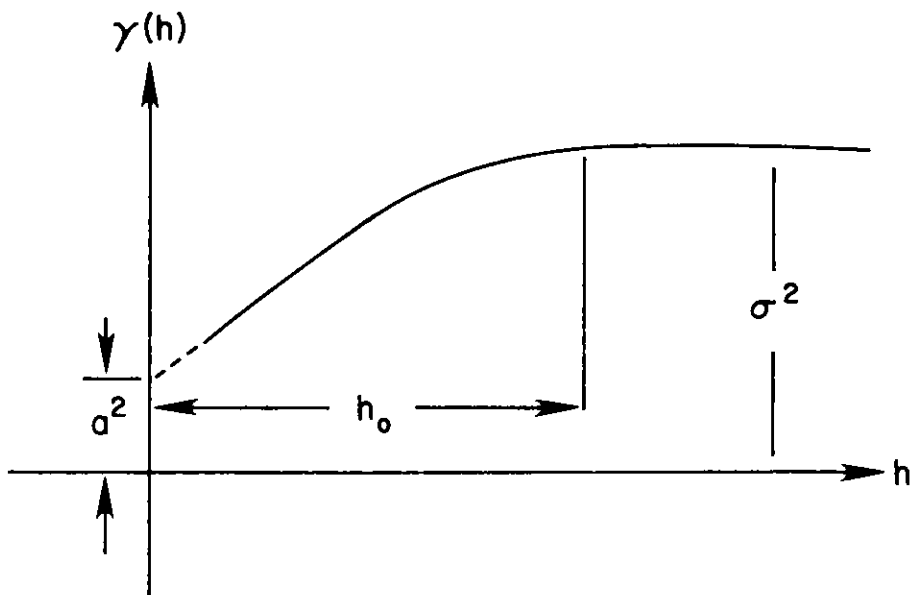
Figure 7.   Typical variogram with variance, σ^2; zone of influence, h_o; and nugget effect, a^2.
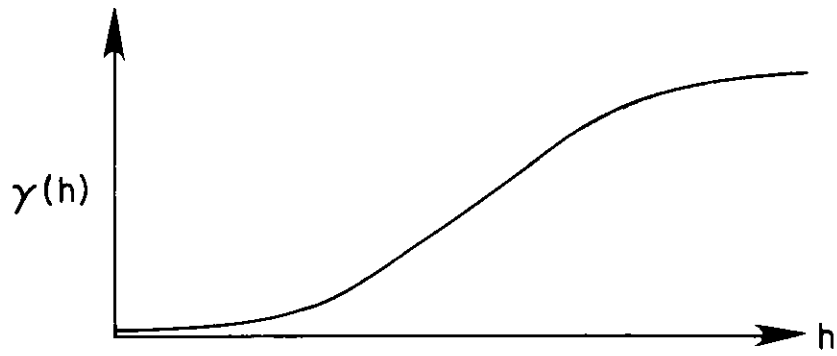
A.
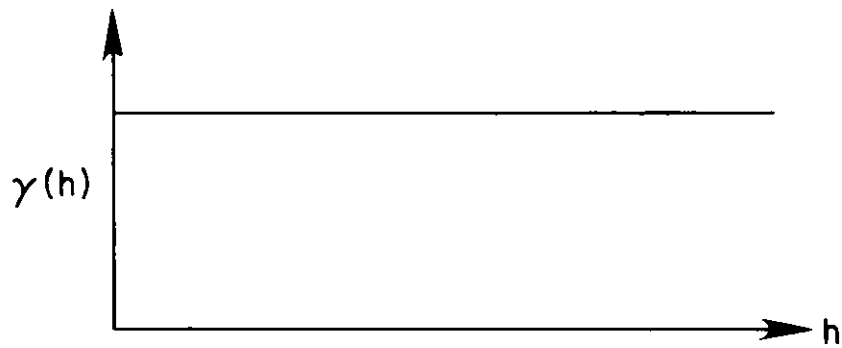
B.
Figure 8.   Theoretical Variograms (A) strong spacial
persistence (large h_o) and (B) complete
independence between grades even at small
spacings.

34

Variograms estimated from actual data have sample randomness and a much more jagged appearance than the idealized figures presented here. Some examples of actual variograms from the uranium data are shown below.

Another measure of spatial persistence useful in geostatistics is the covariance function. It can be defined as $C(h)$, where

$$C(h) = \sigma^2 - \gamma(h) \tag{9}$$

for statistically stationary, isotropic random ore deposits.

Kriged Estimates

The geostatistical procedure of kriging (David, 1977; Journel and Huljbregts, 1978) can be based on either the covariance function or the variogram. In the following, the covariance function will be used. If all assay values are of equal important to the determination of the average grade in some depth zone, a reasonable estimate would be the arithmetic average of the assays. In mathematical terms, if $V(x_i)$ is the assay value at location x_i, and there are n assays available making an estimate of average grade for a zone B, then

$$\hat{V}_B = \frac{1}{n} \sum_{i=1}^{n} V(x_i) \tag{10}$$

where $\hat{V}_B$ is the estimated average grade for the zone.

If all of the assays are not equally important to the determination of the average grade of zone B (for example, some assays may be within the zone and others may be some distance away), then a weighted average of the form

35

$$\hat{\overline{V}}_B = \sum_{i=1}^{n} a_i \, V(x_i),$$

(11)

$$\text{where} \quad \sum_{i=1}^{n} a_i = 1.0$$

(12)

may be more reasonable. For example, nearby values may be weighted more than those far away.

This raises the question, are there systematic procedures for determining the optimal or "best" choices of the weights, a_i. The answer is yes and the procedure is found to depend on the covariance function. The measure of optimality used is that the best weights, $\hat{a}$, are those which minimize the expected square difference between the actual average grade $\overline{V}_B$ and the estimate of that value, $\hat{\overline{V}}_B$. The mathematical procedure for deriving these optimal weights is derived in theorem A-5 of Appendix A. Essentially the procedure reduces to the solution of a system of simultaneous equations whose coefficients and other constants are determined from the covariance function. The general technique is called kriging.

In the closely spaced sample collection of the production or development phases of mineral development, many samples are within a zone of influence of each other and the system of equations may become difficult to solve. However, in reconnaissance sampling the reverse is true. All samples are usually more than a zone of influence apart and the system of equations reduces to the very simple explicit solutions given in theorem A-6 of Appendix A. In fact if the zone of influence is small and the sample spacing is large, the weights are well approximated by 1/n and

36

$$\hat{\bar{V}}_B = \frac{1}{n} \sum_{i=1}^{n} V(x_i) \tag{13}$$

with error variance bounded by

$$\sigma_E^2 = \text{Expected value of } (\hat{\bar{V}}_B - \bar{V}_B)^2 \leq \frac{\sigma^2}{n} + C_{BB}, \tag{14}$$

where C_{BB} can be computed from the geometry of the zone B and the covariance function. In particular, if the variogram is of the simple transitive isotropic form (definition A-1 with very small $s(\Theta)$ and $a = b = h_o$), a convenient upper bound for σ_E^2 is

$$\sigma_E^2 \leq \frac{\sigma^2}{n} + \frac{\pi h_o^2 (\sigma^2 - a^2)}{3B} \tag{15}$$

where B denotes the area of zone B on the mineable surface.

The Sampling Relation in Figure 5

The equation used in Figure 5 was an even simpler version of the relation for σ_E^2. All the equations can be simplified to one-dimensional space (i.e., samples along the strike of the outcrop). The simple transitive variogram becomes

$$\gamma(h) = \begin{cases} a^2 + (\sigma^2 - a^2)|h|/h_o, & \text{if } |h| \leq h_o \\ \sigma^2 & , \text{if } |h| > h_o. \end{cases} \tag{16}$$

and the covariance function is

$$C(h) = \begin{cases} (\sigma^2 - a^2)(1 - |h|/h_o), & \text{if } |h| \leq h_o \\ 0 & , \text{if } |h| > h_o. \end{cases} \tag{17}$$

Under the conditions that all samples are more than a zone of influence apart and are collected at an interior point of zone B more than a zone

of influence from the nearest boundary of B, the expressions C_{BB} and C_{Bi} in theorem A-5 may be explicitly evaluated as

$$C_{Bi} = \frac{1}{L} \int_B C(x-x_i)dx$$

$$= (\sigma^2-a^2)h_o/L \tag{18}$$

and

$$C_{BB} = \frac{1}{L^2} \int_B \int_B C(x-x')dxdx'$$

$$= (\sigma^2-a^2)(h_o/L)(1-h_o/3L), \tag{19}$$

where L is the length of the one-dimensional zone B. For this case, the values of a_i and μ resulting from the solution of the system of equations in theorem A-5 are

$$\hat{a}_i = 1/n \tag{20}$$

$$\hat{\mu} = (\sigma^2-a^2)h_o/L - \sigma^2/n. \tag{21}$$

Hence the expression for σ_E^2 becomes

$$\sigma_E^2 = C_{BB} - \sum_{i=1}^{n} \hat{a}_i C_{Bi} - \hat{\mu}$$

$$= \frac{\sigma^2}{n} + (\sigma^2-a^2)(h_o/L)(1-h_o/3L)-2(\sigma^2-a^2)(h_o/L). \tag{22}$$

Since the probable error is

$$PE = .6745 \ \sigma_E, \tag{23}$$

it follows that the probable error in % is given by

$$PE\% = 67.45 \ \sigma_E/\hat{\overline{V}}$$

$$= 67.45 \ (\sigma/\hat{\overline{V}}) \ [1/n-(1-a^2/\sigma^2)(h_o/L+h_o^2/3L^2)]^{1/2}. \tag{24}$$

If h_o = 10 feet, $\sigma/\bar{V}$ = 0.9, and a^2/σ^2 = 0.62 as the preliminary radio-activity sampling seemed to indicate, the probable error becomes

$$PE\% = 60.7[1/n - 3.8(1/L + 10/3L^2)]^{1/2}. \tag{25}$$

This equation was used to develop the graph in Figure 5 .

The graph served only as a guide for sampling purposes. Subsequently more extensive data arrays were used to refine and adjust the variogram parameters. For example, it was decided to use in the probable error computations of the final resource estimate, the values a^2 = 0 and h_o = 60 feet since these gave conservative bounds for the error. Almost all of the estimated variograms gave values which actually predict smaller probable errors than a^2 = 0 and h_o = 60 feet.

Lognormality of U_3O_8 and ThO_2

The correction of the near-surface tonnage estimates to produce leached uranium endowments, depends critically on the probability law for the population of the larger U_3O_8 values. Previously published investigations have usually found that uranium grade is lognormal. It appeared reasonable to expect lognormal behavior for the Medicine Bow and Sierra Madre deposits.

The grade values which enter the computations consist of the thickness-weighted averages of the grade along each outcrop transect or drill hole as it pierces the mineable surface. The averages are only computed for exceedances of 100 ppm U_3O_8. Let m denote the number of the transects or drill holes which fail to encounter an (unleached) U_3O_8 value exceeding 100 ppm. If there are n transects and drill

holes, then $(n-m)$ of the piercements of the mineable surface encounter

exceedances of 100 ppm. Let

$$\ln U_{m+1} \leq \ln U_{m+2} \leq \ln U_{m+3} \leq \ldots \leq \ln U_n \qquad (26)$$

represent the averages of the logarithm of the grade for those layers

exceeding 100 ppm unleached. The fraction of the piercements with

value less than or equal to $\ln U_r$ is r/n. This is sometimes called

the empirical distribution function,

$$\hat{F}_E(U_k) = r/n, \text{ for } m < r \leq n \qquad (27)$$

and is regarded as a prediction of the distribution function for the

uranium values when uranium $= U_r$. However, this estimate has the

defect that

$$\hat{F}_E(U_n) = 1.0 \qquad (28)$$

and this value cannot be plotted on lognormal probability paper since

1.0 on the probability scale corresponds to $U = \infty$ for these types of

probability. This problem can be circumvented in several ways. One of

the best is advocated by Gumbel (1954) who points out that if $F(u)$ is

the distribution function for the U population, then

$$\{\text{Expected value of } F(U_r)\} = r/(n+1). \qquad (29)$$

With this plotting formula (i.e. $\hat{F}_*(U_r) = r/(n+1)$), the largest value

observed, $\ln U_n$, is plotted versus

$$\hat{F}_*(U_n) = n/(n+1) \qquad (30)$$

on the probability scale. This point can be placed on lognormal paper

with no difficulty.

Thus the procedure used in testing the transect and drill hole accumulated grades for lognormality was as follows. The width-averaged values of the $\ln U_3O_8$ (as corrected approximately to their unleached values) for all exceedances of 100 ppm were ranked in increasing order:

r rank	Average $\ln U_3O_8$	$\hat{F}_*(U_r) = r/(n+1)$
m+1	$\ln U_{m+1}$	$(m+1)/(n+1)$
m+2	$\ln U_{m+2}$	$(m+2)/(n+1)$
m+3	$\ln U_{m+3}$	$(m+3)/(n+1)$
.	.	.
.	.	.
.	.	.
n	$\ln U_n$	$n/(n+1)$.

If the graph of $\ln U_r$ versus $r/(n+1)$, on normal probability paper is approximately a straight line, then the grade accumulations of exceedances of 100 ppm behave approximately like the upper tail of the lognormal.

This procedure was followed for the Medicine Bow and Sierra Madre U_3O_8 and ThO_2 values. The resulting graphs are shown in Figure 9. In each case a straight line appears reasonably consistent with the data. The lognormal parameters, μ and σ^2, can be estimated from the straight lines by the following conventions

$$\hat{\mu} = \text{value of } \ln \text{ where } p = 50 \tag{31}$$

$$\hat{\sigma} = (\text{value of } \ln \text{ where } p = 84.13) - \hat{\mu} , \tag{32}$$

where p is % probability .

Sierra Madre U_3O_8

$\hat{\mu} = 3.40$

$\hat{\sigma} = 0.95$

$+$ $\overline{U_3O_8}$ per encounter

(4 points)

$\hat{\sigma} = 4.35 - 3.40 = 0.95$

$\hat{\mu} = 3.40$

In U_3O_8

0   1   5 10 30 50 70 84 95 99   %

Sierra Madre ThO_2

$\hat{\mu} = 5.22$

$\hat{\sigma} = 0.56$

$+$ $\overline{ThO_2}$ per encounter

(23 points)

$\hat{\sigma} = 5.78 - 5.22 = 0.56$

$\hat{\mu} = 5.22$

In ThO_2

0   1   5 10 30 50 70 84 95 99   %

Medicine Bows U_3O_8

$\hat{\mu} = 5.30$

$\hat{\sigma} = 0.55$

$+$ $\overline{U_3O_8}$ per encounter

(21 points)

$\hat{\sigma} = 5.85 - 5.30 = 0.55$

$\hat{\mu} = 5.30$

In U_3O_8

0   1   5 10 30 50 70 84 95 99   %

Medicine Bows ThO_2

$\hat{\mu} = 5.30$

$\hat{\sigma} = 0.60$

$+$ $\overline{ThO_2}$ per encounter

(22 points)

$\hat{\sigma} = 5.90 - 5.30 = 0.60$

$\hat{\mu} = 5.30$

In ThO_2

0   1   5 10 30 50 70 84 95 99   %

Figure 9.   Lognormal probability plots for uranium and thorium, Sierra Madre and Medicine Bow Mountains.

The predicted values for $\hat{\mu}$ and $\hat{\sigma}$ are listed with each graph in Figure 9. These values will be used later in the section on the leaching formulas and associated resource adjustments.

The Variogram Parameters

As more data was accumulated, additional information became available for computing variogram parameters. The assay values could not be used for this purpose since they were always more than a zone of influence apart. However, additional radioactive count data was collected at close enough spacing to allow the determination of a^2/σ^2 and the zone of influence, h_o. Some examples are shown in Figures 10, 11, and 12. In addition, there were many cases where only upper bounds to the parameters could be determined. A number of such estimates are summarized in Tables 1 and 2. Upper bounds are very relevant, because often they can be used to develop corresponding upper bounds for the probable error. In the resource data analyzed so far, a zone of influence of 60 feet and a nugget effect of 0 appears to give reasonable upper bounds. Actually, the probable errors were computed for both $h_o = 30$ and $h_o = 60$ feet with only slight changes in results. Thus, the error analysis is quite insensitive to h_o and a^2 for the range of values in the data studied.

Figure 10. Variogram typical of conglomerate h, Sierra Madre.
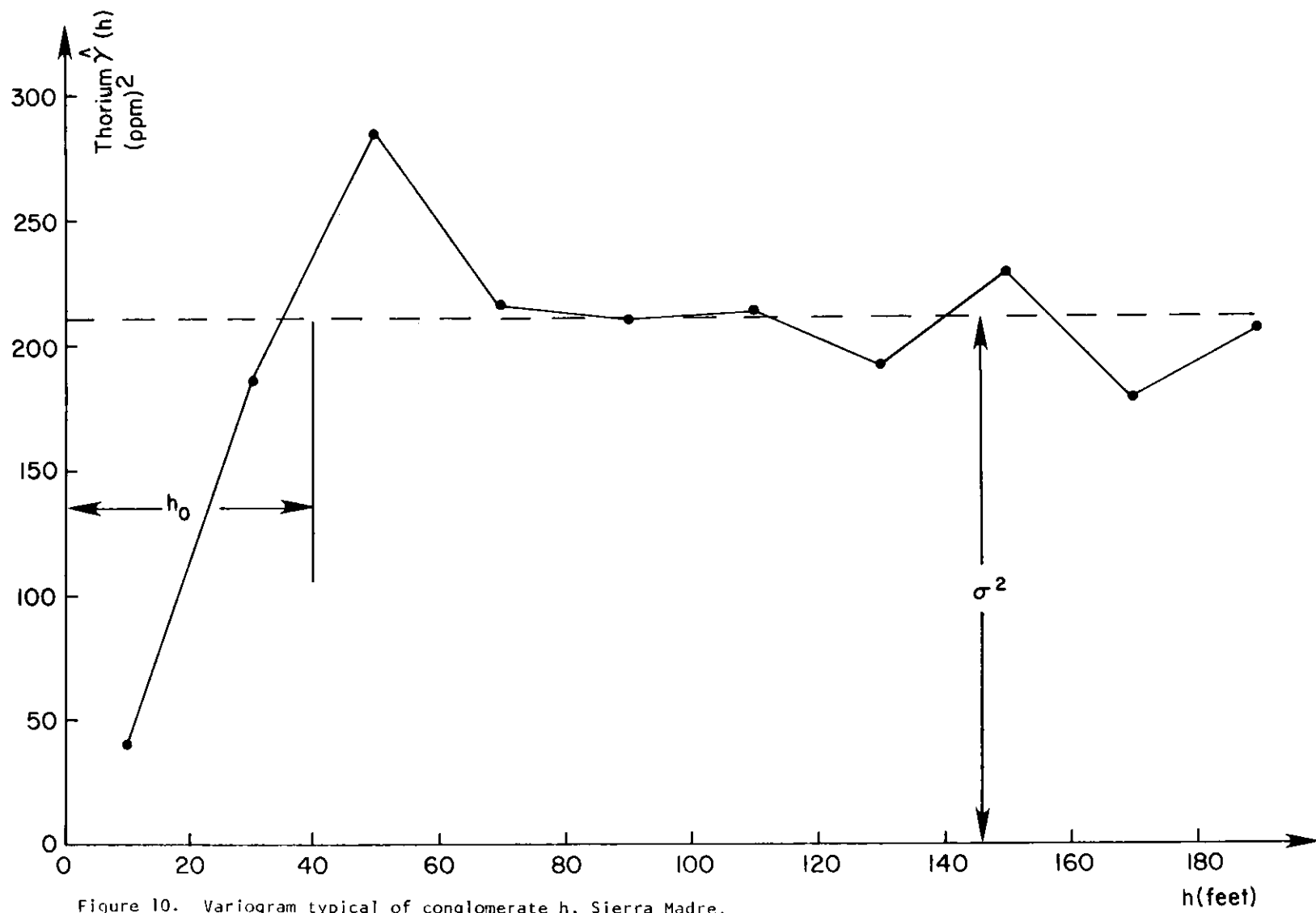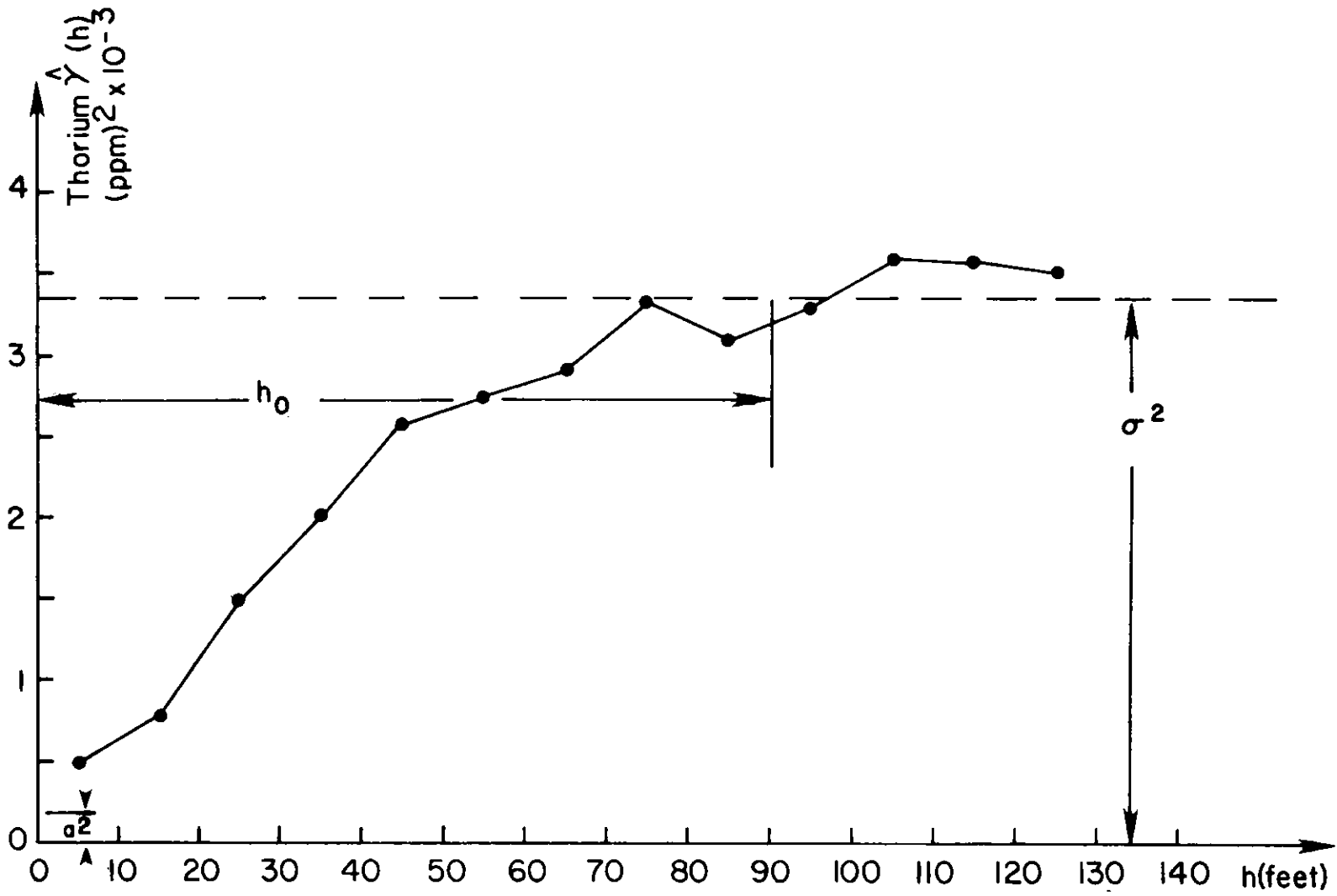
Figure 11.   Variogram typical of conglomerate k, Sierra Madre.

45
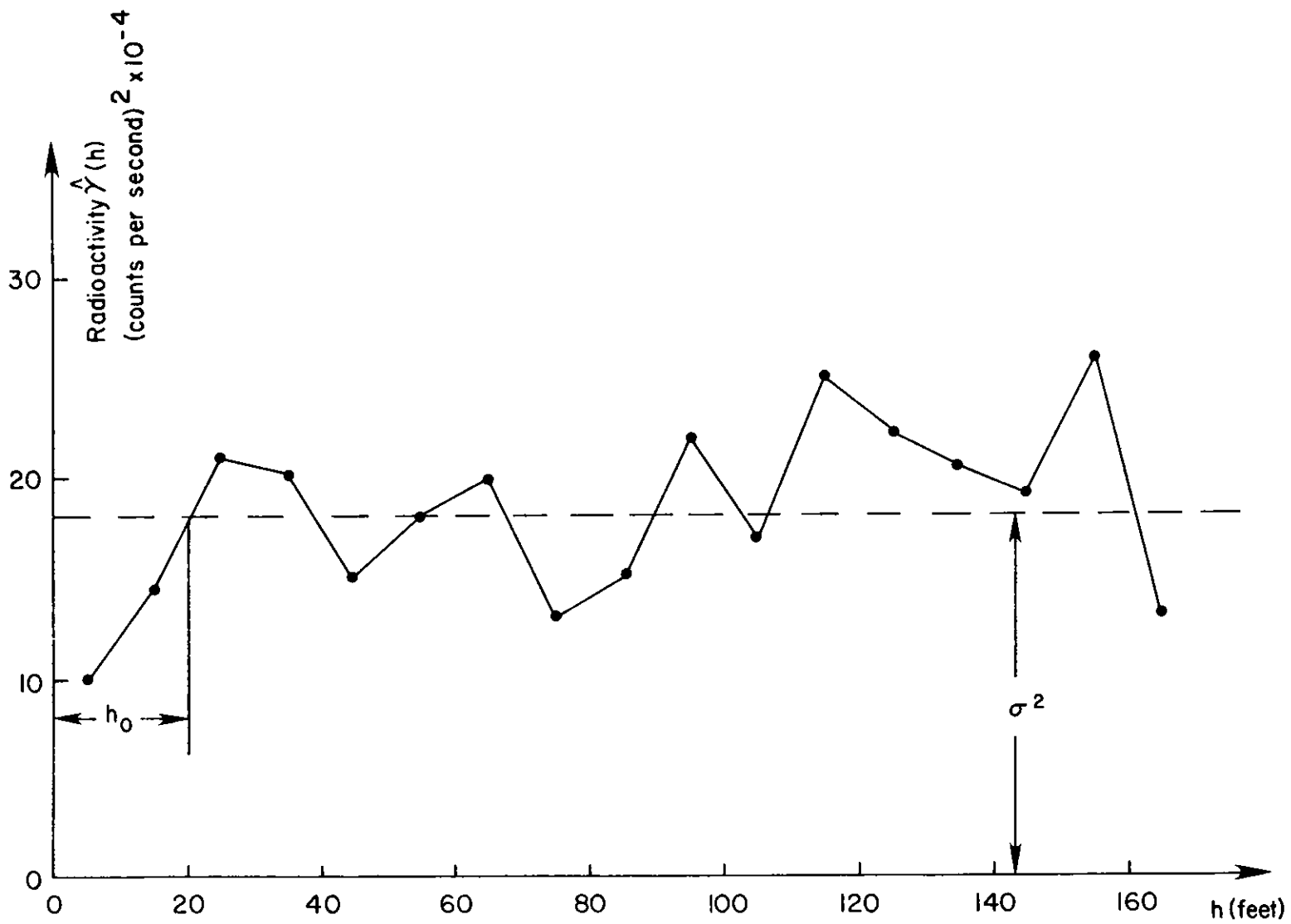
Figure 12. Variogram typical of Onemile Creek area conglomerates.

Rank	Zone of influence, h_0 feet (ranked)	nugget-to-variance ratio a^2/σ^2 (ranked)
1	3	.0
2	3	.03
3	5	.27
4	5	.28
5	6	.55
6	10	.61
7	10 median value	.62 median value
8	14	.63
9	26	.79
10	36	.80
11	45	.81
12	75	.91
13	117	.99

Table 1. Variogram parameters for radioactivity, Carrico Ranch, Sierra Madre. (Note: parameters are ranked separately in increasing size. Average variance of count = 55000 ppm^2).

	Conglomerate	Zone of influence (ft)	Sill Value	Nugget effect
SIERRA MADRE — CARRICO RANCH REGION	G	shows trend		
	H	40	$220(ppmTh)^2$	$1.0(ppmTh)^2$
	I	40	$2200(ppmTh)^2$	$0.0(ppmTh)^2$
	J	shows trend		
	K	90	$3350(ppmTh)^2$	$200(ppmTh)^2$
	L	25	$350(ppmTh)^2$	$100(ppmTh)^2$
MEDICINE BOW — ONE MILE CREEK REGION	Case 1	<10		
	2	40	$35000(cps)^2$	$0(cps)^2$
	3	<10		
	4	<10		
	5	30	$80000(cps)^2$	$0(cps)^2$
	6	20	$18000(cps)^2$	$6000(cps)^2$
	7	<10		

Table 2. Variogram parameters values for data from various portions of the areas in the Sierra Madre and Medicine Bow Mountains

PREDICTION EQUATIONS FOR LEACHING

It appeared reasonable to assume that (1) below some particular depth, the uranium and thorium maintained some fixed functional relation with each other, and (2) above that depth the functional relation required that depth be introduced as an additional variable.

Multivariate stepwise regression was used to search for the critical depth and for the functional relationships. Calculations were made for ln U and ln Th as well as U and Th as measured. The logarithms of the assay values gave substantially better curve fits. After much trial-and-error, the following basic equation was determined to best represent the general features of the relation between ln U, ln Th, and depth, d:

$$\ln U = (a_0 + a_1 e^{-cd} + a_2 e^{-2cd} + a_3 e^{-3cd})$$
$$+ (b_0 + b_1 e^{-cd} + b_2 e^{-2cd} + b_3 e^{-3cd}) \ln Th$$
$$+ \text{random error.} \tag{33}$$

This basically assumes that at any depth, there is a linear relation between ln U and ln Th. However, the intercept and slope of the linear relation are a cubic polynomial of the variable exp(-cd). This allows considerable freedom for the curve to follow the data as it varies with depth. Also, by choosing various values of c, the leaching could be made to reach either great depths or only affect very shallow portions of the deposit.

The general method of analysis consisted of fixing a value of c, and then determining the best coefficients $(a_o, a_1, a_2, a_3, b_o, b_1, b_2, b_3)$ to fit the data by stepwise-multiple regression. The goodness-of-fit, as measured by the fraction of scatter "explained" by the curve fit (a quantity called R^2 in statistical parlance) was then noted for that c value. This was done for many different c values and a graph of R^2 versus c was prepared. The value of c at the maximum R^2 would then be judged as the value most consistent with the data. Based on the R^2 criterion, the value c = .03 was chosen for both the Sierra Madre and the Medicine Bow Areas. Let d_o be the depth at which the variable exp(-cd) dies off to one percent of what it is at d = 0. Then d_o would be the solution to

$$e^{-.03d_o} = .01 \tag{34}$$

or

$$d_o = 154 \text{ feet.} \tag{35}$$

Thus, the c = .03 value implies that the leaching is negligible below d = 154 feet. The functional relations, for d>154 feet would approximately be

$$\ln U = a_o + b_o \ln Th + error. \tag{36}$$

With c = .03, the stepwise regression gave quite adequate curve fits with the formulas:

<u>Sierra Madre</u>

$$\ln U = (-.573 + .158 e^{-.09d}) \tag{37}$$
$$+ (.738 - 1.050 e^{-.03d} + .906 e^{-.06d}) \ln Th$$

(standard deviation of error of fit = .717);

<u>Medicine Bow</u>

$$\ln U = (1.608 - 9.786\ e^{-.03d} + 8.471\ e^{-.09d}) \tag{38}$$
$$+ (.663 - .0947\ e^{-.03d})\ \ln Th$$

(standard deviation of error of fit = .804).

In both equations, the regression explained about 60 percent of the scatter. Thus the equations represent reasonably good trend lines, but there is still substantial scatter (40 percent) about the trend. It should be clearly noted that these equations do not function as prediction equations giving the ln U value for a particular sample as a function of the ln Th and depth for that sample. Rather they establish the surface or trend about which the data scatter.

The equations at substantial depth (>154 feet or so) reduce to the relations for no leaching of:

<u>Sierra Madre</u> (d = ∞)

$$\ln U = -.573 + .738\ \ln Th \tag{39}$$

and

<u>Medicine Bow</u> (d = ∞)

$$\ln U = 1.608 + .663\ \ln Th. \tag{40}$$

These equations can be manipulated to the more conventional form of the uranium to thorium ratio of:

<u>Sierra Madre</u> (d = ∞)
$$(U/Th) = e^{-.573}\ Th^{-.262}$$
$$= .56\ Th^{-.26} \tag{41}$$

and

<u>Medicine Bow</u> $(d = \infty)$

$$(U/Th) = e^{1.608} Th^{-.337} \tag{42}$$

This result was somewhat surprising. The exponent on thorium is quite similar for the two areas (on the order of -.3), but the multiplier is nine times larger in the Medicine Bow area than in the Sierra Madre. It is conjectured that this difference is probably due to the different ages of the formations and some substantial associated depositional or mineralogical differences. Mineralogical analyses performed by Houston (and reported in Volume I, this report) indicate that, although the Medicine Bow deposits have several mineral phases bearing both uranium and thorium, the Sierra Madre units lack any major uranium-bearing minerals.

The relation clearly delineates the observed relationship in the assays that most of the radioactivity in the Carrico Ranch area (Sierra Madre) is due to thorium content, while the Medicine Bow areas have more uranium for the same level of thorium.

Tha amount of leaching at any depth, as stated in terms of difference in logarithms of unleached uranium and leached uranium follows the trend given by subtracting the shallow or depth-dependent relation from the unleached relation holding at depth.

<u>Sierra Madre</u>

$$\text{log increment for leaching} = -.158 \, e^{-.09d}$$
$$+ (1.050 \, e^{-.03d} - .906 \, e^{-.06d}) \ln Th \tag{43}$$

52

<u>Medicine Bow</u>

log increment for leaching = +9.786 $e^{-.03d}$-8.471 $e^{-.09d}$

$\qquad$ + .0947 $e^{-.03d}$ ln Th. $\hspace{3cm}$ (44)

Along the outcrop transects where the major portion of assay data used in the resource calculation was obtained, the log increment for leaching (at d=0) reduces to:

$\qquad$ <u>Sierra Madre</u> (d = 0)

$\qquad$ log increment for leaching =-.158 + .144 ln Th $\hspace{2cm}$ (45)

$\qquad$ <u>Medicine Bow</u> (d = 0)

$\qquad$ log increment for leaching = 1.315 + .0947 ln Th. $\hspace{2cm}$ (46)

Another surprising aspect of the leaching relationships was discovered in the zone between d = zero and d = 30 feet. In planning the analysis, it was more or less assumed that the leaching would be largest at d = zero and decrease along some curve with increasing depth. The formula used in the curve-fitting permits other behavior, however, if the data requires it. A careful examination of the log increment for leaching shows that for larger values of thorium, the amount of leaching increases with depth for about the first 30 feet or so and then begins to decrease steadily with increasing depth. This happens in both the Sierra Madre and in the Medicine Bow areas. Scatter plots of uranium versus depth show that this is a real behavior and not some peculiarity of the analysis procedure. The values at the surface outcrops are slightly richer on the average than those at shallow depths. However,

the number of assays in this 10 to 30 foot zone is quite restricted

and the main curve behavior is controlled primarily by the average

surface values (d = zero) and the trend of the values between 50

feet and 150 feet.

It has been conjectured that the leaching may be strongly affected

by the length of time the moisture stays in contact with the ore as it

percolates downward. Surface moisture would move down rapidly at first

and then slow down somewhat with increasing depth. Thus, the contact

time might be less at d = zero than at d = 20 feet. However, this is

pure speculation.

The leaching adjustments and subsequent tonnage correction procedures

were carefully designed so that they would not be sensitive to whether

this maximum leaching at 30 feet is actually present or not. The data

available at the surface (d=0) and below 50 feet (d>50 feet) were quite

adequate to provide satisfactory accuracy in the determination of the

leaching trend. However, the sparsity of the data for 0<d<50 feet

suggests that the magnitude of the maximum occurring in that interval

may, in part, be related to the well known tendency of polynomial

curve fits to oscillate to unrealistic extremes where data is absent.

As a reasonable approximation to what is probably present, the leaching

curves given in equation (43) and (44) were modified for 0<d<50 feet by

replacing the curve with a straight line interpolation between the

values at d=0 and at d=50 feet. The resulting modified curve was averaged

over the intervals (0,100) and (100, 200) to obtain the leaching

54

correction used in the resource computation. This computation yielded
the results shown in Table 3. Greater depths were essentially unleached,
so the adjustments or corrections were small or zero.

| Area | Depth Interval | |
	0-100	100-200
Medicine Bows	1.406 + .0344 ln Th	.1542 + .0015 ln Th
Sierra Madre	-.0401 + .1357 ln Th	.0162 ln Th

Table 3. Modified averaged log increment for leaching.

The general leaching adjustments proceeded as follows. The log
increment for leaching was added to the logarithm of the measured
uranium and the value of .165 was added to this to adjust the grade to
values for the equivalent logarithm of U_3O_8. The leaching correction
procedure really only affected the top 150 feet of the resource so that
in terms of the total deposit only a small portion was involved. How-
ever, it allowed the surface outcrop assays to become reasonable pre-
dictors of the unleached U_3O_8 grades holding at depth.

All the assay data, as adjusted to unleached equivalent grade,
then could be used to compute accumulations or thickness-averaged
grades for those uranium bearing beds with exceedances of 100 ppm.
These accumulations are tabled in Appendix D. Finally, these accumu-
lated grades were kriged to produce resource estimates in terms of
unleached U_3O_8. The exact details of the kriging will be outlined in
the next seciton. However, it is appropriate to discuss the tonnage
correction used to convert to leached resource estimates in this section
because it is controlled in part by the leaching relations.

As discussed previously, the logarithm of the unleached U_3O_8 accu-
mulations appear to behave according to lognormal probabilities. This
implies that the U_3O_8 will also be lognormal. Also, if B^* represents the

55

subset of the region B where exceedances of 100 ppm are encountered, then the fraction of B^* with grade exceeding some other value, say 200 ppm, can be computed from the lognormal behavior.

For example, as shown in Figure 13, let the area under the curve to the right of ln 100 be area A. This would represent the fraction of B with unleached average grade exceeding 100 ppm. The unleached average grade which would become equal to 100 ppm after leaching would be obtained from:

$$\begin{array}{l}\text{unleached equivalent} \\ \text{of 100 ppm leached}\end{array} = \text{ln 100} + \begin{array}{l}\text{log increment} \\ \text{for leaching}\end{array} \qquad (47)$$

for any particular selected depth. This value on the horizontal axis of Figure 13 is schematically indicated by the downward arrow. Let area A^* be the area under the lognormal curve to the right of the vertical arrow. The two areas, A and A^*, can be interpreted, respectively, as the fraction of B with unleached grade greater than 100 ppm and the fraction of B^* with leached grade greater than 100 ppm. The lognormal curve is characterized by $\hat{\mu}$ (the middle or balance point of the curve) and $\hat{\sigma}$ (the standard deviation parameter). If these values are known, the areas A and A^* can be calculated. Then the tonnage correction is the ratio of area A^* to area A. The basic relation is:

$$\begin{array}{l}\text{fraction of } B^* \text{ with} \\ \text{leached grade>100 ppm}\end{array} = \begin{array}{l}\text{tonnage} \\ \text{correction}\end{array} \times \begin{array}{l}\text{fraction of B} \\ \text{with equivalent} \\ \text{unleached grade>} \\ \text{100 ppm.}\end{array} \qquad (48)$$
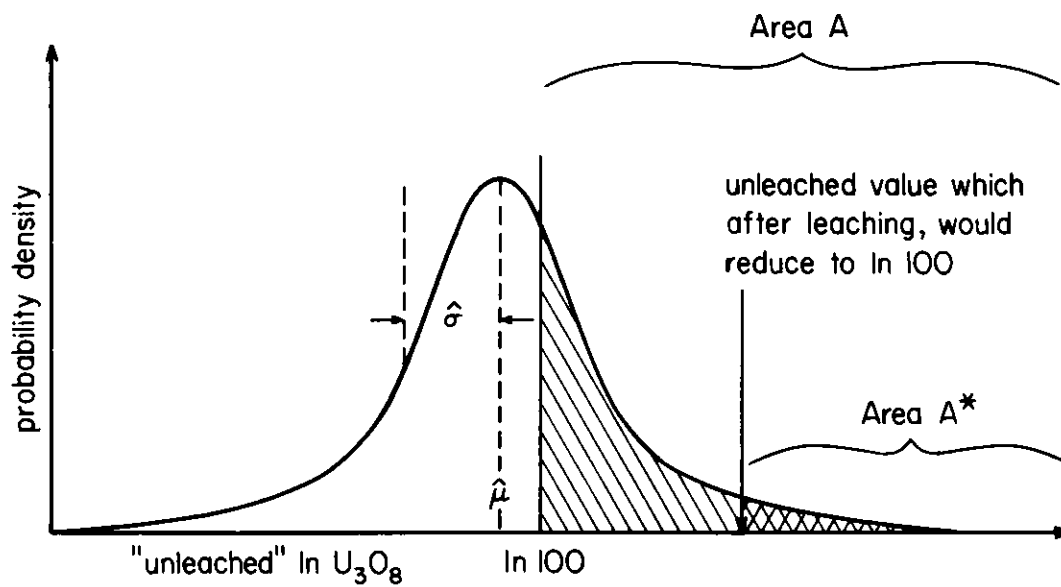
Figure 13. Probability distribution curve illustrating the basis for the tonnage correction.

THE RESOURCE DETERMINATION

The Basic Kriging Relation

The resource determination formula then becomes

$$
\begin{array}{l}
\text{tons } U_3O_8 \\
\text{leached} \\
\text{in a given} \\
\text{depth interal}
\end{array}
=
\begin{array}{l}
\text{area of} \\
\text{mineable} \\
\text{surface}
\end{array}
\times
\begin{array}{l}
\text{average} \\
\text{thickness}
\end{array}
\times
\begin{array}{l}
\text{fraction of} \\
\text{mineable sur-} \\
\text{face with} \\
\text{unleached} \\
\text{grade>100 ppm}
\end{array}
$$

$$
\times
\begin{array}{l}
\text{average unleached} \\
\text{grade for} \\
\text{exceedances of} \\
\text{100 ppm}
\end{array}
\times
\begin{array}{l}
\text{tonnage} \\
\text{correction}
\end{array}
\Big/ \; 11900000.
\tag{49}
$$

The fraction of the mineable surface with unleached grade>100 ppm is
the area of B^* divided by the area of B. This in turn is approximated
by the total number of drill holes and outcrop transects which encoun-
tered beds whose adjusted unleached equivalent grade exceeded 100 ppm,
divided by the total number drill holes and transects piercing the
mineable surface. For example in the Sierra Madre, only two drill holes
and two outcrop transects passed through beds with unleached equivalent
grade greater than or equal to 100 ppm. There were a total of 31 drill
holes or transects that encountered the mineable surface. Then the
fraction would be 4/31. That is 27/31 of the mineable surface does not
experience any exceedances of 100 ppm unleached.

The value 11,900,000 makes the conversion from ppm to tons of
resource. It is based on 11.9 cubic feet per ton, which in turn is the
appropriate value for country rock with a specific gravity of 2.7.

The assumptions under which this resource formula is equivalent to kriging will now be discussed. Let $V^*(\underline{x})$ be the equivalent unleached grade of the deposit at location $\underline{x}(x_1, x_2, x_3)$. From geological considerations and from the limited data available $V^*(\underline{x})$ appears to behave as a stationary random function. Let the adjusted random function $V(\underline{x})$ be defined as

$$V(\underline{x}) = \begin{cases} V^*(\underline{x}), & \text{if } V^*(\underline{x}) \geq 100 \text{ ppm} \\ 0, & \text{otherwise.} \end{cases} \tag{50}$$

The resource in mathematical terms is

$$\text{resource} = \text{correction} \times \iiint\limits_{\text{Deposit}} V(\underline{x})d\underline{x}, \tag{51}$$

where the correction is the depth dependent value which adjusts ppm to tons and makes the tonnage correction for the depth interval involved. In the present study a further modification was introduced in that the inside integral was taken as a perpendicular to the mineable surface and an accumulation was defined as

$$A(x_1, x_2) = \int\limits_{\substack{\text{along } \perp \\ \text{to mineable surface}}} V(\underline{x})dx_3. \tag{52}$$

Then the resource formula becomes the integral over the mineable surface, B, of $A(x_1, x_2)$. Thus,

$$\text{resource} = \text{correction} \times \iint\limits_{B} A(x_1, x_2)dx_1 dx_2 . \tag{53}$$

It was convenient to think in terms of average grade, $\overline{A}(x_1, x_2)$, and total thickness of beds with exceedances of 100 ppm unleached

60

equivalent, $T(x_1, x_2)$. These are mathematically related as

$$\bar{A}(x_1, x_2) = A(x_1, x_2)/T(x_1, x_2).$$ (54)

Thus the resource becomes

resource = correction × (area of B) × (area of B^*/area of B)

$$\times \; (1/\text{area of } B^*) \int_{B^*} \int T(x_1,x_2)\bar{A}(x_1,x_2)dx_1 dx_2.$$ (55)

The integration can be reduced to being over B^* because $\bar{A}(x_1, x_2) = 0$ for the rest of B.

This whole process has reduced the problem to that of estimating the average accumulation over B^*:

$$\text{average accumulation} = \frac{1}{B^*} \int \int A(x_1,x_2)dx_1 dx_2$$

$$= \frac{1}{B^*} \int \int T(x_1,x_2) \, \bar{A}(x_1,x_2)dx_1 dx_2.$$ (56)

This is precisely what kriging as discussed in Appendix A is designed to estimate. The estimate is a weighted average of $\overline{TA}$ over the outcrop and drill hole transects where the weights are determined to minimize the estimate error as shown in Appendix A. Thus the resource estimate becomes

kriged
resource = correction_1 × (area B) × area B^*/area B
estimate (57A)

× (kriged estimate of accumulation over B^*)

= correction_2 × area B × (kriged estimate of accumulation over B). (57B)

61

The resource can be regarded either as a correction times the kriged average over B^* or as a different correction times the kridged estimate over B.

The kriged accumulations are developed in terms of U_3O_8 itself, rather than $\ln U_3O_8$. Actually, it is acceptable practice to use either approach. Kriging based on $\ln U_3O_8$ is called lognormal kriging. However, this study was based on U_3O_8 because it was believed that the kriged estimates represent averages over large volumes for this case. The small zones of influence found (certainly less than 100 feet) would indicate that it is equivalent to average a number of independent random quantities. By the central limit theorem of statistics, the average of a number of lognormal variables will be normally distributed, and not lognormal. Thus the probability behavior for the overall resource values can, in this case, be based on regular normality, even though the original input data is lognormal. Actually, the central limit theorem behavior dominates very quickly. The average of even three of four independent lognormal variable will, to a very good appproximation, behave as a normal variable.

Computation of Probable Error

As shown in the theorem A-6 in Appendix A, the variance of estimate error, for the kriged estimate over B, is

$$\sigma_B^2 \leq \frac{\sigma^2}{n} + \pi h_o^2 (\sigma^2 - a^2)/3B. \tag{58}$$

The corresponding probable error would be

$$PE = .6745\sigma_B \tag{59}$$

and the percentage probable error is

$$PE\% \cong 67.45\hat{\sigma}_B/(\text{kriged estimate of acccumulation over } B). \qquad (60)$$

The probable error is interpreted as the median error due the random-ness of grade and thickness as evidenced by the measured data. Thus, it is a statistical error, not a geological uncertainty factor. Judg-ments concerning geological uncertainty will be discussed later.

In order to apply (58) to the resource estimates in the present model, values have to be assigned to the σ^2, h_o, and a^2 constants; the quantities n and B, (representing the number of transects or drill hole piercements of the mineable surface, and the mineable surface area of the region which is being averaged, respectively) are known from the sampling plan and the assumed geological model.

The estimate of σ_B^2 is quite insensitive to a^2 and h_o. Hence it appears reasonable to accept conservative values for these parameters and obtain a reasonable upper bound for σ_B^2. If a^2 is set to zero, the right-hand side of (58) is made as large as it can get relative to the variation of a^2. From the measured data, it appears quite likely that the overall value of h_o is less than 60 ft. Thus, $a^2=o$ and $h_o=60$ ft. appear to be reasonable choices.

The value of σ^2 is important to the error estimation. In the resource model used, the accumulation, as a function of position on the mineable surface, was taken to be zero if the unleached grade was less than 100 ppm, and was assigned the measured value if the unleached grade exceeded or equaled 100 ppm. Let p be defined as the fraction of the mineable surface with unleached grade $\geq$ 100 ppm (see eg. (49)).

Then the accumulation is a random function over the mineable surface which is zero on p-fraction of the surface and has an average value of mean measured accumulation as determined for those transects or piercements with value $\geq$ 100 ppm. Let $\overline{Acc}$ denote this last average, and let $A\ (x_1,\ x_2)$ be the overall random function which is zero when the accumulations drop below 100 ppm (see eq. (52)). Also let $\overline{Acc^2}$ denote the average of the squared values over this same region.

As shown in eqs (49)-(57), the kriged values reported in the resource estimate may be considered as regional averages of $A\ (x_1,\ x_2)$. Several questions need to be answered before the probable error formulas given earlier can be applied. These are: (1) Is $A\ (x_1,\ x_2)$ stationary? and (2) What is the mean and variance of $A\ (x_1,\ x_2)$?

The accumulations without the 100 ppm cutoff are assumed to be covariance stationary after correction for leaching, with expected lagged product $L(h_1,\ h_2)$, mean μ_o and expected square s_o.

We note that:

$$\mu_A\ = E[A\ (x_1,\ x_2 0] = p\mu_o, \tag{61}$$

$$\sigma_A{}^2 = E[A^2\ (x_1,\ x_2)] = ps_o, \tag{62}$$

$$E[A\ (x_1,\ x_2)\ A\ (x_1+h_1,\ x_2+h_2)] = p^2 L(h_1,h_2). \tag{63}$$

These values do not vary with spatial position, so covariance stationarity is verified.

It follows from the above that reasonable estimates for the mean and variance of A (x_1, x_2) are:

$$\hat{\mu}_A = \text{est. mean } A = p\,\overline{Acc}, \tag{64}$$

$$\hat{\sigma}_A^2 = \text{est. variance } A = p\,\overline{Acc^2} - (p\overline{Acc})^2. \tag{65}$$

This last quantity is the reasonable data-derived value to use as σ^2 in eq. (58). Thus

$$PE\% \leq 67.45 \; \frac{\sqrt{\{p\overline{Acc^2} - (p\overline{Acc})^2\} \; \{\frac{1}{n} + \pi h_o^2/3B\}}}{p\overline{Acc}} \quad . \tag{66}$$

These probable error values are listed in the resource tables.

Probable errors for intervals and overall estimates are estimated from the same formula. The area B is changed in each case to contain the mineable surface area for that region.

The combination of probable errors from several different (and assumed independent) regions requires a different formula. Let R_1, R_2, ..., R_n be n regions with mean values μ_1, μ_2, ..., μ_n and probable errors $(PE)_1$, $(PE)_2$, ..., $(PE)_n$. Then the square probable error of the overall average is the weighted average of the individual square probable errors.

$$\text{P.E. of overall average} = \left[\frac{\sum\limits_{i=1}^{n} \mu_i \, (PE)_i^2}{\sum\limits_{i=1}^{n} \mu_i}\right]^{1/2} \quad . \tag{67}$$

The Resource Computations

The resource calculations are summarized in Tables 4 to 8 for leached U_3O_8. The left column gives the depth interval. The next three

65

columns list the area of mineable surface in each depth interval, the leaching correction as based on the value of the integral of the interval, and the tonnage correction. The fifth column summarizes the resource estimates in terms of equivalent unleached tonnage exceeding 100 ppm. The tonnage correction is multiplied times this to give the sixth column which is the final estimate of the resource endowment for U_3O_8 with grade exceeding 100 ppm. This grade represents an estimate of the in-place, leached tonnage of the ore deposit.

The final column of the table gives the percent probable error as based on the conservative choices of $h_o=60$ feet and $a^2=0$. The probable errors for the U_3O_8 reserves in the Sierra Madre (Table 4) are unexpectedly rather large. However, an examination of the underlying data reveals the probable reason. There were only 4 of 31 transects or drill holes which encountered exceedances of 100 ppm unleached U_3O_8. Among these four, three encountered relatively thin and low grade uranium concentrations, while one was substantially thicker and richer. Thus, the variance of accumulation (thickness X value) was quite substantial and this large variance produced a corresponding large probable error. Because of the small number of encounters (i.e., only four), the estimate of probable error in this case should be regarded as somewhat unreliable and used only as a general indication of magnitude of error.

Since the data was available and may be of interest at some future date, resource estimates were also made for the tons of thorium oxide (ThO_2) exceeding 100 ppm. For this case, the whole leaching adjustment

66

Depth Interval	Area per depth interval of mineable surface (ft.^{2})	Leaching correction for ln U_3O_8	Tonnage correction (adjusted to leached resource)	Unleached tons>100 ppm per depth interval	Resource tons>100 ppm after correction for leaching	% Probable error
0- 100	3,343,000	0.7063	0.2158	8.9	1.9	52.7
100- 200	3,360,000	0.0891	0.8457	9.0	7.6	52.7
200- 300	3,360,000	0	1.000	9.0	9.0	52.7
300- 400	3,360,000	0	1.000	9.0	9.0	52.7
400- 500	3,029,000	0	1.000	8.1	8.1	53.5
500-1000	16,236,000	0	1.000	43.4	43.4	52.7
1000-1500	16,965,000	0	1.000	45.4	45.4	52.7
1500-2000	16,965,000	0	1.000	45.4	45.4	52.7
2000-3000	33,931,000	0	1.000	90.8	90.8	52.7
3000-4000	33,931,000	0	1.000	90.7	90.7	52.7
4000-5000	33,931,000	0	1.000	90.7	90.7	52.7
				Total	442.0 tons	52.7%

Table 4. Summary of Uranium Resource Calculations for Sierra Madre Unit #3.

*These probable errors are unexpectedly rather large. However, an examination of the underlying data reveals the probable reason. There were only 4 of 31 transects or drill holes which encountered exceedance of 100 ppm unleached U_3O_8. Among these four, three encountered relatively thin and low grade uranium concentrations, while one was substantially thicker and richer. Thus, the variance of accumulation (thickness x value) was quite substantial and this large variance produced a corresponding large probable error. Because of the small number of encounters (i.e., only four), the estimate of probable error in this case should be regarded as somewhat unreliable and used only as a general indication of magnitude of error.

Depth Interval	Area per depth interval of mineable surface (ft.^{2})	Leaching correction for $1 n U_3 O_8$	Tonnage correction (adjusted to leached resource)	Unleached tons>100 ppm per depth interval	Resource tons>100 ppm after correction for leaching	% Probable error
0- 100	903,500	1.5484	0.0673	120.0	8.1	17.3
100- 200	831,700	0.1604	0.9302	110.5	102.8	17.3
200- 300	795,600	0	1.000	105.7	105.7	17.3
300- 400	704,100	0	1.000	93.5	93.5	17.4
400- 500	633,100	0	1.000	88.1	88.1	17.6
500-1000	2,243,700	0	1.000	298.1	298.1	16.7
1000-1500	589,200	0	1.000	78.3	78.3	17.7
				Total	774.6 tons	17.3%

Table 5. Summary of Uranium Resource Calculation for Medicine Bow Unit #1.

Depth Interval	Area per depth interval of mineable surface (ft.^{2})	Leaching correction for In U_3O_8	Tonnage correction (adjusted to leached resource)	Unleached tons>100 oon per depth interval	Resource tons>100 ppm after correction for leaching	% Probable error
0- 100	825,900	1.5942	0.0569	109.7	6.2	17.3
100- 200	825,900	0.1624	0.9292	109.7	102.0	17.3
200- 300	859,300	0	1.000	114.2	114.2	17.3
300- 400	798,900	0	1.000	106.1	106.1	17.3
400- 500	783,700	0	1.000	104.1	104.1	17.3
500-1000	1,596,400	0	1.000	212.1	212.1	16.8
1000-1500	147,000	0	1.000	19.5	19.5	21.2
				Total	664.2 tons	17.8%

Table 6. Summary of Uranium Resource Calculations for Medicine Bow Unit #5a.

Depth Interval	Area per depth interval of mineable surface (ft.^{2})	Leaching correction for $\ln U_3O_8$	Tonnage correction (adjusted to leached resource)	Unleached tons>100 ppm per depth interval	Resource tons>100 ppm after correction for leaching	% Probable error
0- 100	702,200	1.5962	0.0509	93.3	4.7	17.4
100- 200	694,200	0.1625	0.9292	92.2	85.6	17.6
200- 300	725,400	0	1.000	96.4	96.4	17.4
300- 400	621,700	0	1.000	82.6	82.6	17.4
400- 500	286,200	0	1.000	38.0	38.0	19.1
500-1000	378,600	0	1.000	50.3	50.3	18.4
				Total	357.6 tons	17.9%

Table 7. Summary of Uranium Resource Calculations for Medicine Bow Unit #5b.

Depth Interval	Area per depth interval of mineable surface (ft.^{2})	Leaching correction for $\ln U_3O_8$	Tonnage correction (adjusted to leached resource)	Unleached tons>100 ppm per depth interval	Resource tons>100 ppm after correction for leaching	% Probable error
0- 100	675,600	1.5498	0.0670	89.7	6.1	17.6
100- 200	675,700	0.1605	0.9302	89.8	83.5	17.6
200- 300	675,700	0	1.000	89.8	89.8	17.6
300- 400	671,200	0	1.000	89.2	89.2	17.6
400- 500	669,000	0	1.000	88.9	88.9	17.6
500-1000	3,325,800	0	1.000	441.8	441.8	16.6
1000-1500	3,163,300	0	1.000	420.2	420.2	16.6
1500-2000	2,992,400	0	1.000	397.5	397.5	16.7
				Total	1617.0 tons	17.2%

Table 8. Summary of Uranium Resource Calculations for Threemile Creek area, Medicine Bow Mountains.

and tonnage correction was unnecessary, since thorium is relatively
unaffected by leaching. These somewhat smaller tables for the tonnage
of ThO_2 exceeding 100 ppm are given in Tables 9 to 13.

Since there may be some interest in what was the maximum value of
U_3O_8 unleached equivalent values which were encountered in the drill
holes where the values did not rise above 100 ppm, the maximum values
encountered in these holes are summarized in Tables 14 and 15. Finally
the overall resource estimates for the Deep Gulch Formation in the
northwestern Sierra Madre and for the Onemile Creek area of the north-
eastern Medicine Bow Mountains are tabulated in Table 16 and 17 for
U_3O_8 and ThO_2 respectively.

Judgements Concerning Geological Uncertainty

Any evaluation of uranium resources is strongly dependent on a
geologic understanding of the geometry of the mineralized bodies. The
geostatistical resource estimate presented in this report reflects our
current understanding of the structure and stratigraphy of the Onemile
Creek area and the Carrico Ranch area, based on surface mapping at a
scale of 1:1200 and on subsurface, drill-core data. In both areas, the
mineralized units have been folded at least twice, faulted, and intruded
by mafic magmas. As a consequence of this complex deformational history
(and in spite of detailed mapping and reconnaissance drilling) there are
still geologic uncertainties in extrapolating outcrop information into
areas of poor outcrop and into the subsurface. For this report, we have
evaluated what we consider to be the most reasonable geometry of the

72

Depth Interval	Area per Depth Interval ot Mineable Surface	Resource Tons >100 ppm	% Probable Error
0- 100	3,343,000	126.6	16.0
100- 200	3,360,000	126.7	16.0
200- 300	3,360,000	126.7	16.0
300- 400	3,360,000	126.9	16.0
400- 500	3,029,000	114.2	16.0
500-1000	16,236,000	612.5	15.8
1000-1500	16,965,000	640.0	15.8
1500-2000	16,965,000	639.7	15.8
2000-3000	33,931,000	1230.0	15.8
3000-4000	33,931,000	1280.0	15.8
4000-5000	33,931,000	1280.0	15.8
Total		6353.3 Tons	15.9%

Table 9. Summary of Thorium Resource Calculations for Sierra Madre Unit #3.

Depth Interval	Area per Depth Interval of Mineable Surface $(ft.^2)$	Resource Tons>100 ppm	% Probable Error
0- 100	903,500	62.6	15.2
100- 200	831,700	57.6	15.4
200- 300	795,600	55.1	15.4
300- 400	704,100	48.8	15.5
400- 500	633,100	45.9	15.5
500-1000	2,243,700	155.4	14.8
1000-1500	589,200	40.8	15.6
Total		466.2 tons	15.3%

Table 10. Summary of Thorium Resource Calculations for Medicine Bow Unit #1.

Depth Interval	Area per Depth Interval of Mineable Surface $(ft.^2)$	Resource Tons>100 ppm	% Probable Error
0- 100	825,900	57.2	15.4
100- 200	825,900	57.2	15.4
200- 300	859,300	59.5	15.2
300- 400	798,900	55.3	15.4
400- 500	783,700	54.3	15.4
500-1000	1,596,400	110.6	14.9
1000-1500	147,000	10.2	18.7
Total		404.3 Tons	15.8%

Table 11. Summary of Thorium Resource Calculations for Medicine Bow Unit #5a.

Depth Interval	Area per Depth Interval of Mineable Surface (ft.^{2})	Resource Tons >100 ppm	% Probable Error
0- 100	702,200	48.6	15.5
100- 200	694,200	48.1	15.5
200- 300	725,400	50.2	15.5
300- 400	621,700	43.0	15.6
400- 500	286,200	19.8	16.8
500-1000	378,600	26.2	16.3
	Total	235.9 Tons	15.9%

Table 12. Summary of Thorium Resource Calculations for Medicine Bow Unit #5b.

Depth Interval	Area per depth interval of Mineable Surface (ft.^{2})	Resource tons>100 ppm	% Probable error
0- 100	675,600	46.8	15.5
100- 200	675,700	46.8	15.5
200- 300	675,700	46.8	15.5
300- 400	671,200	46.5	15.5
400- 500	669,000	46.3	15.5
500-1000	3,325,800	230.4	14.6
1000-1500	3,163,300	219.1	14.6
1500-2000	2,992,400	207.3	14.8
Total		890.0 tons	15.2%

Table 13. Summary of Thorium Resource Calculations for Threemile Creek area, Medicine Bow Mountains.

Drill Core	Unit 1		Unit 2		Unit 4	
	Unt	Th	Unt	Th	Unt	Th
SM-1	3.7	20	29	$130^{(250)}$	18	56
SM-1A	64.0	400	35.0	$26^{(230)}$	14	140
SM-2	no encounter		15	$110^{(120)}$	12.2	$17^{(64)}$
SM-3	21	28	36	$100^{(220)}$	no encounter	
JP-1	4.6	9	27	97	26	220
JP-2	29	220	26	150	22	$20^{(34)}$
JP-3	4.2	15	no encounter		no encounter	
JP-4	42	170	no encounter		14	22

Table 14. Highest uranium and thorium values from units 1, 2, 4 from drill cores in the Sierra Madre.
*Value in parentheses indicates highest spot sample.

Lithologic Units

Drill Hole or transect	1		2		3		4		5	
	U_3O_8	ThO_2	U_3O_8	ThO_2	U_3O_8	ThO_2	U_3O_8	ThO_2	U_3O_8	ThO_2
EMB-1	C(1)	C(1)	C(1)	C(1)	C(1)	C(1)	24.8	21.6	NE	
EMB-2	NE		NE		NE		E-ND		E-ND	
EMB-3	NE		NE		NE		NE		NE	
EMB-4	NE		NE		NE		NE		NE	
EMB-6	NE		NE		NE		E-ND		C(2,3)	C(2,3)
EMB-7	NE		NE		NE		C(2)	C(2)	C(2,3)	C(2,3)
EMB-8	NE		NE		NE		E-ND		C(3)	C(3)
EMB-9	NE		NE		NE		NE		C(3)	C(3)
EMB-10	NE		NE		NE		NE		C(3)	84.2
EMB-11	NE*		NE*		NE*		NE*		NE*	
MB-16	C(1)	C(1)	C(1)	C(1)	34.8	29.6	NE		NE	
T1A	C(1)	C(1)	C(1)	C(1)	NE		NE		NE	
T1B	C(1)	C(1)	C(1)	C(1)	NE		NE		NE	
T1C	C(1)	C(1)	C(1)	C(1)	NE		NE		NE	
T2	C(1)	96.7	C(1)	C(1)	20.8	92.2	14.0	51.2	NE	
T3	NE		NE		NE		NE		C(3)	C(3)
T4	NE		NE		NE		C(2)	C(2)	NE	
T5	NE		NE		NE		C(2)	C(2)	C(2,3)	C(2,3)
T6	NE		NE		NE		87.6	61.8	75.8	C(3)
T7	NE		NE		NE		NE		C(3)	C(3)
T8	NE		NE		NE		C(2)	C(2)	C(2,3)	C(2,3)

NE - Not encountered by drill hole or transect
NE*- Units encountered do not correlate with these lithologic units
C(1)- Used in resource calculation; number indicates which resource
    geometry includes this unit:
        1- Unit 1, Onemile Creek area
        2- Unit 5a, Onemile Creek area
        3- Unit 5b, Onemile Creek area
U_3O_8 and ThO_2 are reported in ppm and maximum ThO_2 may not be from same sample as maximum U_3O_8.

Table 15. Maximum uranium and thorium values <100 ppm encountered in Magnolia Formation lithologic units, Medicine Bow Mountains.

Depth Interval (feet)	Deep Gulch Formation Northwestern Sierra Madre Mountains		Magnolia Formation Northeastern Medicine Bow Mountains	
	Tons U_3O_8 >100 ppm	Probable Error %	Tons U_3O_8 >100 ppm	Probable Error %
0- 100	1.9	52.7*	25.1	16.6
100- 200	7.6	52.7	378.9	16.7
200- 300	9.0	52.7	406.0	16.7
300- 400	9.0	52.7	371.4	16.7
400- 500	8.1	53.5	319.1	16.7
500-1000	43.4	52.7	1002.2	16.5
1000-1500	45.4	52.7	518.0	16.6
1500-2000	45.4	52.7	397.5	16.7
2000-3000	90.8	52.7		
3000-4000	90.7	52.7		
4000-5000	90.7	52.7		
Total	442.0 tons	52.7%	3418.2 tons	16.7%

Average grade for U_3O_8 exceeding 100 ppm	130.2 ppm	305.7 ppm
Average total thickness of beds with U_3O_8 exceeding 100 ppm	1.5 feet	6.1 feet
Thickness per bed	0.6 feet	0.95 feet
Map area	12 sq. miles	2.5 sq. miles

Table 16. Resource summary for tons U_3O_8 with grade exceeding 100 ppm for the listed areas, together with other basic statistics.

*See footnote on Table 4.

Depth Interval (feet)	Deep Gulch Formation Northwestern Sierra Madre Mountains		Magnolia Formation Northeastern Medicine Bow Mountains	
	Tons ThO_2 >100 ppm	Probable Error %	Tons ThO_2 >100 ppm	Probable Error %
0- 100	126.6	16.0	215.2	14.8
100- 200	126.7	16.0	209.6	14.8
200- 300	126.7	16.0	211.7	14.8
300- 400	126.9	16.0	193.6	14.8
400- 500	114.2	16.0	166.4	14.8
500-1000	612.5	15.8	522.5	14.5
1000-1500	640.0	15.8	270.1	14.6
1500-2000	639.7	15.8	207.3	14.8
2000-3000	1280.0	15.8		
3000-4000	1280.0	15.8		
4000-5000	1280.0	15.8		
Total	6353.3 tons	15.9%	1996.4 tons	14.7%
Average grade for ThO_2 exceeding 100 ppm	265.5 ppm		284.5 ppm	
Average total thickness of beds with ThO_2 exceeding 100 ppm	1.5 feet		3.5 feet	
Thickness per bed	0.6 feet		0.8 feet	
Map area	12 mi^2		2.5 mi^2	

Table 17. Resource summary for tons ThO_2 with grade exceeding 100 ppm for the listed areas, together with other basic statistics.

mineralized units. However, in this section it is fruitful to examine

other feasible geologic interpretations which could result in either

larger uranium reserve estimates (terms "optimistic" interpretations) or

smaller reserves estimates ("pessimistic" interpretations).

For the Medicine Bow areas, there are three major uncertainties in

interpreting the subsurface extent of mineralized units in the Magnolia

Formation. The first two, the plunge of the major syncline and the shape

and extent of the mafic intrusive bodies, involve outcropping Magnolia

Formation of both the Onemile Creek and the Threemile Creek areas. The

third deals with the possibility of subcropping Magnolia Formation un-

conformably underlying the Cascade Quartzite east of Onemile Creek.

The major structure in the Onemile Creek area is a faulted and

intruded, tight to isoclinal overturned syncline. Figure 14 shows two

possible plunges for this syncline. Figure 14a, an inclined syncline,

is consistent with the macroscopic pattern of the Magnolia Formation

which can be traced through the Threemile Creek area over a distance of

6 miles to the southwest, into an area of open, upright folds with sub-

horizontal fold axes. Figure 14b, a reclined syncline, is suggested by

mesoscopic fold configurations in the Onemile area. We have used the

inclined fold geometry of 14a in our resource estimate because it explains

regional relationships better and because we believe the mesoscopic fold

structures are related to a superposed fold system which is well documented

by stereonet plots of bedding foliations and lineations. Nevertheless,

if the reclined fold plunge of 14b were used, the resources estimate would

change. Figure 15 and 16 show schematic east-west cross-sections of part

of the Onemile syncline using both interpretations. With the reclined
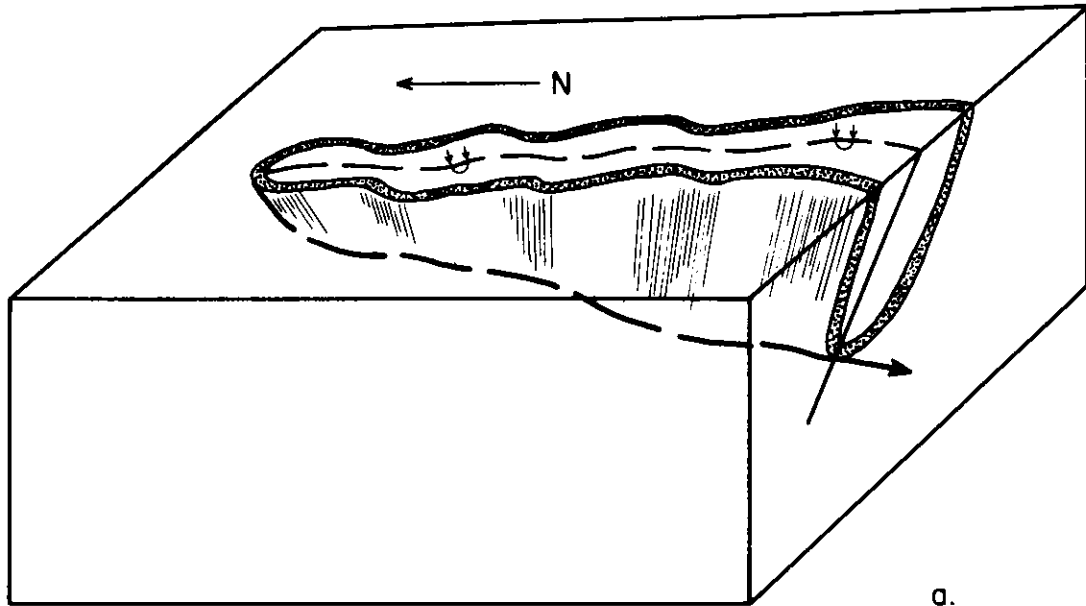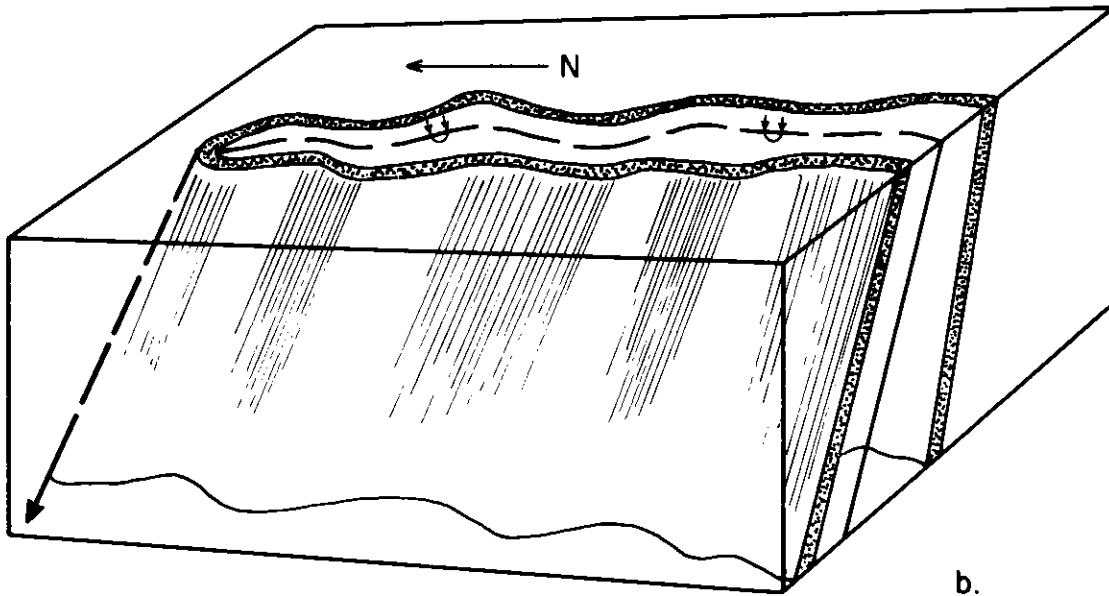
Figure 14. Schematic diagrams of possibe styles of folding in the Onemile Creek area: a) inclined, b) reclined. Heavy dashed line with arrow shows plunge of fold.
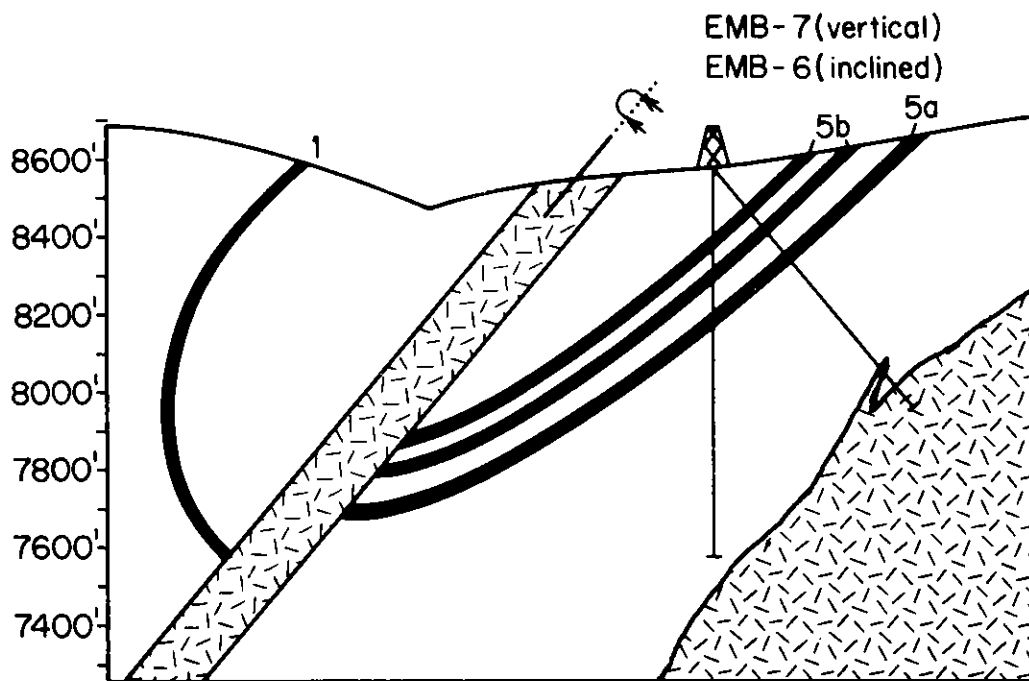
a. Inclined fold with mafic sill.
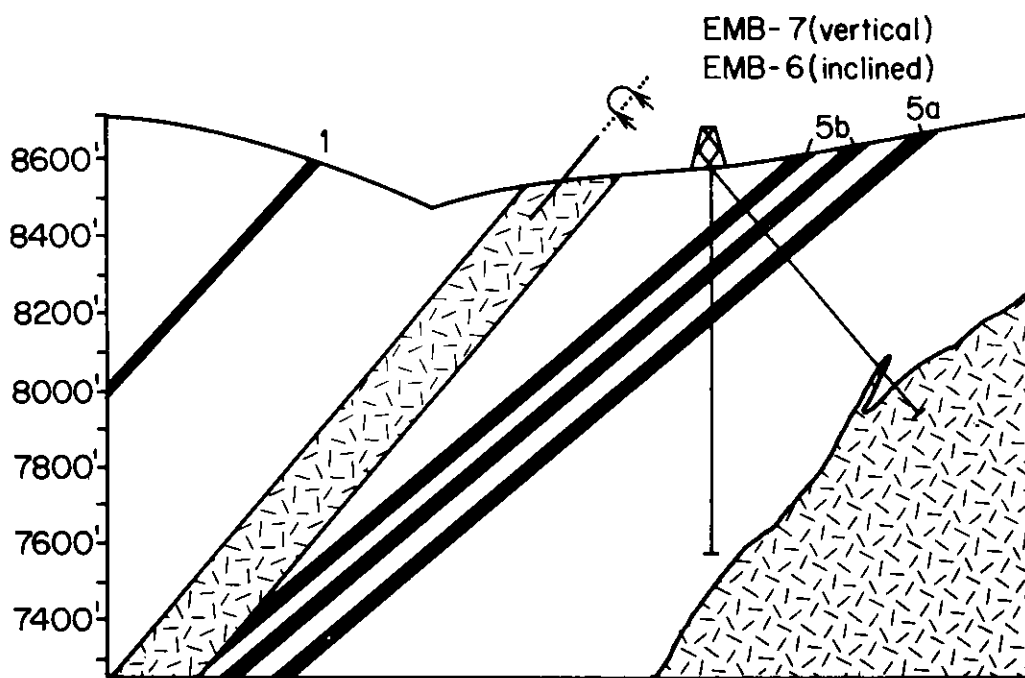
b. Reclined fold with mafic sill.

Figure 15. Possible fold geometries with mafic bodies modelled as sills.
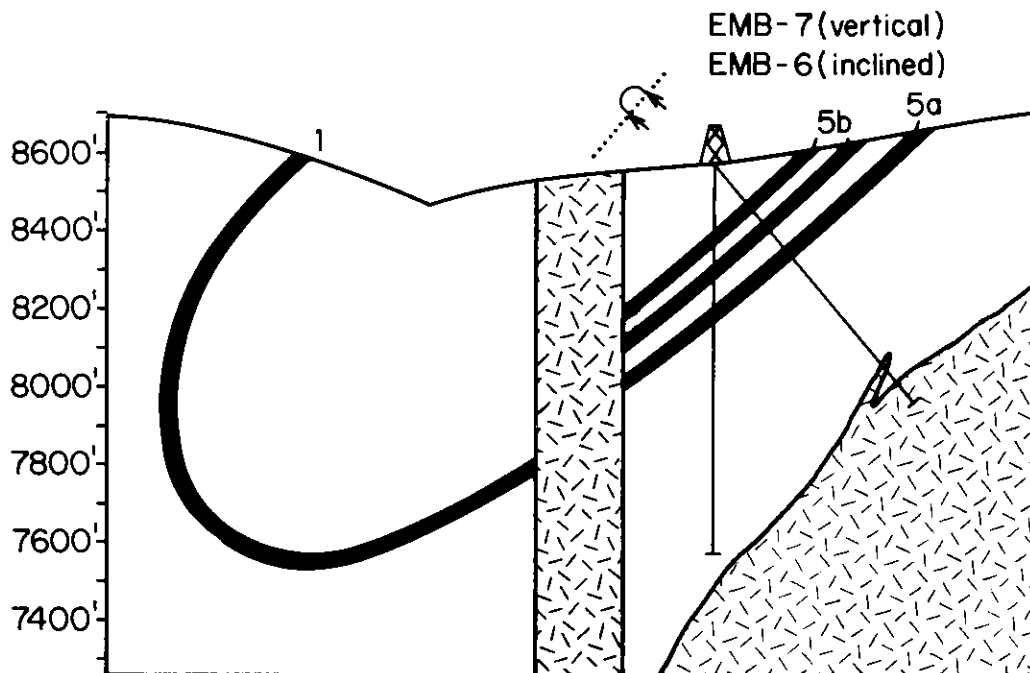
a. Inclined fold with vertical dike.
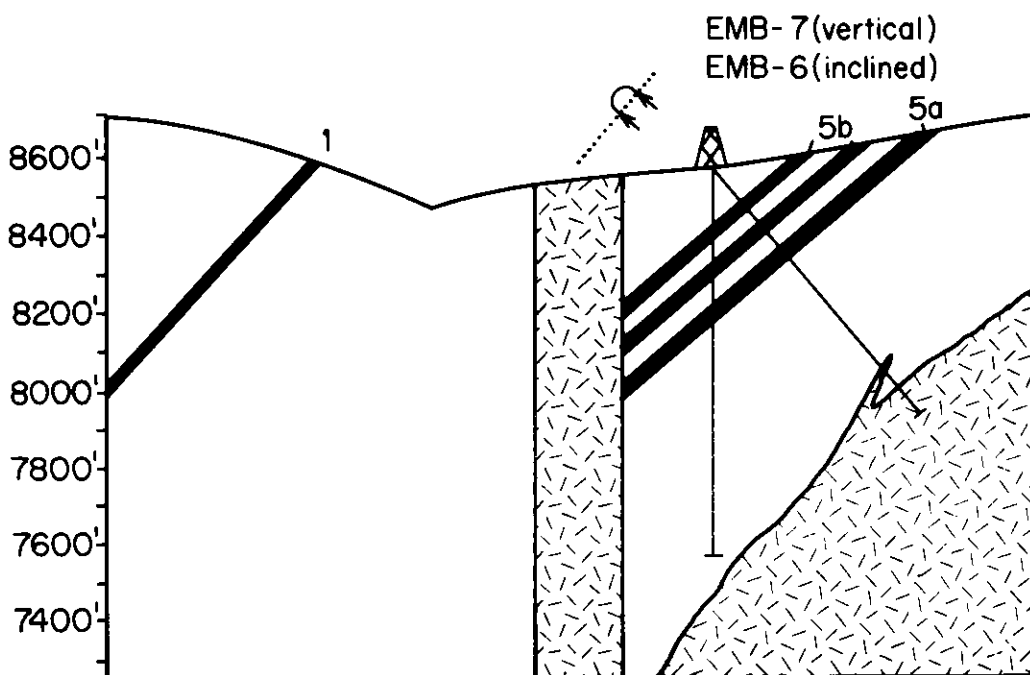
b. Reclined fold with vertical dike.

Figure 16. Possible fold geometries with mafic bodies modelled as vertical dikes.

syncline 14b, mineralized zones would extend to greater depths (averaging 2000 feet instead of 1000 feet) and the reserve figure would be increased by a factor of about 2, if extended to the required depth of 5000 feet. Projection of the Threemile Creek geometry as an inclined syncline to 5000 feet was considered unsupported by our subsurface information but this projection would also double the reserve figure.

The problem of the shape of mafic intrusive bodies is also illustrated in Figures 15 and 16. We believe that the bodies are mainly sill-like and that they were intruded along bedding planes and faults which parallel the axial plane of the fold. However, the bodies could either thicken or thin with depth or remain fairly uniform in thickness. Figure 15, which represents our favored interpretation of sill-like shapes, gives a reasonably optimistic uranium resource estimate, Figure 16, showing geologically unreasonable vertical mafic dikes, would give a pessimistic estimate. If the latter were used, the resource number could be decreased by a factor of .5.

The third problem, of the possibility of subcropping Magnolia east of Onemile Creek, is difficult to evaluate and we have neglected such a possibility in our resource estimate. However, Figure 3 (map) shows the hinge of the major syncline to be offset left laterally into this area so there may be mineralized Magnolia in the subcrop. If so, it is conceivable that the resource estimate should be increased by a factor of 1.5 or 2.

Table 17 summarizes what we consider to be the extremes of optimistic versus pessimistic geologic interpretations in the Medicine Bow area and how they would affect the present resource number (R) reported earlier.

TABLE 18

Possible optimistic geometry

Reclined folds	– –	2R
Buried Magnolia Formation	– –	2R

Most optimistic	– –	4R

Present geometry used

Inclined folds, no buried Magnolia Formation, mafic sills	– –	R

Most likely	– –	R

Most pessimistic geometry

Vertical mafic dikes	– –	.5R
Most pessimistic	– –	.5R

We believe our present interpretation is geologically most reason-able but other geologic interpretations could increase the estimate by a factor up to 4 times or decrease it by about one-half.

For the Sierra Madre area, geologic uncertainties in interpreting the structure of the Deep Gulch Formation of the Carrico Ranch area involve the subsurface projection of the unit. The unit maintains a fairly uniform overturned dip of about 50 degrees for a lateral distance of at least four miles and drill data indicate these dips remain uniform in the subsurface at least to depths of 500 - 1000 feet. Therefore, we have projected it farther, to depths of 5000 feet, in our reserve estimate.

However, the overturned beds are part of a large overturned reclined syncline, plunging west, which has only been partly defined; we have not found the equivalent beds in the upright limb of the syncline on the surface and we believe there are large reverse faults parallel to the

axial planes of the folds. As a consequence, it is possible that the mineralized unit is truncated at levels shallower than 5000 feet, (Figure 17B), decreasing the reserve estimate, or is repeated by folding, (Figure 17A), increasing the estimate. Figure 17 shows these two possibilities plus the interpretation used in our resource estimate (17C). The pessimistic interpretation could decrease the estimate by a factor of .2; the optimistic interpretation could increase the estimate by a factor of 2 or 3. The present, optimistic and pessimistic estimations for the Sierra Madre are summarized in Table 19.

TABLE 19

Optimistic	Present	Pessimistic
Repeated Folding-2 or 3R	Continuous Dip-R	Reverse Faulting-.2R
Most optimistic-2R to 3R	Most likely-R	Most Pessimistic-.2R

A quantitative statistical version of this geological uncertainty, as based on a careful consideration of the factors previously outlined is shown in Table 20.

Geologists Subjective Probability

Actual Resource	Sierra Madre Area	Medicine Bow Area
R/2	.15	.05
R	.75	.50
2R	.05	.25
3R	.05	.20
Expected Actual Resource	1.075R	1.625R

Table 20. Estimated (subjective) probabilities the actual resource is less or more than that derived from the geostatistical analysis.
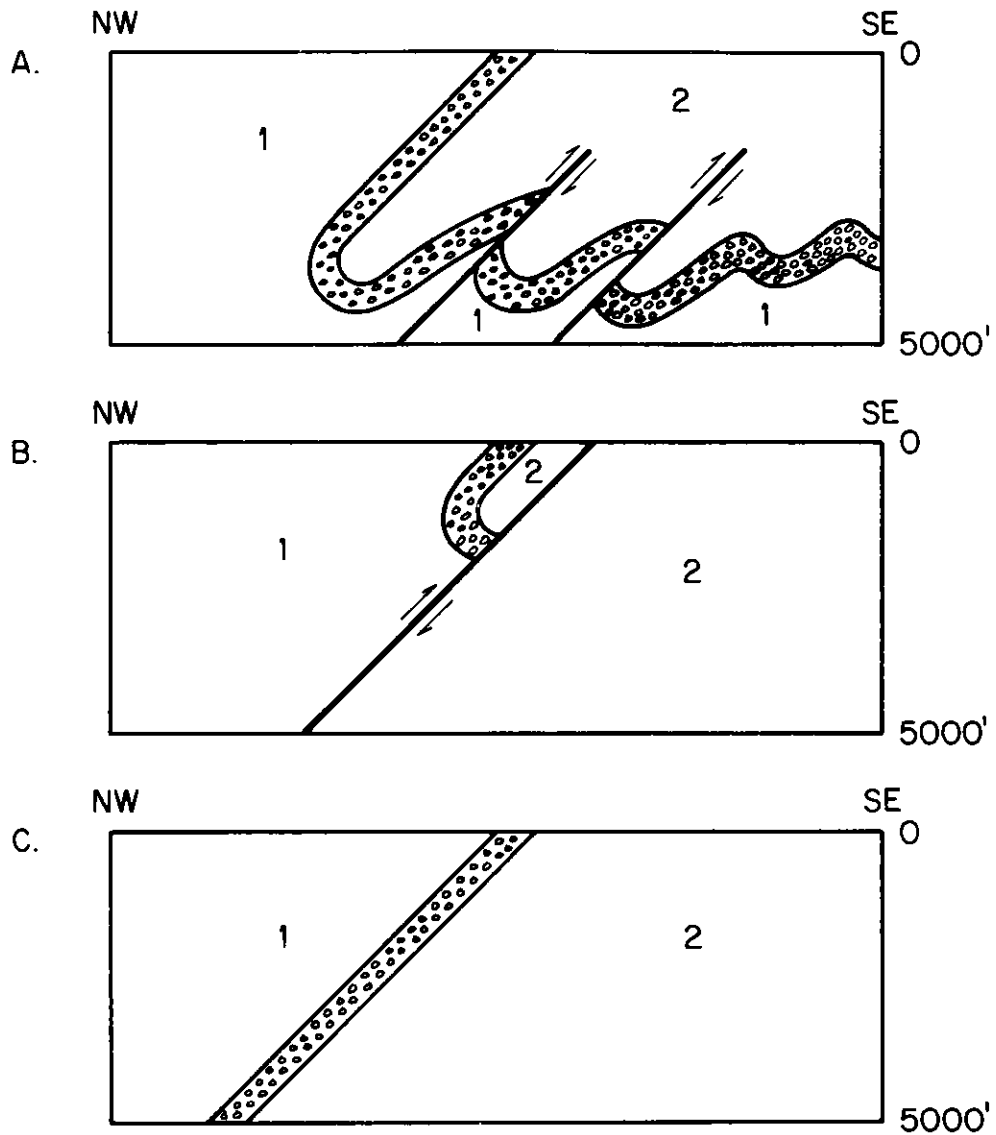
Figure 17. Optimistic (A), pessimistic (B) and favored (C) interpretations of the subsurface extent of the Deep Gulch Formation in the Northwest Sierra Madre. 1 = basement gneiss; $\underset{\circ}{\overset{\circ}{\circ}}\overset{\circ}{\circ}\circ$ = Deep Gulch Formation; 2 = quartzites and metavolcanic rocks of the Phantom Lake metamorphic Suite.

This may be interpreted in words as suggesting that geological judg-

ment gives very little chance for much more resource being found in

the Sierra Madre, but there may be as much as 62 percent more tonnage

than estimated in the Medicine Bow Mountains. This all is, of course,

very speculative but it does provide some measure of the geological

uncertainties involved in the interpretations.

SUMMARY AND CONCLUSIONS

1. The uranium endowment in Precambrian pebble conglomerate metased-
    iments in the Sierra Madre and Medicine Bow Mountains of south-
    eastern Wyoming was determined through an investigation which
    carefully coordinated geology with mining geostatistics.

2. The resource assessment consisted of four phases of activity.
    These were (a) a detailed geological study of the three-dimen-
    sional geometry of the uranium-bearing rocks, (b) the collection
    of samples from outcrop transects and drill core according to
    planned systematic geostatistical procedures, (c) the transfor-
    mation of the assay values to unleached equivalents, the develop-
    ment of resource estimates by kriging, and the reverse transfor-
    mation to leached uranium endowment, and (d) the integrated geo-
    logical and statistical interpretation of these results to pro-
    duce final resource estimates and error predictions.

3. Leaching was carefully studied so that the outcrop assay data
    could be converted to unleached equivalent U_3O_8 content and then
    be used to predict the uranium endowment at depth where little
    data was available. Leaching was found to be negligible at
    depths greater than 154 feet. The amount of leaching in outcrop
    samples was found to be somewhat less than that at 50 feet or so.

4. The geostatistical methodology used in the assessment is outlined
    in detail. The only trend found to be significant in the depos-
    its was that due to leaching. This nonstationarity was removed
    by transformation to equivalent unleached U_3O_8. The resulting

stationary regionalized variable was analyzed by a type of optimal weighed averaging called kriging. This produced estimates of the average accumulation over the test area and predictions of the probable error of these averages. The sampling was so designed that the kriging procedure reduced to ordinary arithmetic averaging. Upper bounds to the estimate error was determined by the kriging mathematics. Derivations of the mathematical formulas used are given in Appendix A.

5. As an interesting additional resource assessment, the endowment of thorium for exceedances of 100 ppm was also calculated for the study areas. The same geostatistical procedures were used, except that the leaching adjustment and reverse transformation was unnecessary.

6. The uranium endowment was computed as 442 tons $\pm$ 53% for the Deep Gulch Formation in the Sierra Madre, and as 3,418 tons $\pm$ 17% for the Magnolia Formation of the Medicine Bow Mountains. The corresponding thorium endowment was 6,353 tons $\pm$ 16% for the Sierra Madre and 1,996 tons $\pm$ 15% for the Medicine Bow Mountains. The errors stated here are probable errors. The actual error has a probability of 50% of being larger than this and 50% of being smaller. A 90% confidence interval would be 2.96 times this probable error.

7. The geological model used in the analysis involved subjective interpretations of the various sources of geological information. In general, the interpretations made were chosen to be slightly

conservative. A careful analysis of the amount the resource

might change under various alternative interpretations is out-

lined. The basic conclusions are presented in Tables 18, 19, and

20. In the Medicine Bows, under the most pessimistic interpreta-

tion the resource could be about half the value calculated in

the current investigation and under the most optimistic interpre-

tation, it might be four times larger than that calculated. Sim-

ilarly in the Sierra Madre, the most pessimistic interpretation

would yield a reduction by 80% of the current reserve estimation,

and the most optimistic version would increase the estimation up

to a factor of 3.

8. The relations developed from the study of leaching have signifi-

    cant bearing on various geological questions concerning the two

    areas. The substantial difference between the leaching relations

    suggest that mineralogical differences, age differences, deposi-

    tional history, or other factors may distinguish the two areas.

REFERENCES CITED

David, M., 1977, Geostatistical Ore Reserve Estimation, Elsevier, Amsterdam, 364 p.

Graff, P., 1979, A Review of the stratigraphy and uranium potential of early Proterozoic (Precambrian X) metasediments in the Sierra Madre, Wyoming: Contributions to Geology, v. 17, no. 2, p. 149-157.

Gumbel, E. J., 1954, Statistical theory of extreme values and some practical applications: Applied Math Series 33, National Bureau Standards, Washington, D. C.

Houston, R. S., and Karlstrom, K. E., 1980, Precambrian uranium-bearing quartz-pebble conglomerates: exploration model and United States resource potential: Bendix Field Engineering Corporation Open File Report CJBX (80-1), 510 p.

Journel, A. G. and Huljbregts, Ch., 1978, Mining Geostatistics, Academic Press, New York, 600 p.

Karlstrom, K. E. and Houston, R. S., 1979, Stratigraphy of the Phantom Lake Metamorphic Suite and Deep Lake Group and a review of the Precambrian tectonic history of the Medicine Bow Mountains: Contributions to Geology, v. 17, no. 2, p. 111-133.

APPENDIX A

Mathematical Derivations

APPENDIX - DERIVATIONS

Definition A-1

A radial, transitive variogram with elliptical zone of influence is defined as

$$\gamma(h_1, h_2) = \sigma^2 , \text{ for } h_1^2 + h_2^2 > h_o^2 (\theta) \tag{A-1}$$

and

$$\gamma(h_1, h_2) = a^2 \{1 - \exp[-(h_1^2 + h_2^2)/2 \; s^2(\theta)]\}$$

$$+ (\sigma^2 - a^2) \sqrt{h_1^2 + h_2^2} / h_o(\theta), \tag{A-2}$$

for $h_1^2 + h_1^2 \leq h_o^2 (\theta)$,

where

$$\theta = \text{arc tan } (h_2/h_1) \tag{A-3}$$

$$s^2(\theta) = A^2 B^2 / [A^2 \sin^2(\theta - \psi) + B^2 \cos^2(\theta - \psi)] \tag{A-4}$$

$$h_o^2(\theta) = a^2 b^2 / [a^2 \sin^2(\theta - \phi) + b^2 \cos^2(\theta - \phi)] \tag{A-5}$$

and $s(\theta)$ is small compared with the scale of measurement of h_1, and h_2. Both $s(\theta)$ and $h_o(\theta)$ define ellipses with long axes in the ψ and ϕ angular directions in (h_1, h_2) space.

The covariance function corresponding to this variogram is zero for $h_1^2 + h_2^2 > h_o^2 (\theta)$ and

$$C(h_1, h_2) = a^2 \exp[-(h_1^2 + h_2^2)/2s^2(\theta)]$$

$$+ (\sigma^2 - a^2) [1 - \sqrt{h_1^2 + h_2^2}/h_o(\theta)] \tag{A-6}$$

for $h_1^2 + h_2^2 \leq h_o^2(\theta)$.

Definition A-2

Let $V(x, y)$ be some resource variable of economic interest at location (x, y). Let B specify some area within which the average value of $V(x, y)$, denoted by $\overline{V}_B$, is of importance.
Stated in formulas

$$\overline{V}_B = (1/B) \int_B\!\int V(x, y) \, dx \, dy \tag{A-7}$$

where B is also interpreted as the area of B where that is appropriate. The expression, $V(x, y)$, will be considered a stationary random function with variogram $\gamma(h_1, h_2)$, covariance $C(h_1, h_2)$, and mean μ.

Theorem A-3

The theoretical mean of $\overline{V}_B$ is given by

$$\sigma_B^2 = \text{Variance } [\overline{V}_B] = (1/B)^2 \int_B\!\int \int_B\!\int C(x-x', y-y') \, dx \, dy \, dx' \, dy'. \tag{A-8}$$

Proof

$$E[\overline{V}_B] = E[(1/B) \int_B\!\int V(x, y) \, dx \, dy]$$

$$= (1/B) \int_B\!\int \mu \, dx \, dy = \mu. \tag{A-9}$$

$$\text{Variance } [\overline{V}_B] = E[\{(1/B) \int_B\!\int V(x, y) \, dx \, dy - \mu\}^2]$$

$$= E[(1/B)^2 \int_B\!\int \int_B\!\int \{V(x, y)-\mu\}\{V(x', y')-\mu\} \, dx \, dy \, dx' \, dy']$$

$$= (1/B)^2 \int_B\!\int \int_B\!\int C(x-x', y-y') \, dx \, dy \, dx' \, dy'. \tag{A-10}$$

Definition A-4

Suppose that the value of $V(x, y)$ is known by sampling at the points (x_1, y_1), (x_2, y_2), ..., (x_n, Y_n). A reasonable estimate $\hat{\bar{V}}_B$ of the quantity $\bar{V}_B$ is provided by a linear combination of the sample values

$$\hat{\bar{V}}_B = \sum_{i=1}^{n} a_i \, V(x_i, y_i). \tag{A-11}$$

It seems reasonable to require that $\hat{\bar{V}}_B$ be an unbiased estimate. This condition implies that

$$\sum_{i=1}^{n} a_i = 1.0 \tag{A-12}$$

because

$$\mu = E[\hat{\bar{V}}_B] = \sum_{i=1}^{n} a_i \, E[V(x_i, y_i)] = \sum_{i=1}^{n} a_i \mu. \tag{A-13}$$

Theorem A-5 (David, 1977; Journel and Huljbregts, 1978)

The constants $\hat{a}_i$; $i = 1, 2, \ldots, n$, which minimize the estimation error variance, σ_E^2, defined by

$$\sigma_E^2 = E[(\hat{\bar{V}}_B - \bar{V}_B)^2], \tag{A-14}$$

subject to the side condition

$$\sum_{i=1}^{n} \hat{a}_i = 1.0 \tag{A-15}$$

are the solution to the matrix equation

$$\begin{bmatrix} C_{11} & C_{12} & C_{13} & \cdots & C_{1n} & 1 \\ C_{21} & C_{22} & C_{23} & \cdots & C_{2n} & 1 \\ C_{31} & C_{32} & C_{33} & \cdots & C_{3n} & 1 \\ \cdot & \cdot & \cdot & & \cdot & \cdot \\ \cdot & \cdot & \cdot & & \cdot & \cdot \\ \cdot & \cdot & \cdot & & \cdot & \cdot \\ C_{n1} & C_{n2} & C_{n3} & \cdots & C_{nn} & 1 \\ 1 & 1 & 1 & \cdots & 1 & 0 \end{bmatrix} \times \begin{bmatrix} \hat{a}_1 \\ \hat{a}_2 \\ \hat{a}_3 \\ \cdot \\ \cdot \\ \cdot \\ \hat{a}_n \\ \hat{u} \end{bmatrix} = \begin{bmatrix} C_{B1} \\ C_{B2} \\ C_{B3} \\ \cdot \\ \cdot \\ \cdot \\ C_{Bn} \\ 1 \end{bmatrix} \qquad (A-16)$$

where

$$C_{ij} = C(x_i - x_j, \ y_i - y_j) \qquad (A-17)$$

and

$$C_{Bi} = (1/B) \int_B\!\int C(x - x_i, \ y - y_i) \ dx \ dy \qquad (A-18)$$

An estimate of the estimation error variance is given by

$$\hat{\sigma}_E^2 = C_{BB} - \sum_{i=1}^{n} \hat{a}_i \ C_{Bi} - \hat{u} \qquad (A-19)$$

where

$$C_{BB} = \sigma_B^2 \qquad (A-20)$$

defined in (A-3).

Proof

By the method of Lagrangian multipliers, $\hat{a}_i$, will be the result of minimizing Q where

$$Q = \sigma_E^2 + 2u\left(\sum_{i=1}^{n} a_i - 1.0\right) \qquad (A-21)$$

with the added condition that

$$\sum_{i=1}^{n} a_i = 1.0.$$

(A-22)

Now

$$Q = E\left[\left\{\sum_{i=1}^{n} a_i V(x_i, y_i) - (1/B) \int_B \!\! \int V(x, y)\ dx\ dy\right\}^2\right]$$

$$+ 2u\left(\sum_{i=1}^{n} a_i - 1.0\right)$$

$$= E\left[\left\{\sum_{i=1}^{n} a_i <V(x_i, y_i)-\mu> - (1/B \int_B \!\! \int < V(x, y)-\mu>dx\ dy\right\}^2\right]$$

$$+ 2u\left(\sum_{i=1}^{n} a_i - 1.0\right)$$

$$= \sum_{i=1}^{n} \sum_{j=1}^{n} a_i a_j C_{ij} - 2 \sum_{i=1}^{n} a_i\ C_{Bi} + C_{BB}$$

$$+ 2u\left(\sum_{i=1}^{n} a_i - 1.0\right).$$

(A-23)

Consequently

$$\frac{\partial Q}{\partial a_k} = 2\sum_{i=1}^{n} a_i C_{ki} - 2C_{Bk} + 2u.$$

(A-24)

If $\hat{a}_i$ and $\hat{u}_i$ are the values which make $\partial Q/\partial a_k = 0$, then

$$\sum_{i=1}^{n} C_{ki}\ \hat{a}_j + \hat{u} = C_{Bk}$$

(A-25)

for $K = 1, 2, \ldots, n$. This system of simultaneous equations corresponds to the matrix equation stated in the theorem.

The value of Q when $\hat{a}_i$ and $\hat{u}$ are substituted into the formula gives a reasonable estimate of σ_E^2 as

$$\hat{\sigma}_E^2 = \sum_{i=1}^{n} \sum_{j=1}^{n} \hat{a}_i \hat{a}_j C_{ij} - 2 \sum_{i=1}^{n} \hat{a}_i C_{Bi} + C_{BB} \, . \tag{A-26}$$

This formula can be simplified by multiplying both sides of eq. (A-25) by $\hat{a}_k$ and summing over $k=1, 2, \ldots, n$.
This gives

$$\sum_{k=1}^{n} \sum_{i=1}^{n} C_{ki} \hat{a}_i \hat{a}_k + \hat{u} \sum_{k=1}^{n} \hat{a}_k = \sum_{k=1}^{n} \hat{a}_k C_{Bk} \, . \tag{A-27}$$

Since $\sum_{k=1}^{n} \hat{a}_k = 1.0$, the previous equation can be substituted into eq. (A-26) to yield

$$\hat{\sigma}_E^2 = C_{BB} - \sum_{i=1}^{n} \hat{a}_i C_{Bi} - \hat{u} \, . \tag{A-28}$$

Theorem A-6

Suppose that

$$C_{ij} = \begin{cases} \sigma^2, & \text{if } i=j \\ 0, & \text{if } i \neq j \end{cases} \tag{A-29}$$

and that the indices $i = 1, 2, \ldots, n$ can be divided into two sets, $S_1 = \{i; \ 1 \leq i \leq m\}$ and $S_2 = \{i; \ m < i \leq n\}$ such that

$$C_{Bi} \neq 0 \quad , \text{ if } i \in S_1 \tag{A-30}$$

$$C_{Bi} = 0 \quad , \text{ if } i \in S_2 \tag{A-31}$$

where the symbol "ϵ" should be read as "belongs to". That is samples more than a zone of influence away have subscripts in S_2, while those within a zone of influence of the block being estimated will have subscripts in S_2.

Under these assumptions, the solution to the martix equation in A-5 is

$$\hat{a}_i = \begin{cases} (1/n) + C_{Bi}/\sigma^2 - \sum_{k=1}^{m} C_{Bk}/n\sigma^2, & \text{if } i \in S_1 \\ (1/n) - \sum_{k=1}^{m} C_{Bk}/n\sigma^2, & \text{if } i \in S_2 \end{cases} \qquad \text{(A-32)}$$

$$\hat{u} = (1/n) \sum_{k=1}^{m} C_{Bk} - \sigma^2/n \qquad \text{(A-33)}$$

and

$$\sigma_E^2 = \sigma^2/n + C_{BB} - (2/n) \sum_{k=1}^{m} C_{Bk} - \sum_{k=1}^{m} C_{Bk}^2/\sigma^2$$

$$+ \left(\sum_{k=1}^{m} C_{Bk} \right)^2/n\sigma^2. \qquad \text{(A-34)}$$

Proof

The inverse of

$$\begin{bmatrix} \sigma^2 & 0 & 0 & \ldots & 0 & 1 \\ 0 & \sigma^2 & 0 & \ldots & 0 & 1 \\ 0 & 0 & \sigma^2 & \ldots & 0 & 1 \\ \cdot & \cdot & \cdot & & \cdot & \cdot \\ \cdot & \cdot & \cdot & & \cdot & \cdot \\ \cdot & \cdot & \cdot & & \cdot & \cdot \\ 0 & 0 & 0 & \ldots & \sigma^2 & 1 \\ 1 & 1 & 1 & \ldots & 1 & 0 \end{bmatrix}$$

is

$$\frac{1}{n\sigma^2} \begin{bmatrix} n-1 & -1 & -1 & \cdots & -1 & \sigma^2 \\ -1 & n-1 & -1 & \cdots & -1 & \sigma^2 \\ -1 & -1 & n-1 & \cdots & -1 & \sigma^2 \\ \cdot & \cdot & \cdot & & \cdot & \cdot \\ \cdot & \cdot & \cdot & & \cdot & \cdot \\ \cdot & \cdot & \cdot & & \cdot & \cdot \\ -1 & -1 & -1 & \cdots & n-1 & \sigma^2 \\ \sigma^2 & \sigma^2 & \sigma^2 & & \sigma^2 & -\sigma^4 \end{bmatrix} .$$

The theorem then follows from theorem A-5.

Theorem A-7

For the variogram in Definition (A-1), assuming $s(\theta)$ is small enough so that the exponential can be ignored,

$$0 \le C_{Bi} \le \pi ab \ (\sigma^2 - a^2)/3B; \tag{A-35}$$

$$C_{BB} < \pi ab \ (\sigma^2 - a^2)/3B. \tag{A-36}$$

An upper bound for $\hat{\sigma}_E^2$, providing C_B/σ^2 is negligible, is

$$\hat{\sigma}_E^2 < (\sigma^2/n) + \pi ab(\sigma^2 - a^2)/3B. \tag{A-37}$$

Proof

If the elliptical base for the variogram is entirely enclosed within B, then

$$\int_B\!\!\int C(x - x', \ y - y') \ dx \ dy = \pi ab(\sigma^2 - a^2)/3. \tag{A-38}$$

The rest of the relations follow from theorem A-6.

105

107

Table B-1

SUMMARY OF AREAS PER DEPTH INTERVAL FOR SIERRA MADRE

Unit 3: Strike Length = 23615 feet

Segment	Av. El.	Area per depth interval (sq. ft.)										
		0-100	100-200	200-300	300-400	400-500	500-1000	1000-1500	1500-2000	2000-3000	3000-4000	4000-5000
Carrico Ridge #1	7685	282523	331775	331775	331775	0	1094512	1824187	1824187	3648375	3648375	3648375
Inferred Geometry A, Between Carrico Ridge #1 and #2	7670	104708	170085	170085	170085	170085	850454	850454	840454	1700908	1700908	1700908
Inferred Geometry B, Between Corrico Ridge #1 and #2	7772	107744	123165	123165	123165	123165	615804	615804	615804	1231692	1231692	1231692
Carrico Ridge #2	7870	104739	95306	95306	95306	95306	476547	476547	476547	953095	953095	953095
Inferred Geometry Between Carrico Ridge #2 and #3	7883	100695	115322	115322	115322	115322	576286	576286	576286	1152573	1152573	1152573
Carrico Ridge #3	7957	104839	93545	93545	93545	93545	467725	467725	467725	935450	935450	935450
Inferred Geometry Between Carrico Ridge #3 and Fault	7855	130625	165625	165625	165625	165625	828125	828125	828125	1656250	1656250	1656250
Deep Gulch #5	7762	342428	242598	242598	242598	242598	1212863	1212863	1212863	2425726	2425726	2425726
Deep Gulch #4	7805	26972	30525	30525	30525	30525	152600	152600	152600	305200	305200	305200
Deep Gulch #3A	7821	150625	158618	158618	158618	158618	793030	793030	793030	1586061	1586061	1586061
Deep Gulch #3B	8003	119730	86163	86163	86163	86163	430782	430782	430782	861564	861564	861564
Inferred Geometry Deep Gulch #2	8041	163125	163187	163187	163187	163187	815875	815875	815875	1631750	1631750	1631750
Deep Gulch #1	7987	152073	132232	132232	132232	132232	661138	661138	661138	1322277	1322277	1322277
Inferred Geometry Between Deep Gulch #1 and Manning Ridge #1	7948	552875	583406	583406	583406	583406	2916937	2916937	2916937	5833875	5833875	5833875
Manning Ridge #1	7960	146616	112014	112014	112014	112014	560088	560088	560088	1120176	1120176	1120176
Inferred Geometry Between Manning Ridge #1 and #2	7849	193737	194459	194459	194459	194459	972262	972262	972262	1944525	1944525	1944525
Manning Ridge #2A	7977	103664	81983	81983	81983	81983	410118	410118	410118	820236	820236	820236
Manning Ridge #2B	7977	11422	97583	97583	97583	97583	487899	487899	487899	975798	975798	975798
Inferred Geometry Between Manning Ridge #2 and #3	7962	169446	196581	196581	196581	196581	982869	983869	982869	1965738	1965738	1965738
Manning Ridge #3	8060	44549	44549	44549	44549	44549	222736	222736	222736	445473	445473	445473
Inferred Geometry Between Manning Ridge #3 and Fault	7995	127130	141425	141425	141425	141425	707100	707100	707100	1414200	1414200	1414200
Total Area for Intervals		3343065	3360148	3360148	3360148	3028373	16235753	16965428	16965428	33930942	33930942	33930842
Cumulative Area		3343065	6703213	10063361	13423509	16451882	32687635	49653064	66618492	100549434	134480376	168411318

Carrico Ridge # I. Width=2875'

Transect # 1
Transect # 2
Transect # 3
Transect # 4
Transect # 5

SM-2 ⊙ 100

End of Rotated Block

0'—
202.5'
100
0' 550.0'
1000 380.7'
1000'
2000 1549.7'
2000'
3000 2916.7'
3000'
4000 4187.7'
4000'
5000'
5000 5456.8'

Inferred Geometry, A, Between Carrico Ridge # I and # 2. Width =1160'

0'
100 171.6'
500 758.1'
1000'
1000 1491.2'
2000'
3000' 2000 2957.5'
4000'
3000 4423.8'
5000'
4000 5890.1'
6000'
7000'
5000 7356.4'

Sierra Madre Unit # 3

Figure B-1

109
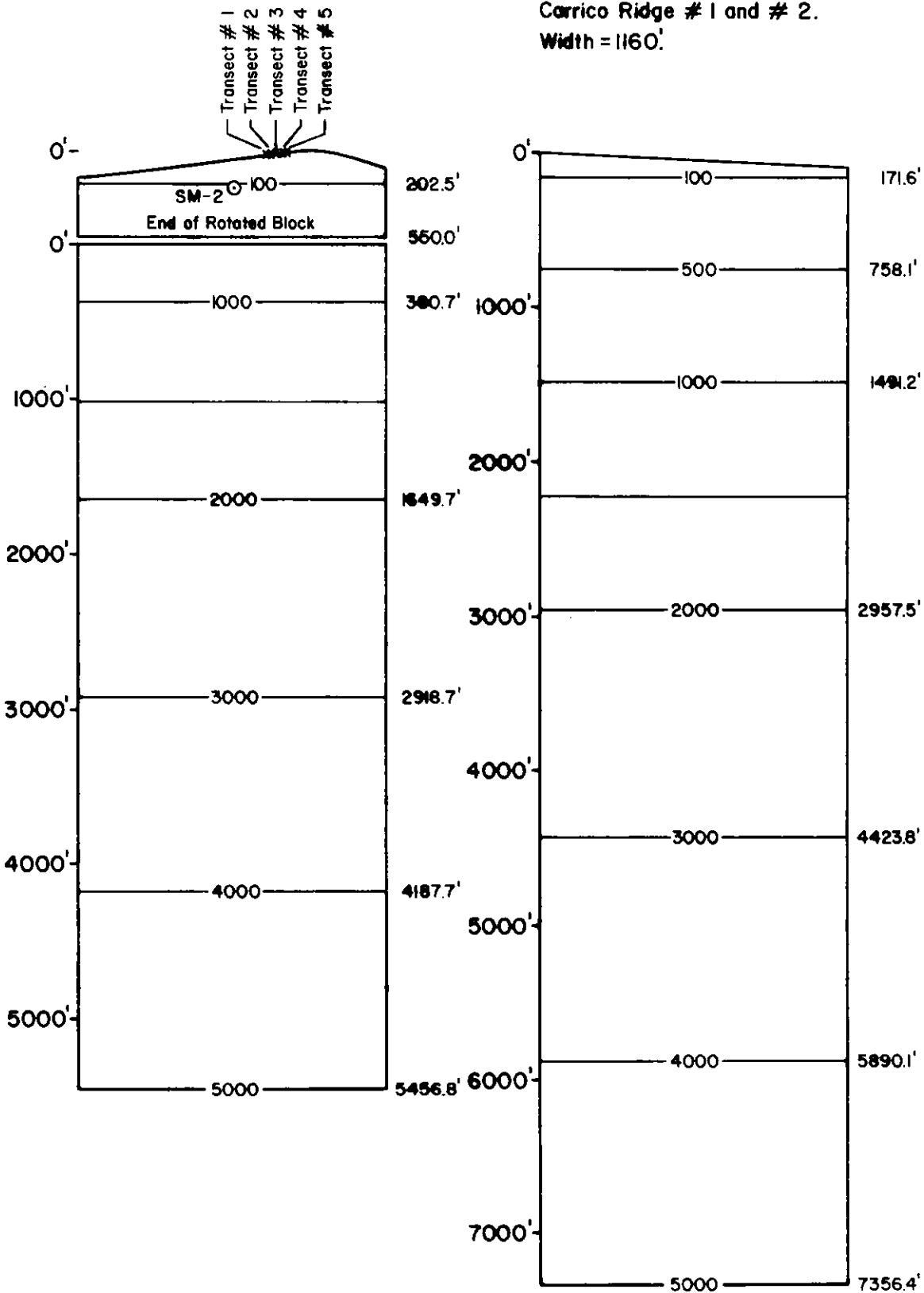
Inferred Geometry, B, Between Carrico Ridge # 1 and # 2. Width = 840'

Depth	Value
0'	
100	246.6'
500	833.1'
1000	1566.2'
2000	3032.5'
3000	4498.8'
4000	5965.1'
5000	7431.4'

Carrico Ridge # 2. Width = 650'

Transect # 9, Transect # 8, Transect # 7, Transect # 6

SM-1
SM-1A

Depth	Value
0'	
100	190.6'
500	777.1'
1000	1510.2'
2000	2976.5'
3000	4442.8'
4000	5909.1'
5000	7375.4'
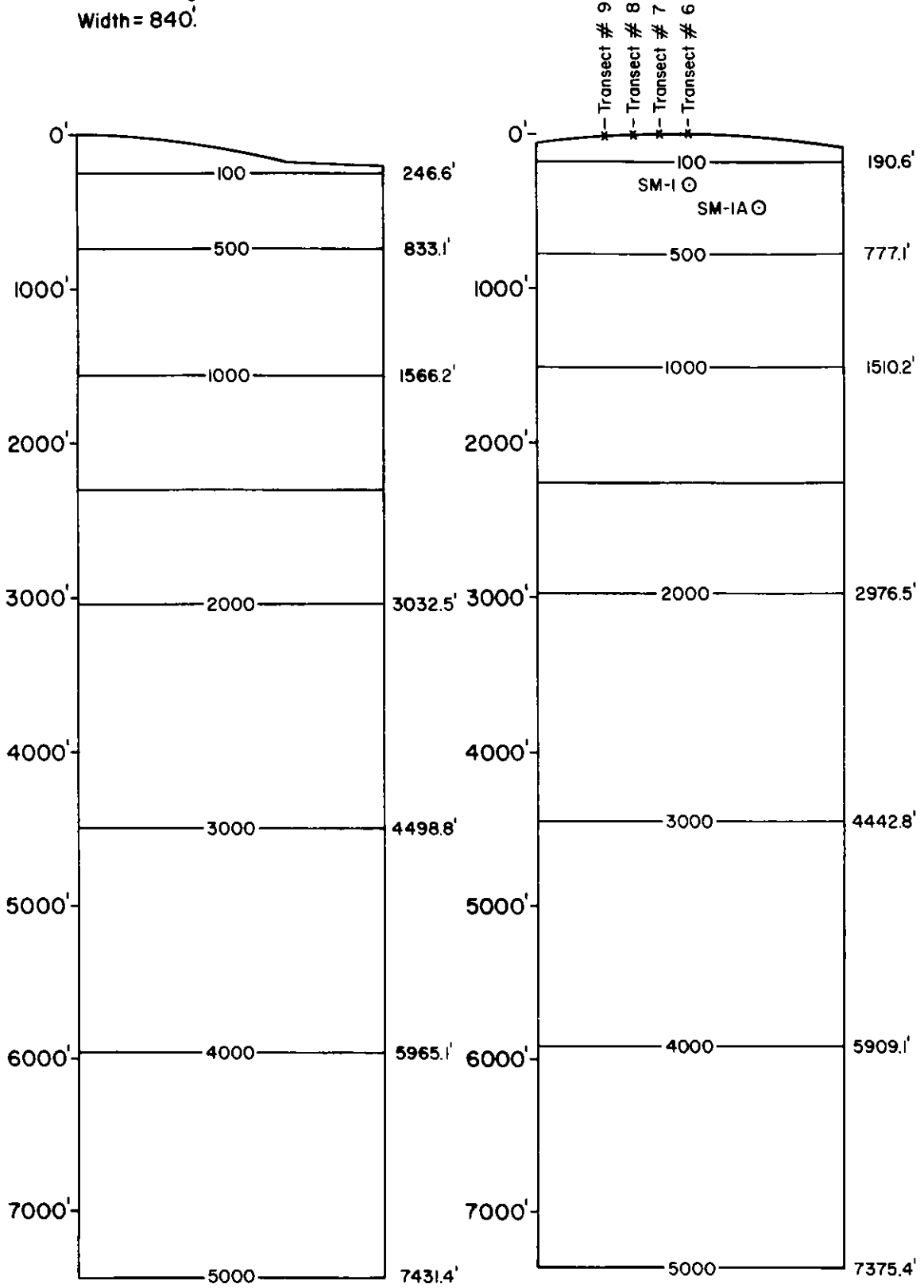
Sierra Madre Unit # 3

Figure B-2

110

Inferred Geometry Between Carrico Ridge # 2 and # 3. Width = 815'

Depth	Value
100	191.1'
500	757.1
1000	1464.2'
2000	2878.4'
3000	4292.6'
4000	5706.8'
5000	7121.6'
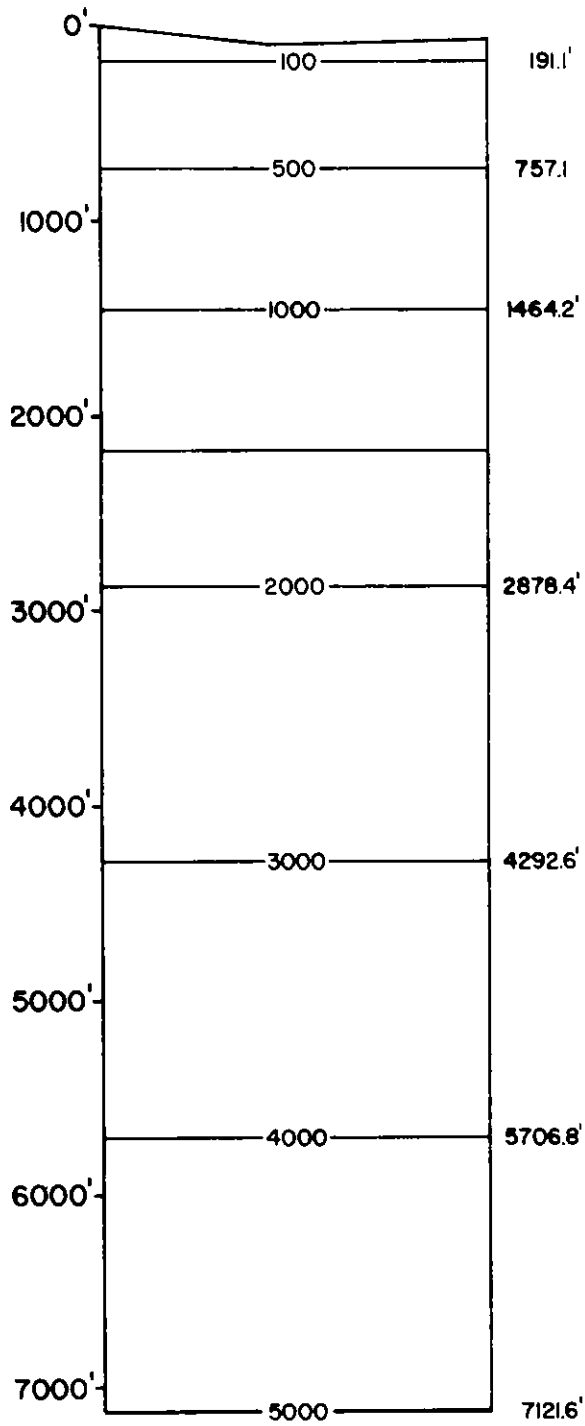
Carrico Ridge # 3. Width = 706'

Transect # 12 Transect # 11 Transect # 10

Depth	Value
100	195.5'
500	725.5'
1000	1388.0'
2000	2713.0'
3000	4038.0'
4000	5363.0'
5000	5688.0'
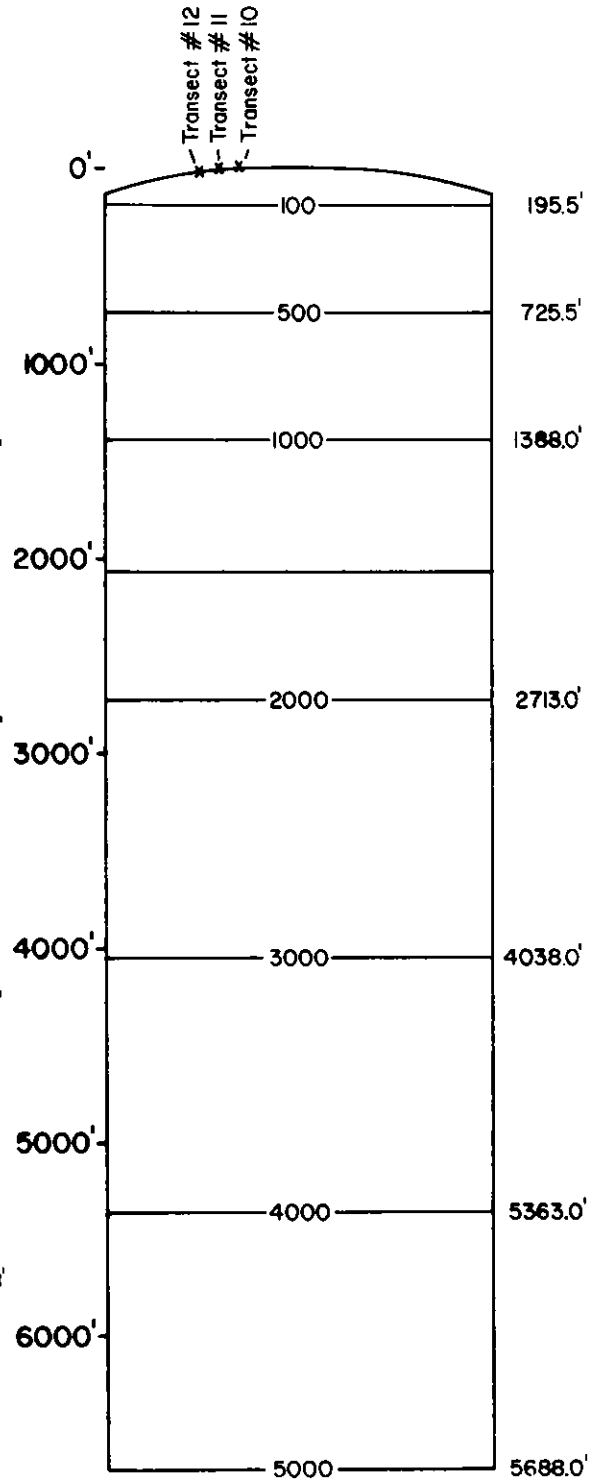
Sierra Madre Unit # 3

Figure B-3

Inferred Geometry Between
Carrico Ridge # 3 and fault.
Width = 1250'
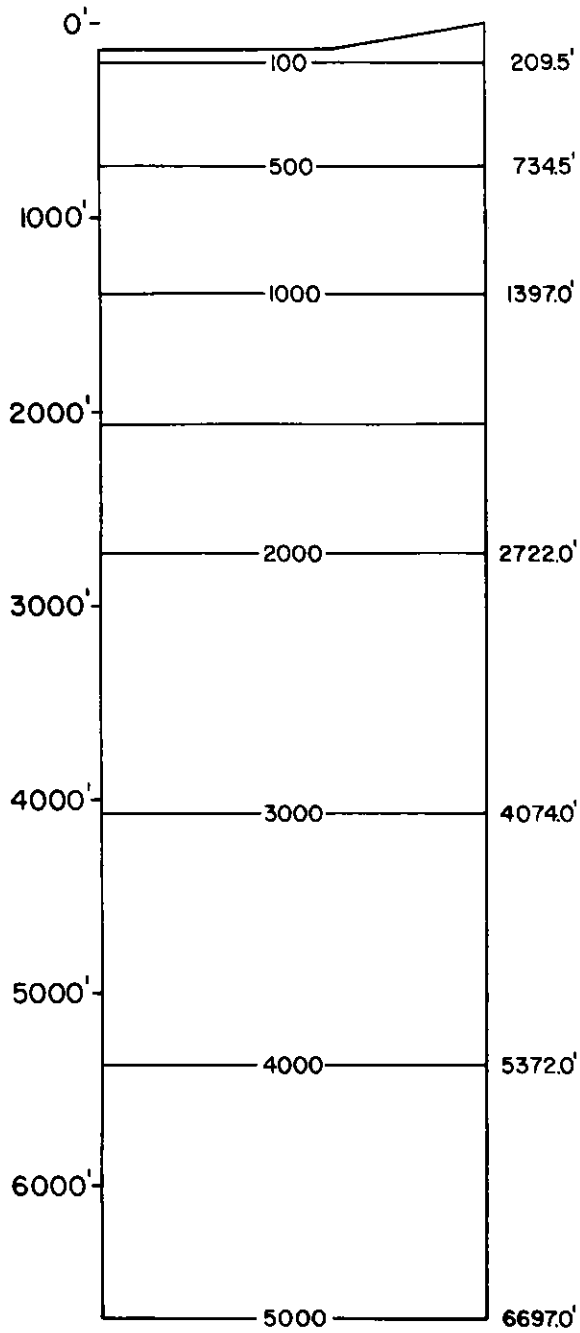
Deep Gulch # 5. Width = 1685'
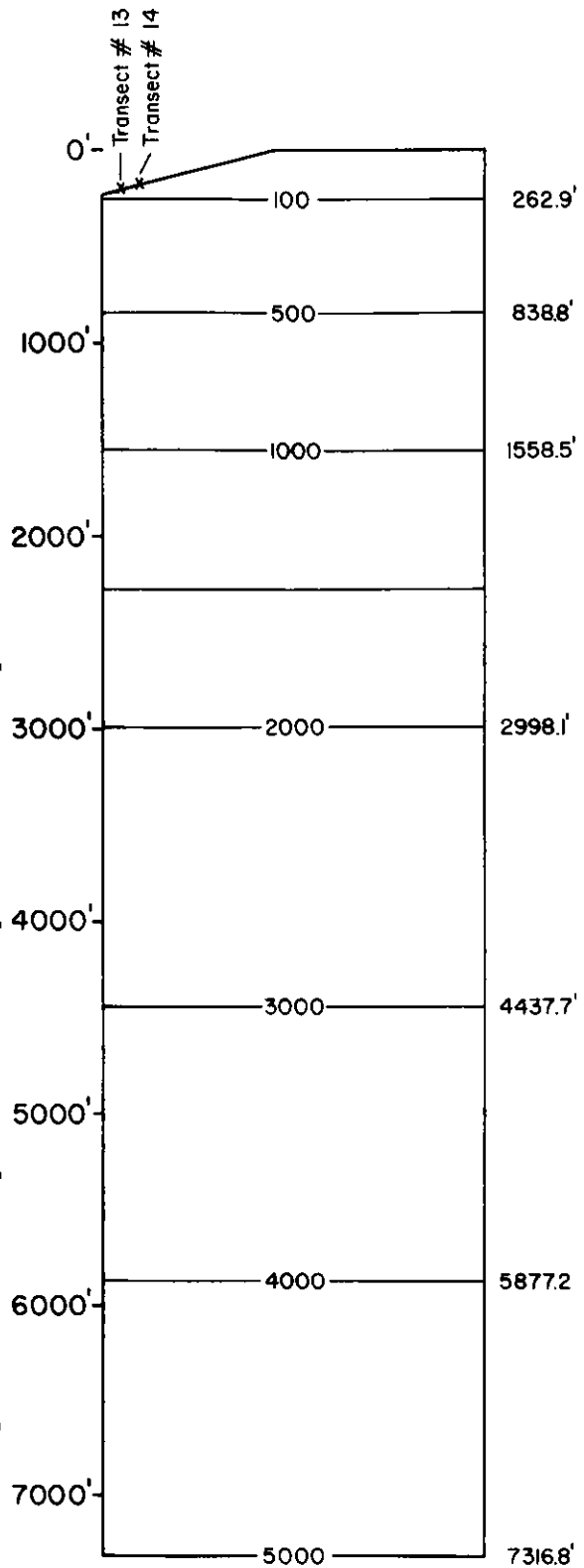
Sierra Madre Unit # 3
Figure B-4

Deep Gulch # 4. Width = 250'

Deep Gulch # 3A. Width = 1215'
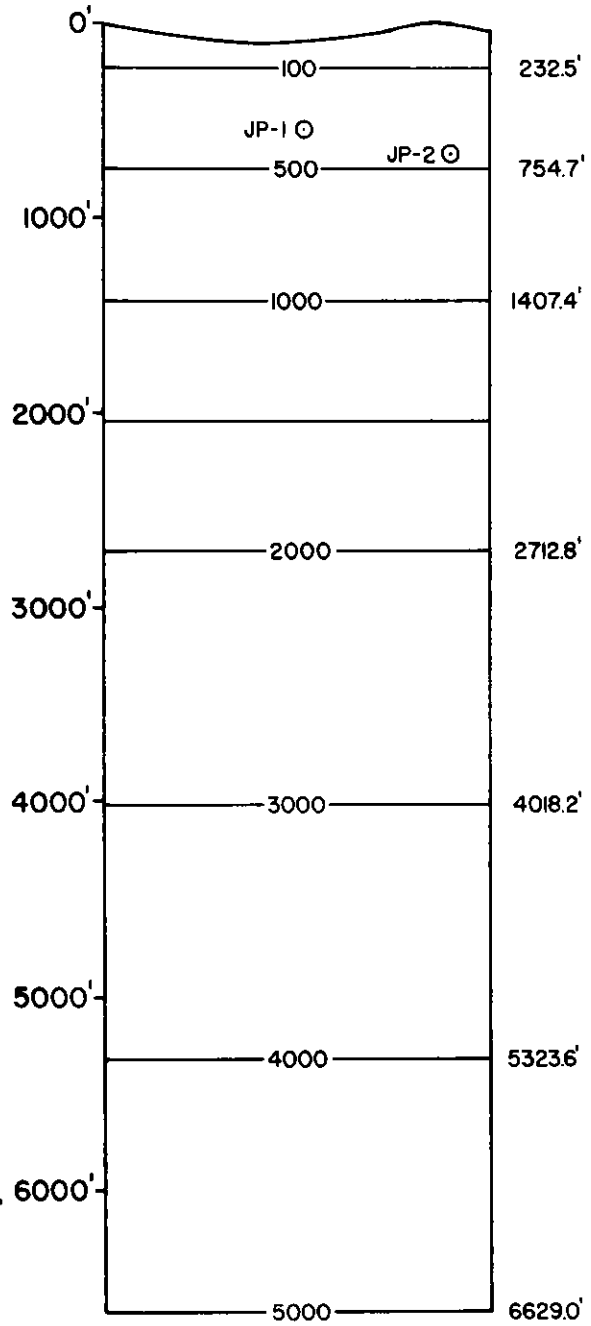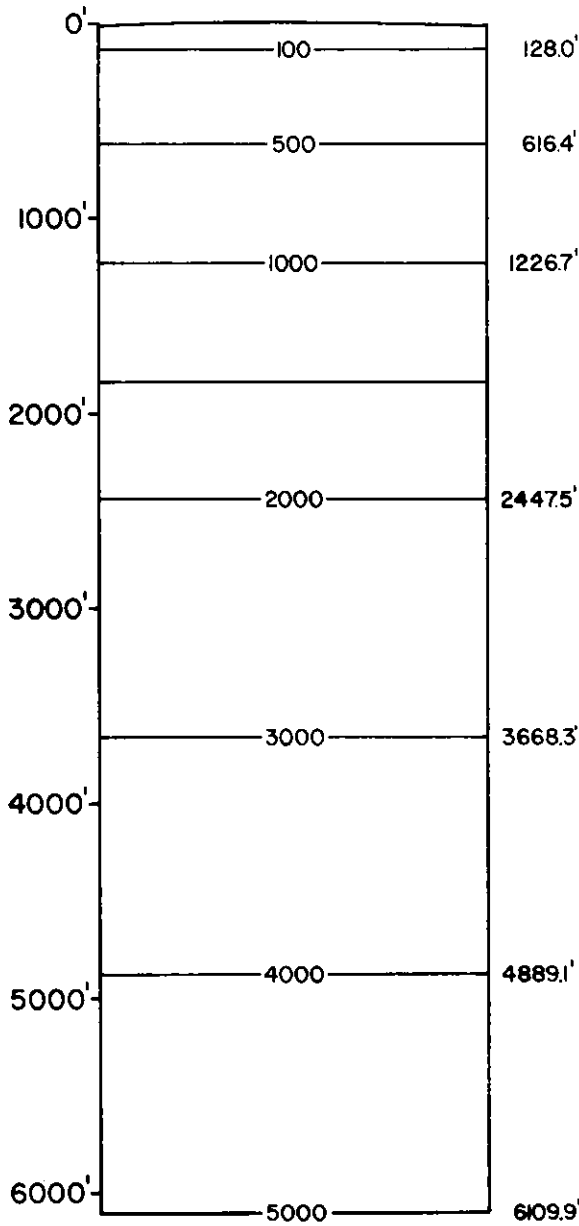
Sierra Madre Unit # 3

Figure B-5

Deep Gulch # 3B. Width 660'
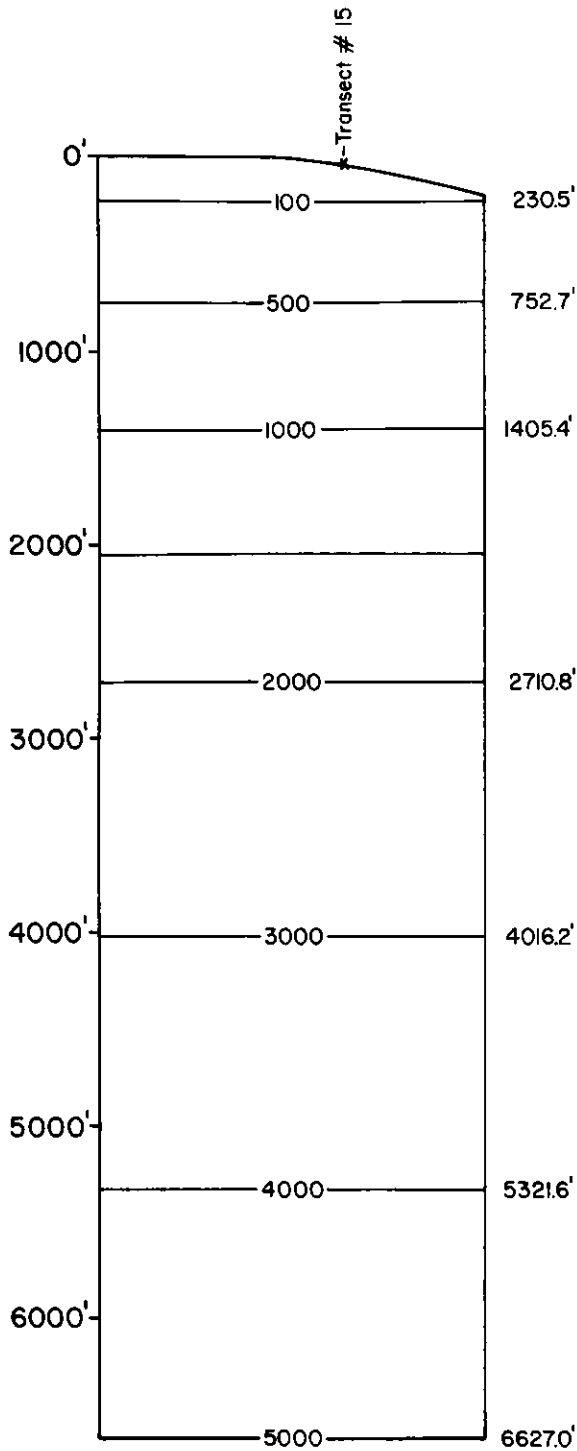
Inferred Geometry, Deep Gulch
2. Width = 1250'

x—Transect # 15

Deep Gulch # 3B	Inferred Geometry
0'	0'
100 — 230.5'	100 — 155.6'
500 — 752.7'	500 — 677.7'
1000'	1000'
1000 — 1405.4'	1000 — 1330.4
2000'	2000'
2000 — 2710.8'	2000 — 2635.8'
3000'	3000'
3000 — 4016.2'	3000 — 3941.2'
4000'	4000'
5000'	5000'
4000 — 5321.6'	4000 — 5246.0'
6000'	6000'
5000 — 6627.0'	5000 — 6552.0'
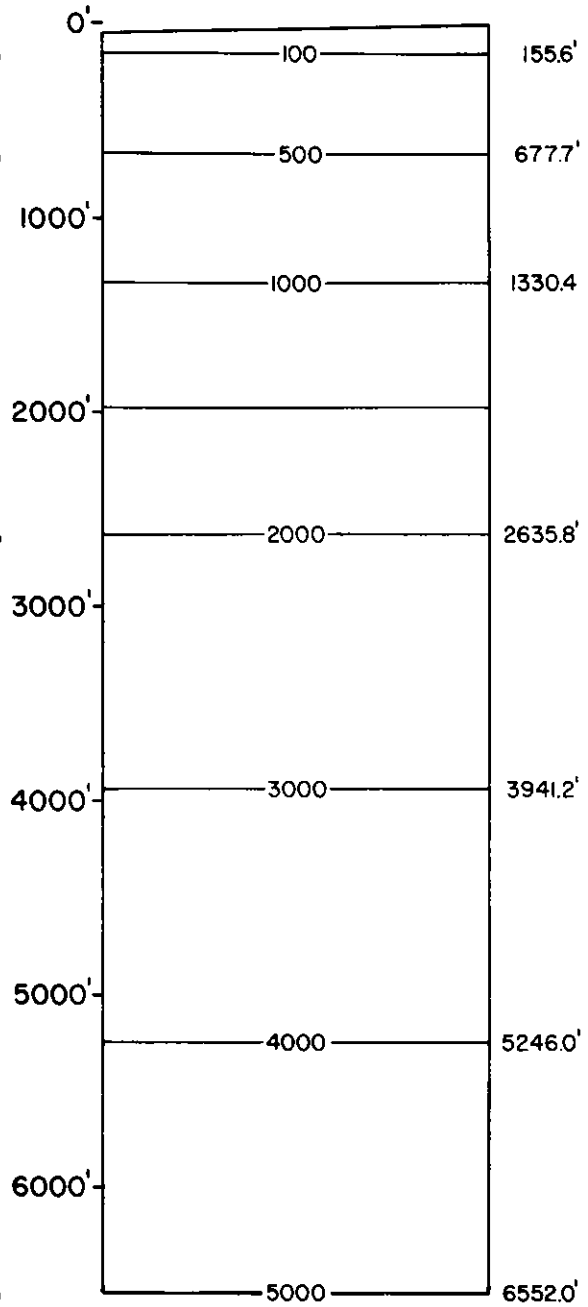
Sierra Madre Unit # 3

Figure B-6

Deep Gulch # I. Width = 935.'
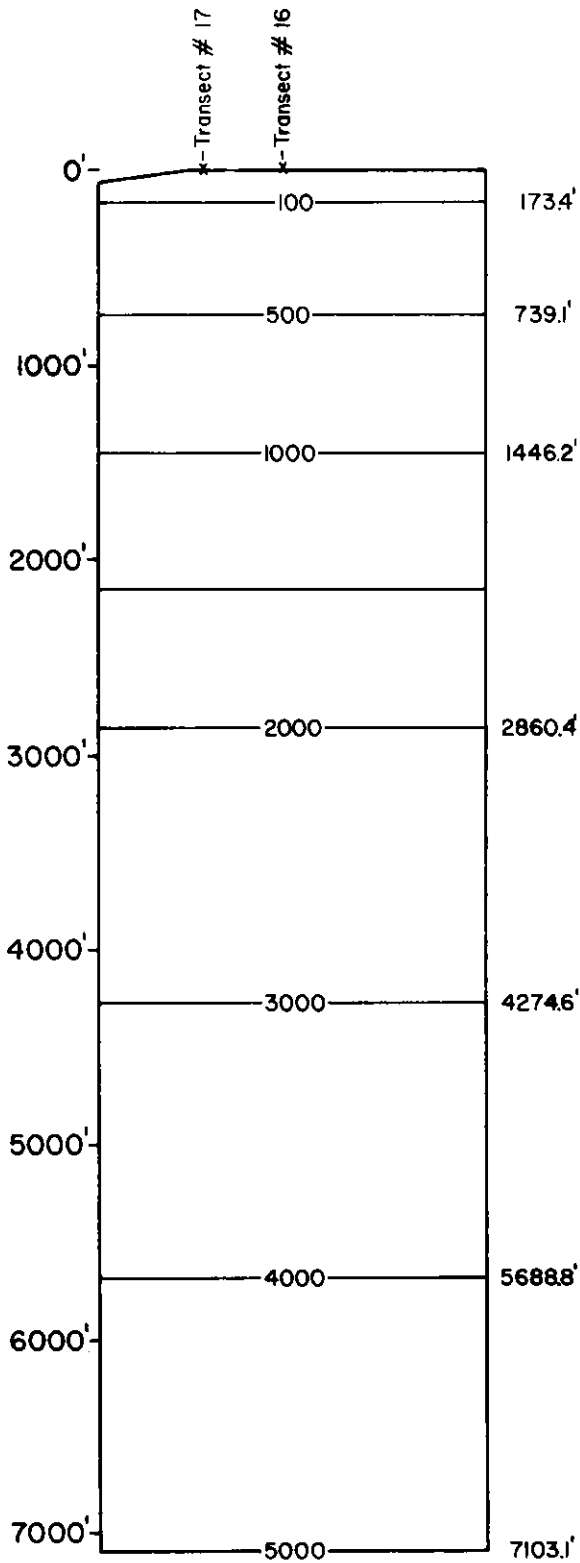
Inferred Geometry Between
Deep Gulch # I and Manning
Ridge # I. Width = 3750.'
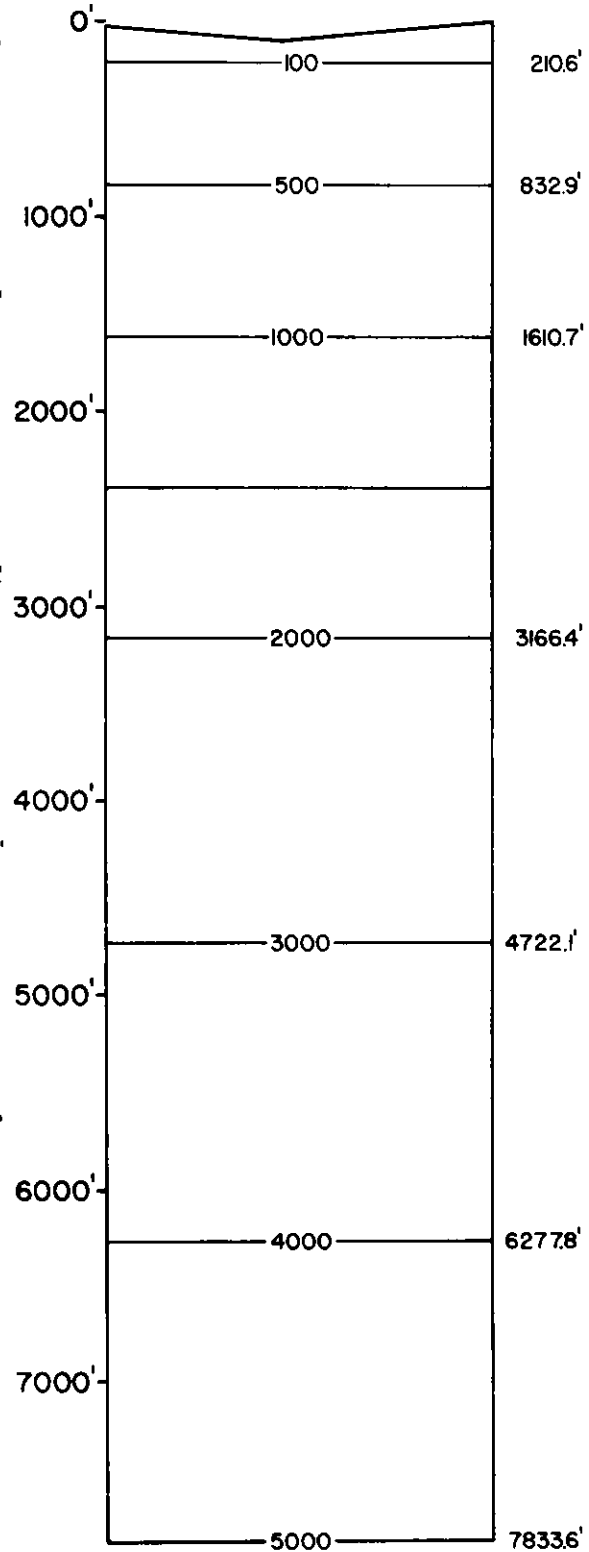
Sierra Madre Unit # 3

Figure B-7

115

Manning Ridge #1. Width=720.'

Transect #20
Transect #19
Transect #18

0'
100 — 217.6'
JP-4 ⊙
500 — 839.9'
1000'
1000 — 1617.7'
2000'
3000'
2000 — 3173.4'
4000'
5000'
3000 — 4729.2'
6000'
4000 — 6284.9'
7000'
5000 — 7840.6'
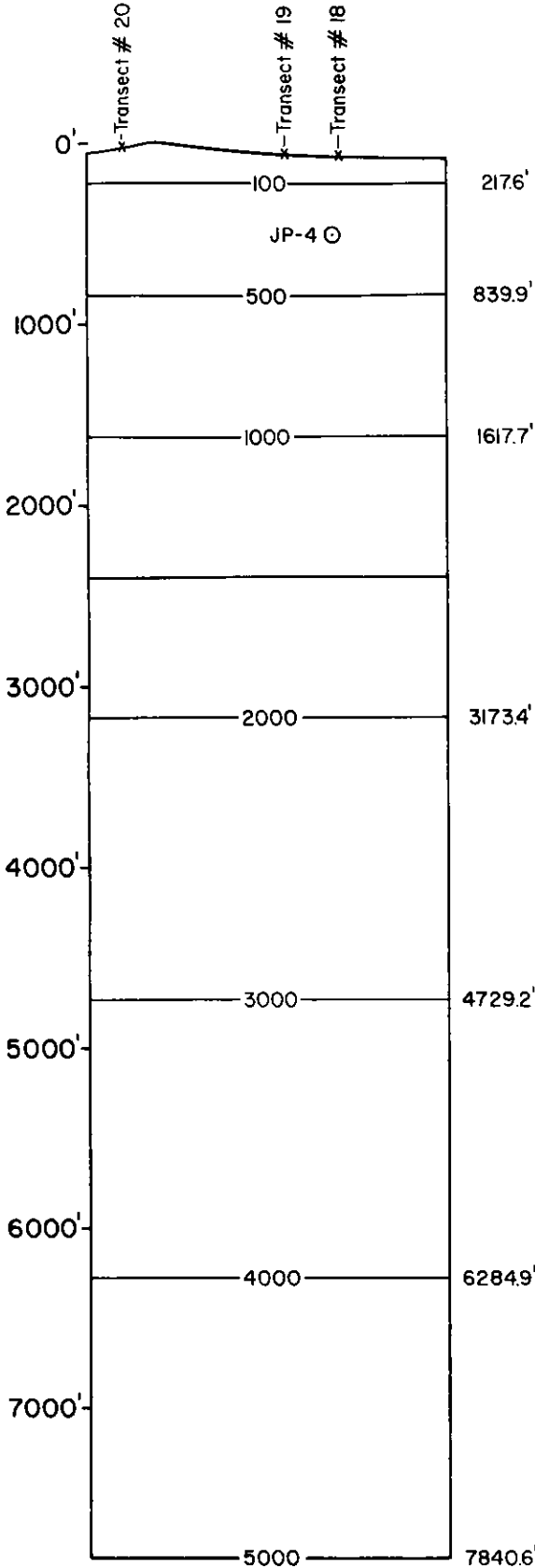
Inferred Geometry Between
Manning Ridge #1 and #2.
Width=1375.'

0'
100 — 248.4'
500 — 814.1'
1000'
1000 — 1521.2'
2000'
3000'
2000 — 2935.4'
4000'
3000 — 4349.6'
5000'
4000 — 5763.8'
6000'
7000'
5000 — 7178.0'
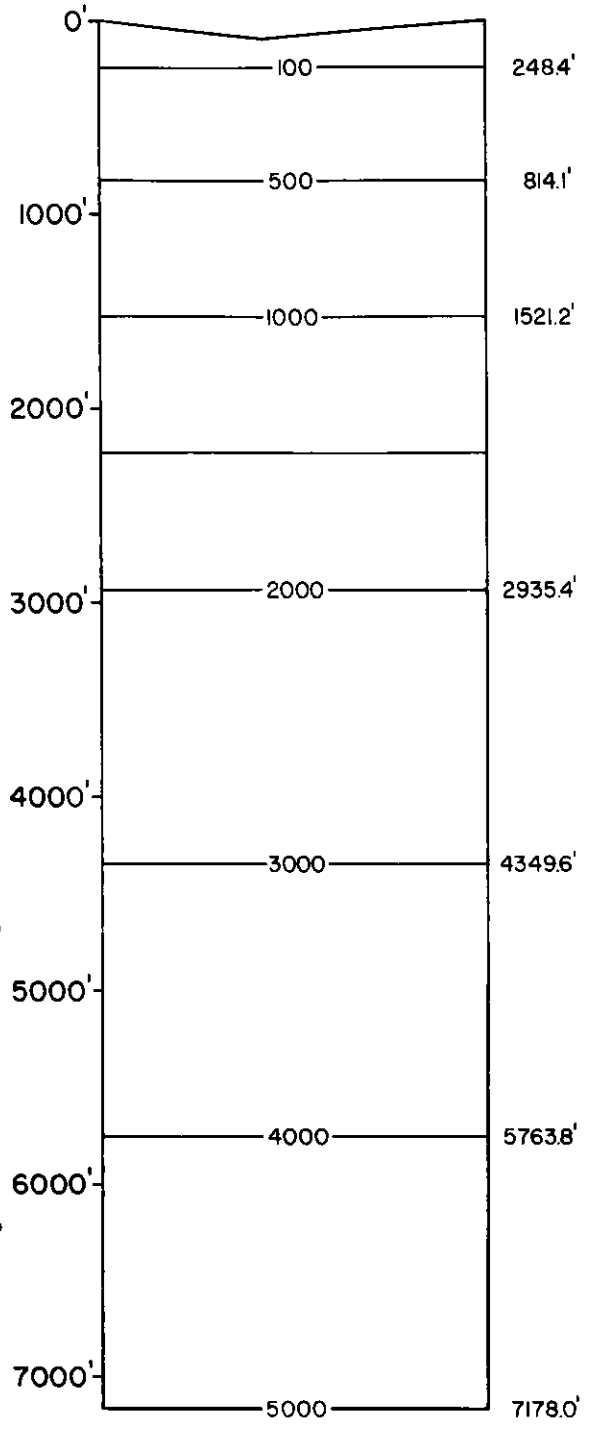
Sierra Madre Unit # 3
Figure B-8

116

Manning Ridge # 2A. Width 580'

Transect # 22A
Transect # 21A

100	187.4'
500	753.1'
1000	1460.2'
2000	2874.4'
3000	4288.6'
4000	5702.8'
5000	7117.1'
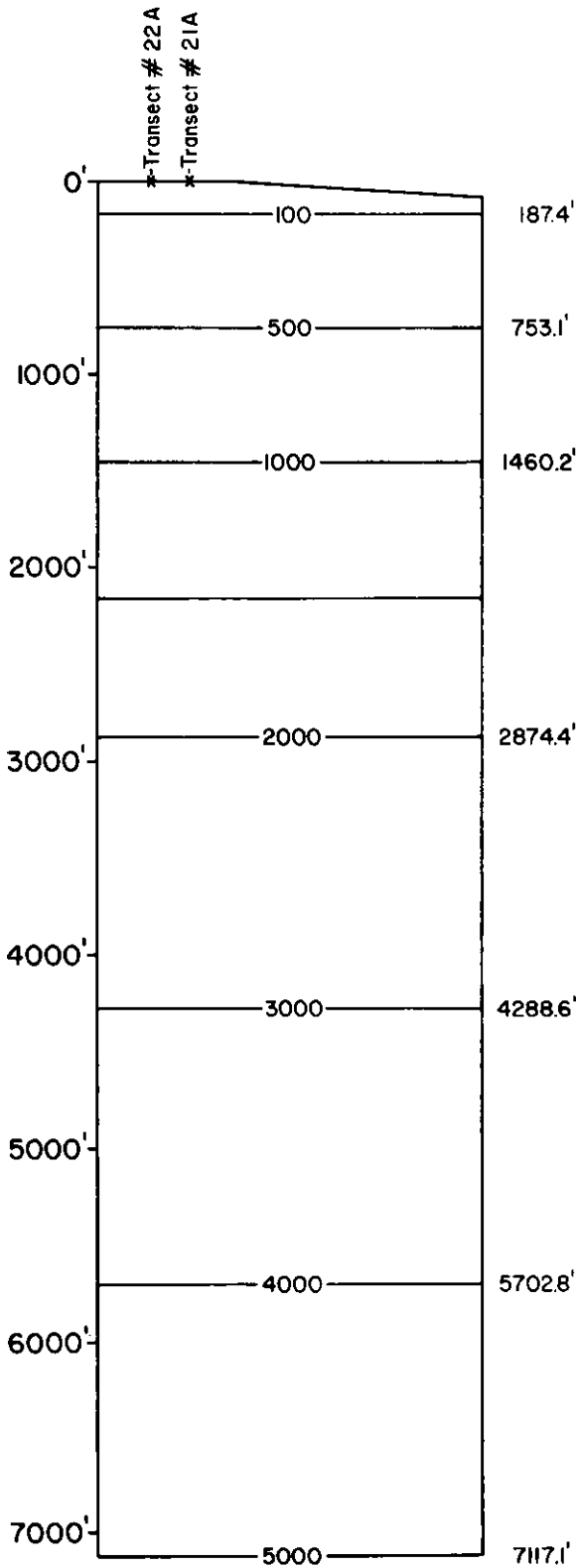
Manning Ridge # 2B. Width 690'

Transect # 22B
Transect # 21B

100	187.4'
500	753.1'
1000	1460.2'
2000	2874.4'
3000	4288.6'
4000	5702.8'
5000	7117.1'
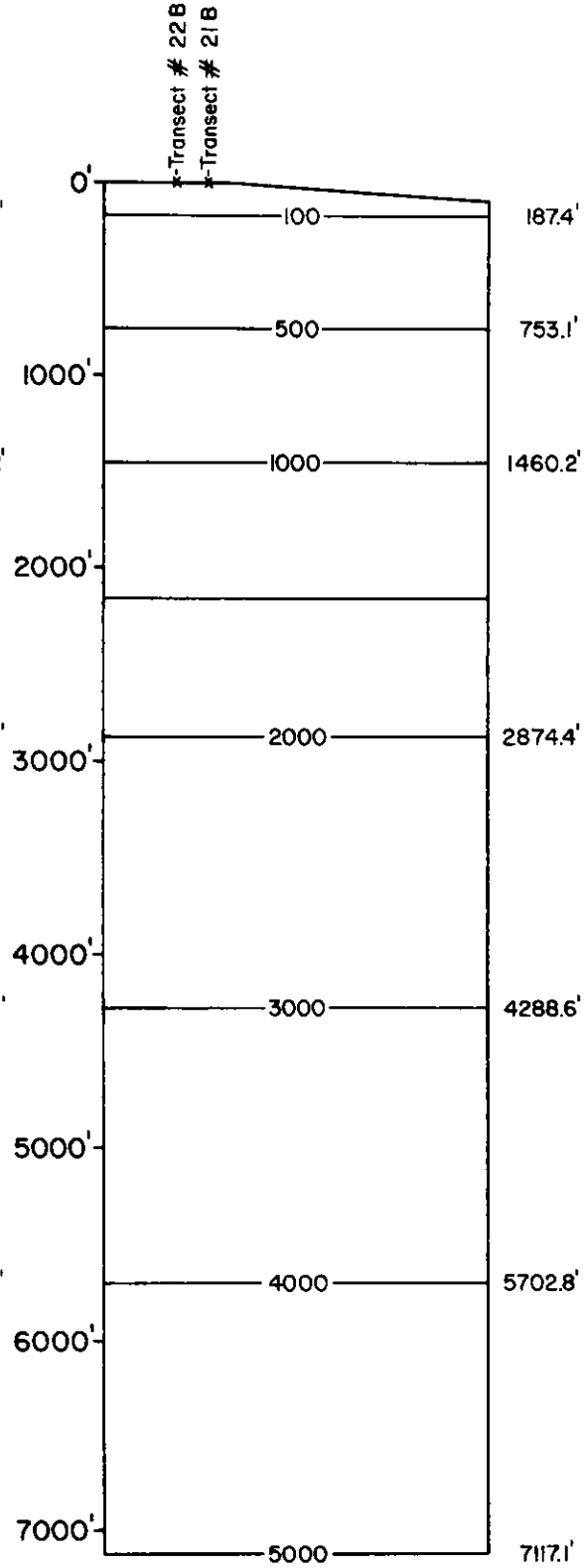
Sierra Madre Unit # 3

Figure B-9

Inferred Geometry Between Manning Ridge # 2(A,B) and # 3. Width=1390.'

0'

— 100 — 261.4'

— 500 — 817.1'

1000'

— 1000 — 1524.2'

2000'

— 2000 — 2938.4'

3000'

4000'

— 3000 — 4352.6'

5000'

— 4000 — 5766.8'

6000'

7000'

— 5000 — 7181.0'

Manning Ridge # 3. Width=315.'

← Transect # 24

← Transect # 23

0'

— 100 — 141.4'

— 500 — 707.1'

1000'

— 1000 — 1414.2'

2000'

— 2000 — 2828.4'

3000'

4000'

— 3000 — 4242.6'

5000'

— 4000 — 5656.8'

6000'

7000'

— 5000 — 7071.1'
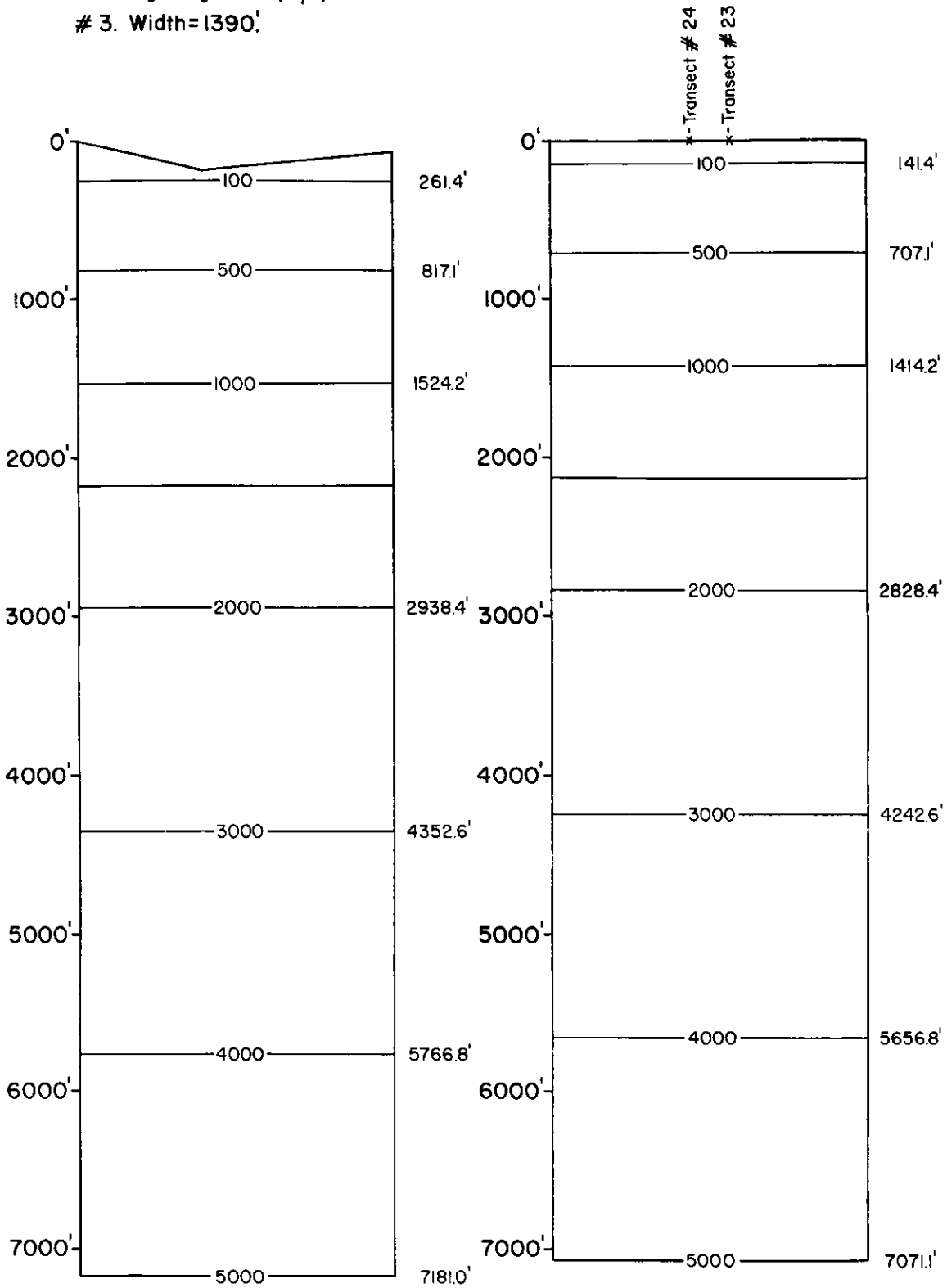
Sierra Madre Unit # 3

Figure B-10

Inferred Geometry East of
Manning Ridge # 3.
Width = 1000'.

0'

100 — 233.4'

500 — 799.1'

1000'

1000 — 1506.2'

2000'

2000 — 2920.4'

3000'

3000 — 4334.6'

4000'

5000'

4000 — 5748.8'

6000'

7000'

5000 — 7163.0'
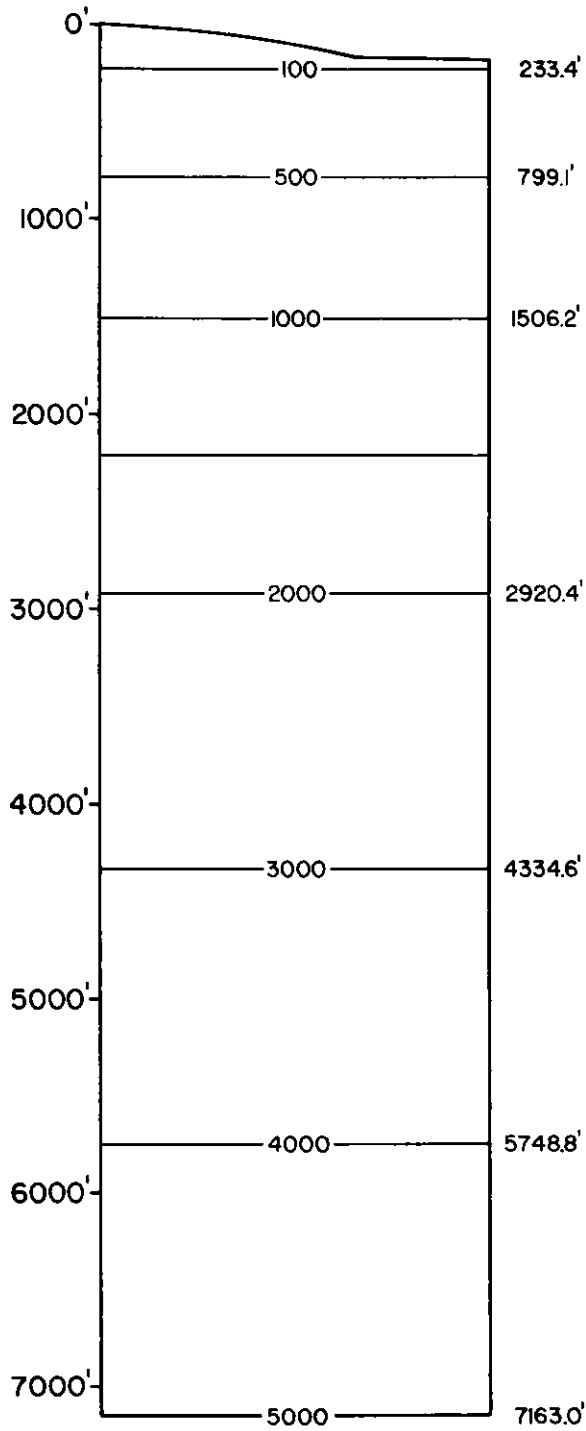
Sierra Madre Unit # 3

Figure B-11

Table B-2

SUMMARY OF AREAS PER DEPTH INTERVAL FOR MEDICINE BOW

Area per depth interval (sq. ft.)

SEGMENT NUMBER	AVE. EL.	0-100	100-200	200-300	300-400	400-500	500-1000	1000-1500
Unit 5a: East Limb, Strike Length = 3580 feet								
1	8850	43750	43750	43750	56250	71320	20350	
2	8770	64500	64500	64500	64500	64500	191350	
3	8710	89250	89250	89250	89250	144375	212250	
4	8700	95625	95625	95625	95625	147250		
5	8640	42500	42500	42500	42500	42500	213900	5625
6	8600	63000	63000	63000	63000	63000	107250	45150
7	8420	60000	60000	60000	60000	60000	68000	
8	8500	70000	70000	70000	87500	26250		
9	8535	78000	78000	78000	78000	40000	43750	
Unit 5a: Eastern Syncline, Strike Length = 1475 feet								
1	8420	52500	52500	52500	52500	37365		
2	8450	25000	25000	25000	26200			
3	8480	54375	54375	87812				
4	8510	39375	39375	39375	39375	39375	303750	46250
5	8510	48000	48000	48000	48000	48000	435840	49890

(Unit 5a totals include both east limb and eastern syncline portions)

Total area for intervals		825875	825875	859312	798700	783935	1596440	146915
Cumulative area		825875	1651750	2511062	3309762	4093697	5690137	5837052

SEGMENT NUMBER	AVE. EL.	0-100	100-200	200-300	300-400	400-500	500-1000	1000-1500
Unit 5b: East Limb, Strike Length = 3100 feet								
1	8800	36000	36000	36000	12750			
2	8825	38750	38750	38750	46500			
3	8760	52000	52000	52000	52000	52000	17500	
4	8707	78750	78750	78750	78750	28500		
5	8670	58750	58750	58750	38750			
6	8640	26000	26000	26000	26000	33250	90250	
7	8530	102000	105000	150000	180000			
8	8500	89250	78750	57750				
9	8500	25250	25250	34500				
Unit 5b: Eastern Syncline, Strike Length = 1620								
1	8660	27500	25900	24000	22385	16250	52650	
2	8595	60000	60000	60000	60000	60000	152500	
3	8555	25000	25000	27400	27400	27400	31620	
4	8530	36000	36000	36000	36000	36000	27600	
5	8510	32750	32750	39300	39300	32725	6507	
6	8590	14170	15312	6250	1875			

(Unit 5b totals include both east limb and eastern syncline portion)

Total area for intervals		702170	694212	725450	621710	286125	378627	
Cumulative area		702170	1396380	2121830	2743540	3029665	3408292	

SUMMARY OF AREAS PER DEPTH INTERVAL FOR MEDICINE BOW

Area per depth interval (sq. ft.)

SEGMENT NUMBER	AVE. EL.	0-100	100-200	200-300	300-400	400-500	500-1000	1000-1500	1500-2000
Unit 1: West Limb, Strike Length = 2975									
1	8700	94375	56790	15900					
2	8600	57000	60125	62405	64920	67375	156740	12145	
3	8660	56170	56170	71750	45920	51250	189000		
4	8620	91875	91875	91875	88200	82232	323415		
5	8580	75600	73375	60480	51300	47300	125850		
Unit 1: Southern Limb, Strike Length = 3430									
1	9250	78750	78750	78750	67500	58500	188175		
2	9230	87500	87500	87500	75000	67500	275000	162500	
3	9260	70000	70000	70000	60000	52000	178125	53200	
4	9215	51000	51000	51000	51000	51000	90250		
5	9205	30625	30625	30625	31500	17500	13125		
6	9200	37500	37500	37500	30000	30000	78125		
7	9150	20000	20000	20000	20800	16000	77350		
8	9120	20400	20400	20400	20400	21250	90100	38400	
9	9040	60000	60000	60000	60000	60000	262500	156250	
10	8985	37500	37500	37500	37500	41250	196875	166775	
Unit 1: Normal Limb, Strike Length = 575									
1	9190	4000							
2	9180	17500							
3	9170	13750							

(Unit 1 totals include the west limb, southern limb, and normal limb portions)

|		0-100	100-200	200-300	300-400	400-500	500-1000	1000-1500	1500-2000
Total area for intervals		903545	831610	795685	704040	663160	2243630	589270	
Cumulative area		903545	1735155	2530840	3234880	3898040	6141670	6730940	
Three Mile Creek: Strike Length = 6025									
1	9280	123750	123750	123750	119350	117150	566500	518415	508100
2	9360	121000	121000	121000	121000	121000	605000	577730	600220
3	9390	109200	109200	109200	109200	109200	546000	573200	529300
4	9360	128700	128700	128700	128700	128700	643500	597575	539925
5	9400	93600	93600	93600	93600	93600	468000	434600	385400
6	3980	99450	99450	99450	99450	99450	497250	461760	429490
Total area for intervals		675650	675650	675650	671250	669050	3325750	3163280	2992435
Cumulative area		675650	1351300	2026950	2698200	3367250	6693000	9856280	12848715

N

structure contours

outcrop pattern

MAP VIEW

top of bed

intrusive rocks

0   500   1000 ft
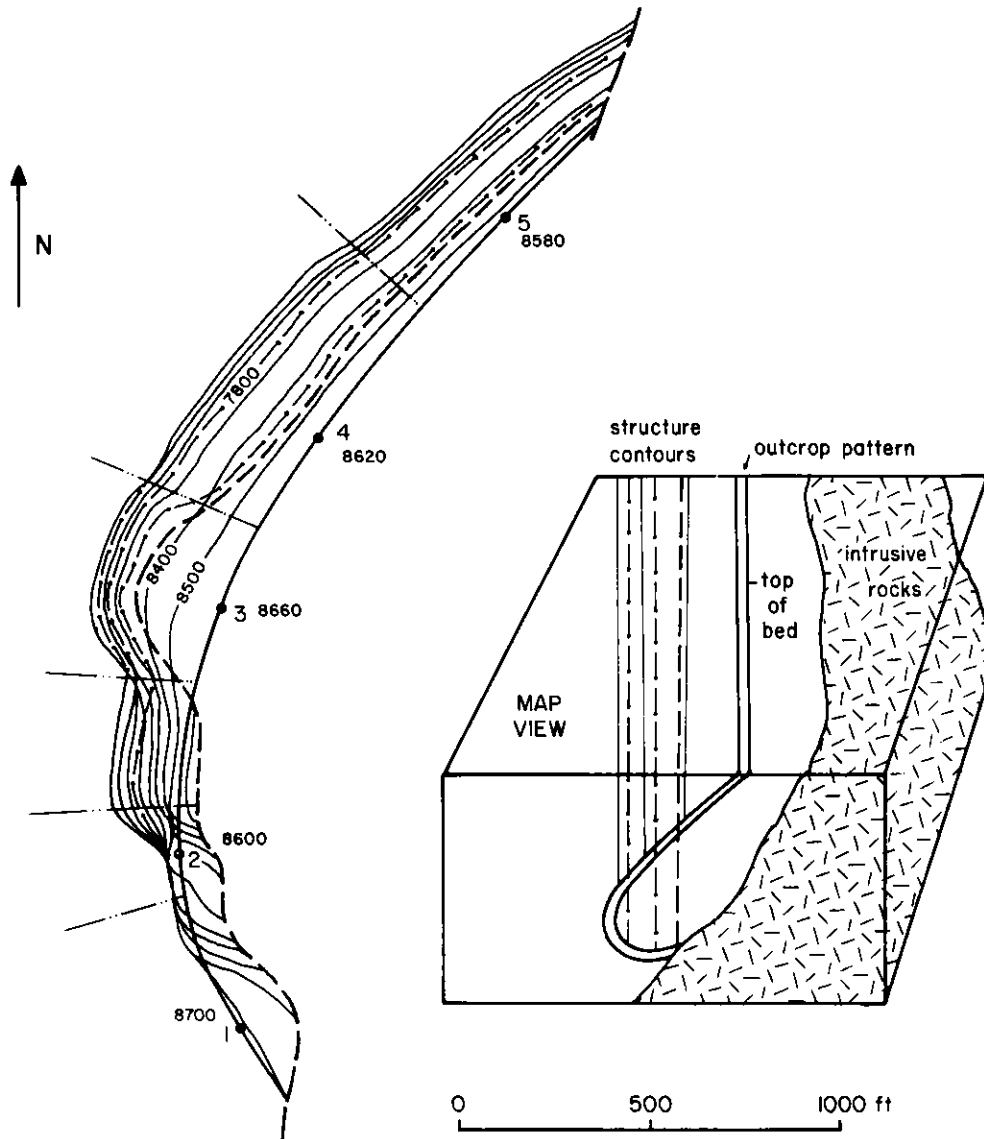
EXPLANATION

Datum is mean sea level
Contour interval 100 feet

————·— Structure contour on overturned portion of bed (see inset)

—·—·— Structure contour on normal portion of bed (see inset)

——— — Contact with intrusive rocks

—·—·— Area segment boundary

8580
•5 Reference point for area segment with reference elevation

Figure B-12. Structure contours on top of mineable Unit 1, overturned west limb of Onemile Creek Syncline, Onemile Creek area, Medicine Bow Mountains.

Sec. 6   T18N
Sec. 7   R78W
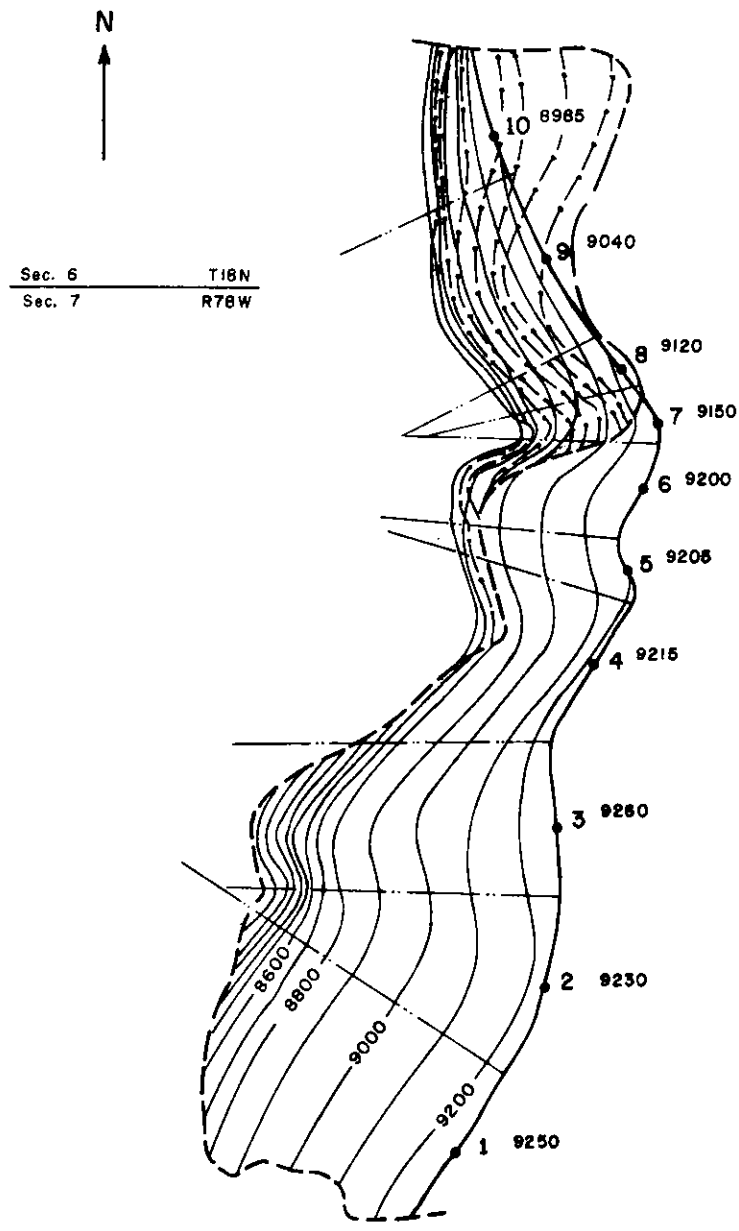
Explanation as on sheet for Unit 1, overturned west limb
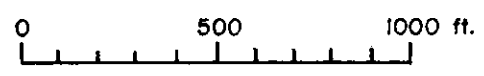
Figure B-13.
Structure contours on top of mineable Unit 1, overturned southern limb of Onemile Creek syncline, Onemile Creek area, Medicine Bow Mountains.
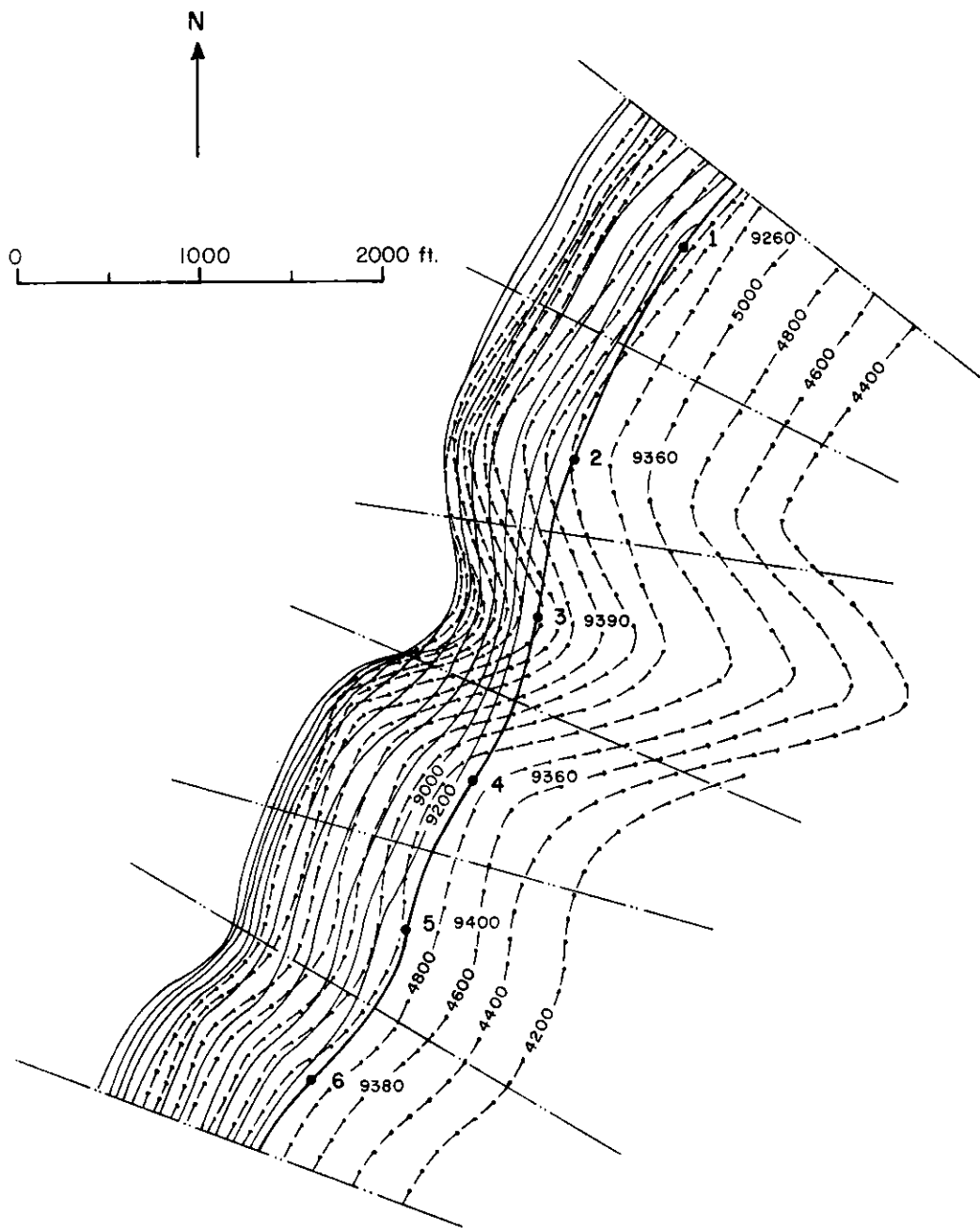
Explanation as on Unit 1, overturned west limb
Contour interval 200 feet

Figure B-14.
Structure contours on top of
principal radioactive unit in
Threemile Creek area, Medicine
Bow Mountains.

EXPLANATION FOR
STRUCTURE CONTOUR MAPS

5b

Elevations in feet, datum mean sea level.
Contour interval 100 feet.

⬭ Outcrop pattern

——— Structure contour

—— — Projected contact between unit and
intrusive rocks.

—··— Area segment boundary

8555 Reference point for area segment with
●3   reference elevation in feet.

N 0   500   1000 feet
   0   100   200   300 meters

5a

Sec.6 | Sec.5
T18N
R78W
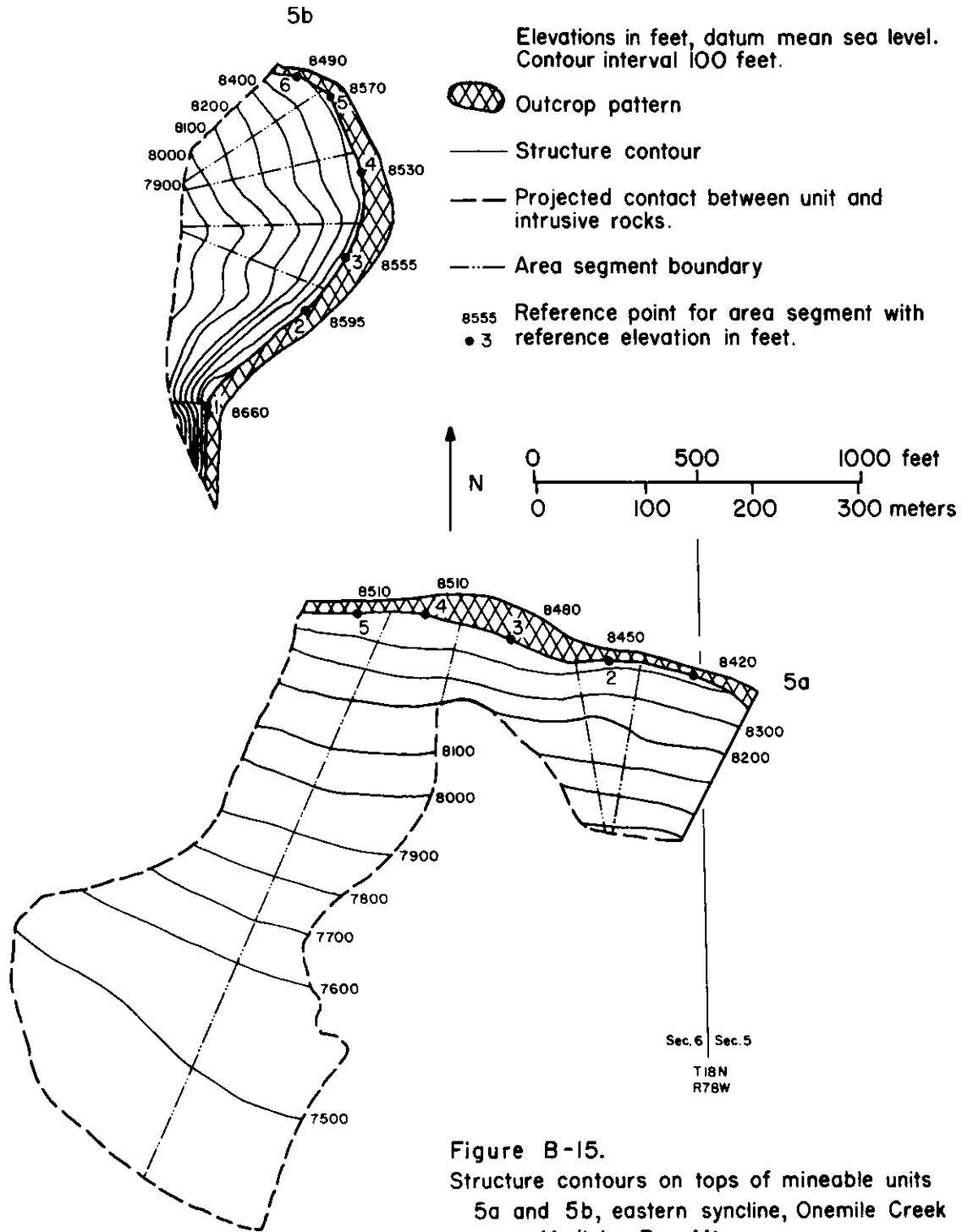
Figure B-15.
Structure contours on tops of mineable units
5a and 5b, eastern syncline, Onemile Creek
area, Medicine Bow Mtns.

125

Figure B-16
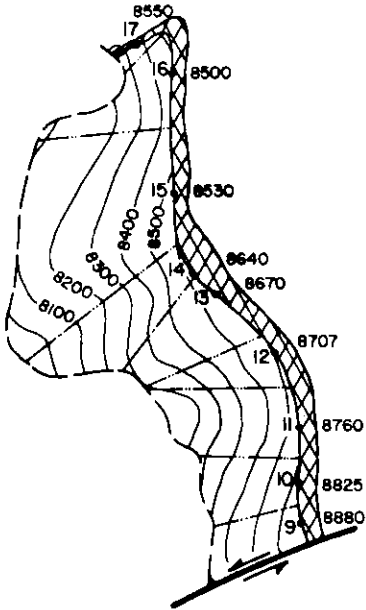
Structure contours on top of mineable unit
5b, east limb of Onemile Creek
Syncline, Onemile Creek area.
Explanation as on sheet for eastern
syncline.

T 18N
R78W

Sec. 6	Sec. 5
Sec. 7	Sec. 8

N

```
0          1000         2000 feet
|___|___|___|___|___|___|___|
0          300          600 meters
```
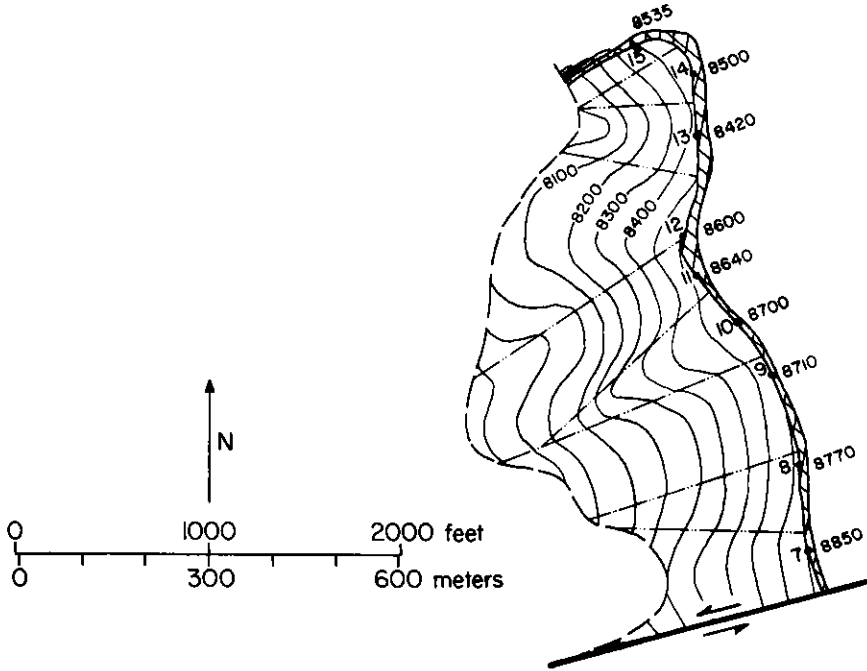
Structure contours on top of mineable unit
5a, east limb of Onemile Creek
Syncline, Onemile Creek area.
Explanation as on sheet for eastern
syncline.

T 18N
R78W

Sec. 6	Sec. 5
Sec. 7	Sec. 8

126

Appendix C

Graphical Presentation of Placement
and True Thickness of Ore Beds in
the Outcrop Transects and the Drill
Holes.

Sierra Madre Unit #3

Figure C-1. Thickness and U,Th values of Unit 3, Deep Gulch Conglomerate from transects 1, 2 and 3, Carrico Ranch, northwest Sierra Madre. ND = NO DATA AVAILABLE
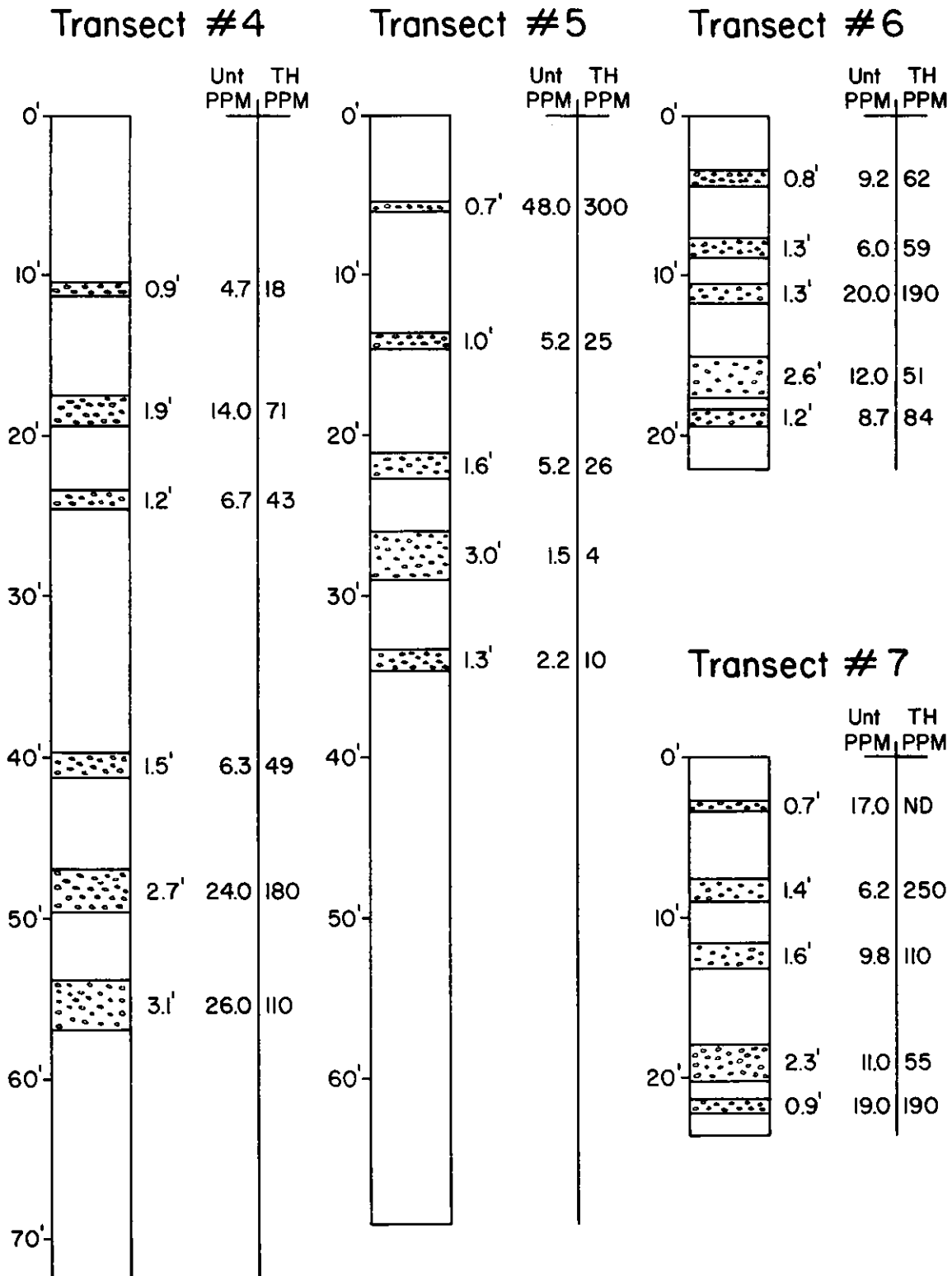
Figure C-2. Thickness and U,Th values of Unit 3, Deep Gulch Conglomerate from transects 4, 5, 6 and 7, Carrico Ranch, northwest Sierra Madre. ND = NO DATA AVAILABLE

Transect # 8

	Unt PPM	TH PPM
0.7'	3.3	14
0.9'	12.0	92
1.8'	8.7	15
0.5'	8.7	84

Transect # 10

	Unt PPM	TH PPM
2.3'	12.0	120
1.0'	8.1	50
3.2'	43.0	220

Transect # 11

	Unt PPM	TH PPM
2.0'	23.0	110
1.3'	3.8	23
2.4'	26.0	120

Transect # 9

	Unt PPM	TH PPM
0.7'	15.0	120
0.8'	16.0	110
2.4'	7.3	25
0.7'	5.8	58

Figure C-3.   Thickness and U,Th values of Unit 3, Deep Gulch
   Conglomerate from transects 8, 9, 10 and 11, Carrico Ranch,
   northwest Sierra Madre.
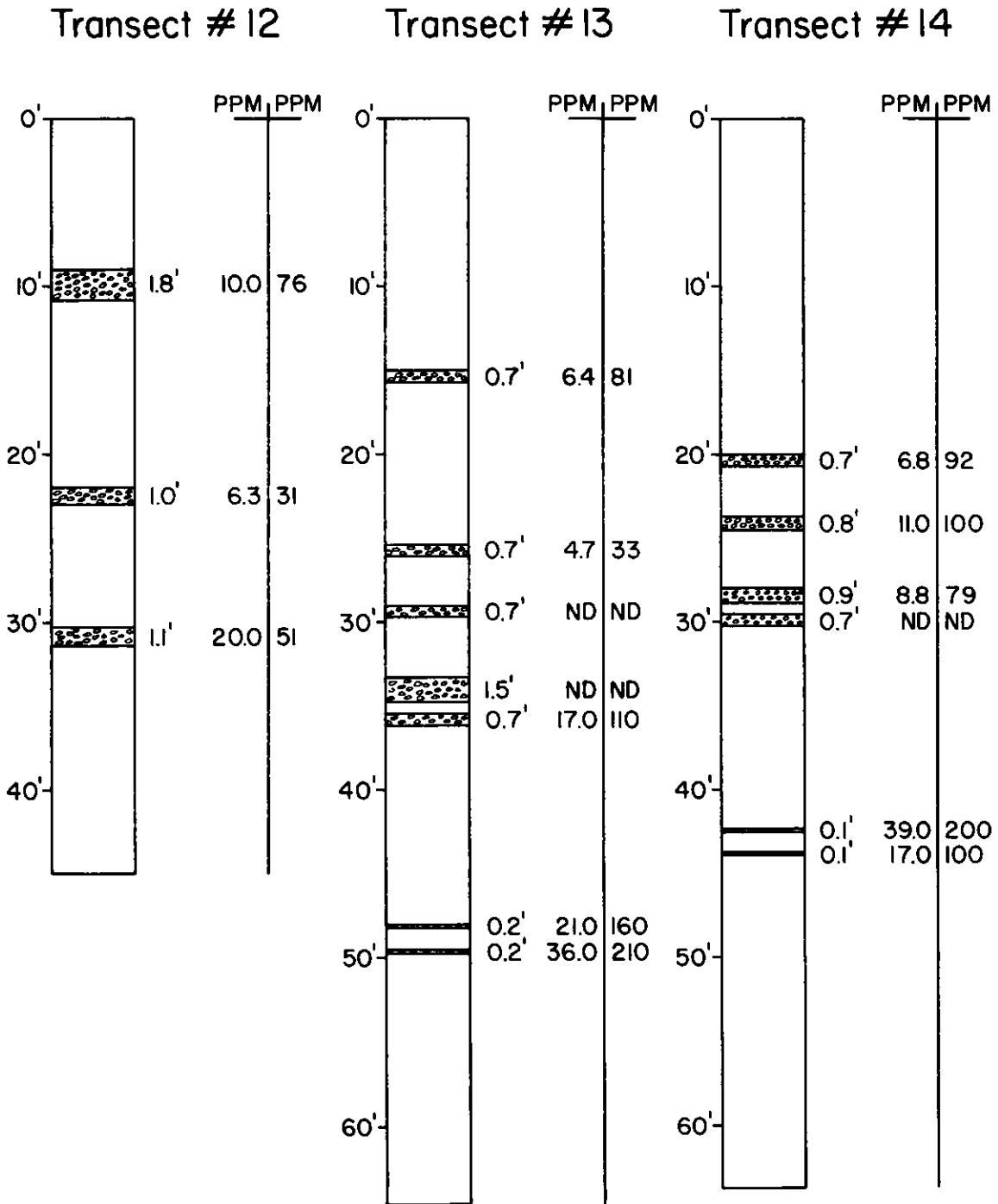
Figure C-4. Thickness and U,Th values of Unit 3, Deep Gulch Conglomerate from transects 12, 13 and 14, Carrico Ranch and Deep Gulch, northwest Sierra Madre. ND = NO DATA AVAILABLE

Transect #15   Transect #16   Transect #17

| | Unt | TH |
| | PPM | PPM |

| | Unt | TH |
| | PPM | PPM |

| | Unt | TH |
| | PPM | PPM |

0'   0'   0'

10'   10'   0.5' 56.0 150   10'   0.3'   0.9   3
                             0.3' 16.0   87

                             0.6'   4.6   29   0.7'   ND   ND
                             0.7' 11.0   61   0.6'   2.5   2

20'   20'   20'

                             0.5' 24.0 190   0.6' 24.0   ND
                             0.3' 19.0 260   0.4'   ND   ND

30'   30'   30'

40'   1.7'   ND   ND

50'
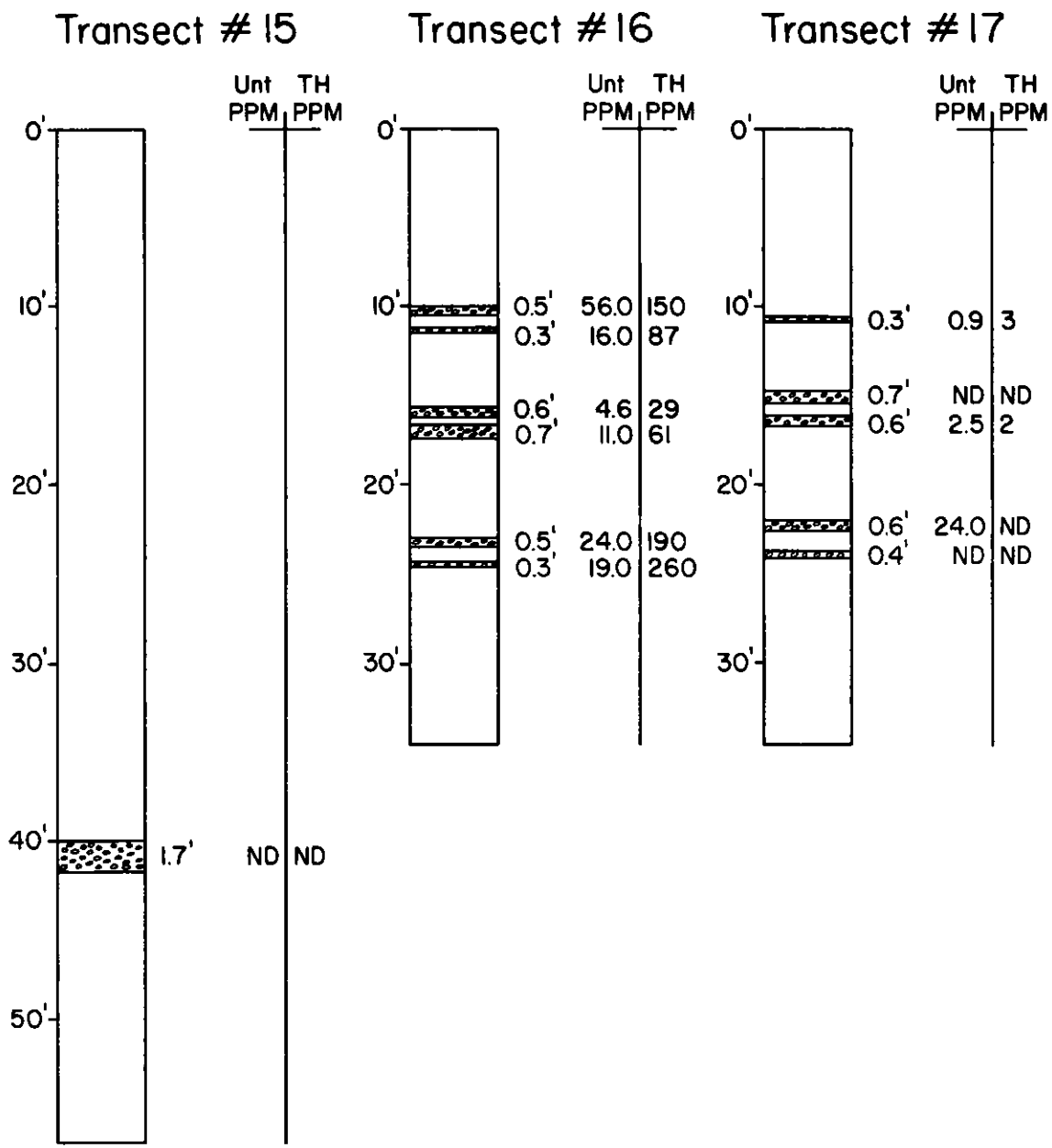
Figure C-5. Thickness and U,Th values of
    Unit 3, Deep Gulch Conglomerate from   ND = NO DATA AVAILABLE
    transects 15, 16 and 17, Deep Gulch,
    northwest Sierra Madre.

132

Transect #18

	Unt PPM	TH PPM
0.6'	20.0	370
0.2'	3.1	27
0.3'	7.0	220
0.6'	2.7	150
0.3'	2.4	11
0.4'	2.5	10
0.3'	4.3	19
0.4'	2.3	14
0.4'	10.0	56
0.3'	6.1	30
0.8'	13.0	63

Transect #19

	Unt PPM	TH PPM
0.7'	5.8	32
0.8'	6.5	240
0.7'	11.0	280
0.4'	6.5	32
0.4'	6.2	41
0.3'	6.4	31
0.2'	3.4	16
0.7'	10.0	90

Transect #20

	Unt PPM	TH PPM
0.3'	8.7	77
0.8'	4.2	45
0.5'	5.7	69
0.2'	3.1	38
0.4'	6.1	86
0.5'	3.7	37
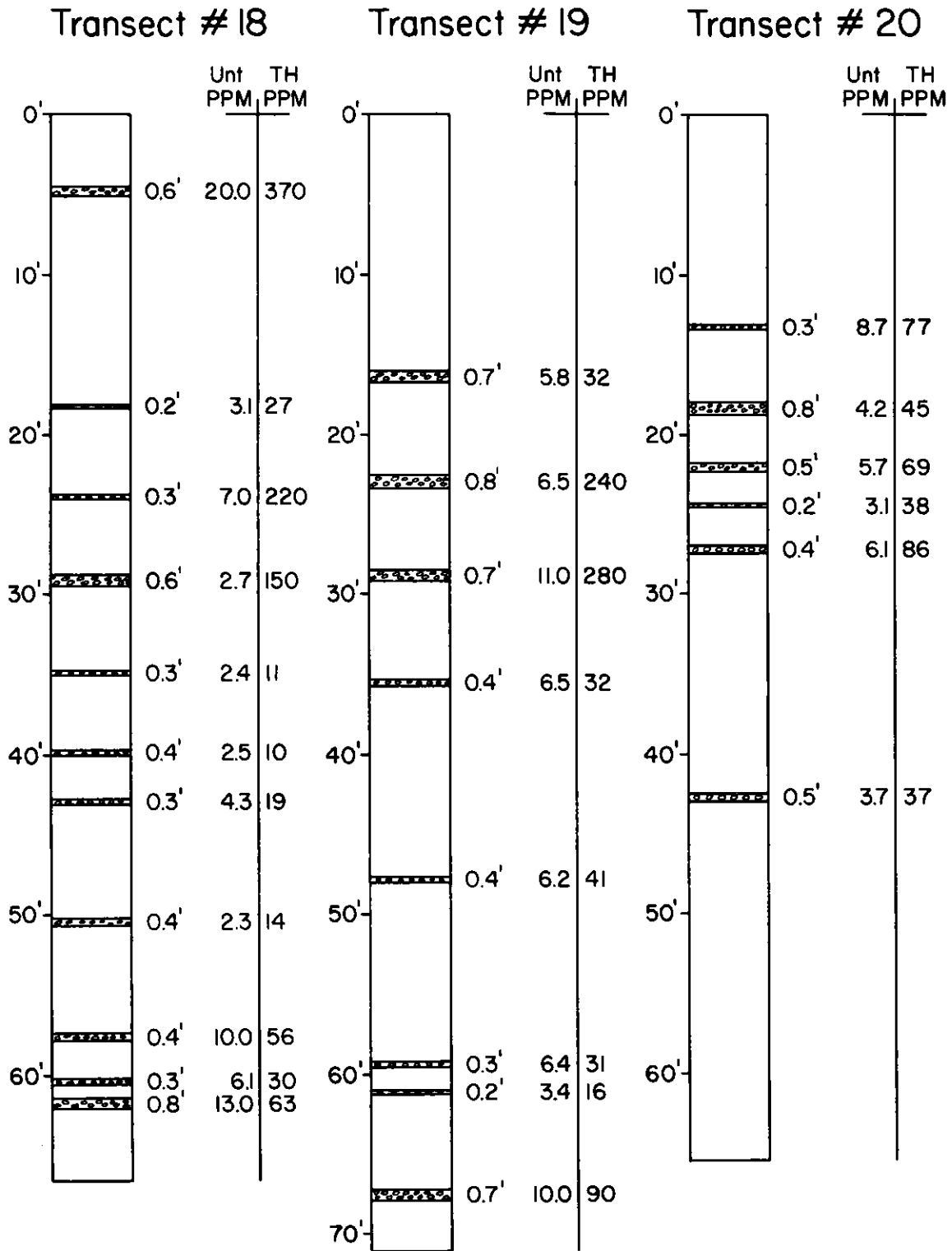
Figure C-6. Thickness and U,Th values of Unit 3, Deep Gulch
Conglomerate from transects 18, 19, 20, Manning Ranch,
northwest Sierra Madre.

133

Transect # 21A

	Unt PPM	TH PPM
0.1'	12.0	120
0.7'	17.0	210
0.3'	9.0	150
0.5'	9.4	55
0.2'	9.1	150
0.1'	8.6	71

Transect # 21B

	Unt PPM	TH PPM
0.3'	7.4	26
0.2'	4.9	150
0.5'	5.0	120

Transect # 22A

	Unt PPM	TH PPM
0.3'	ND	54
1.0'	15.0	290
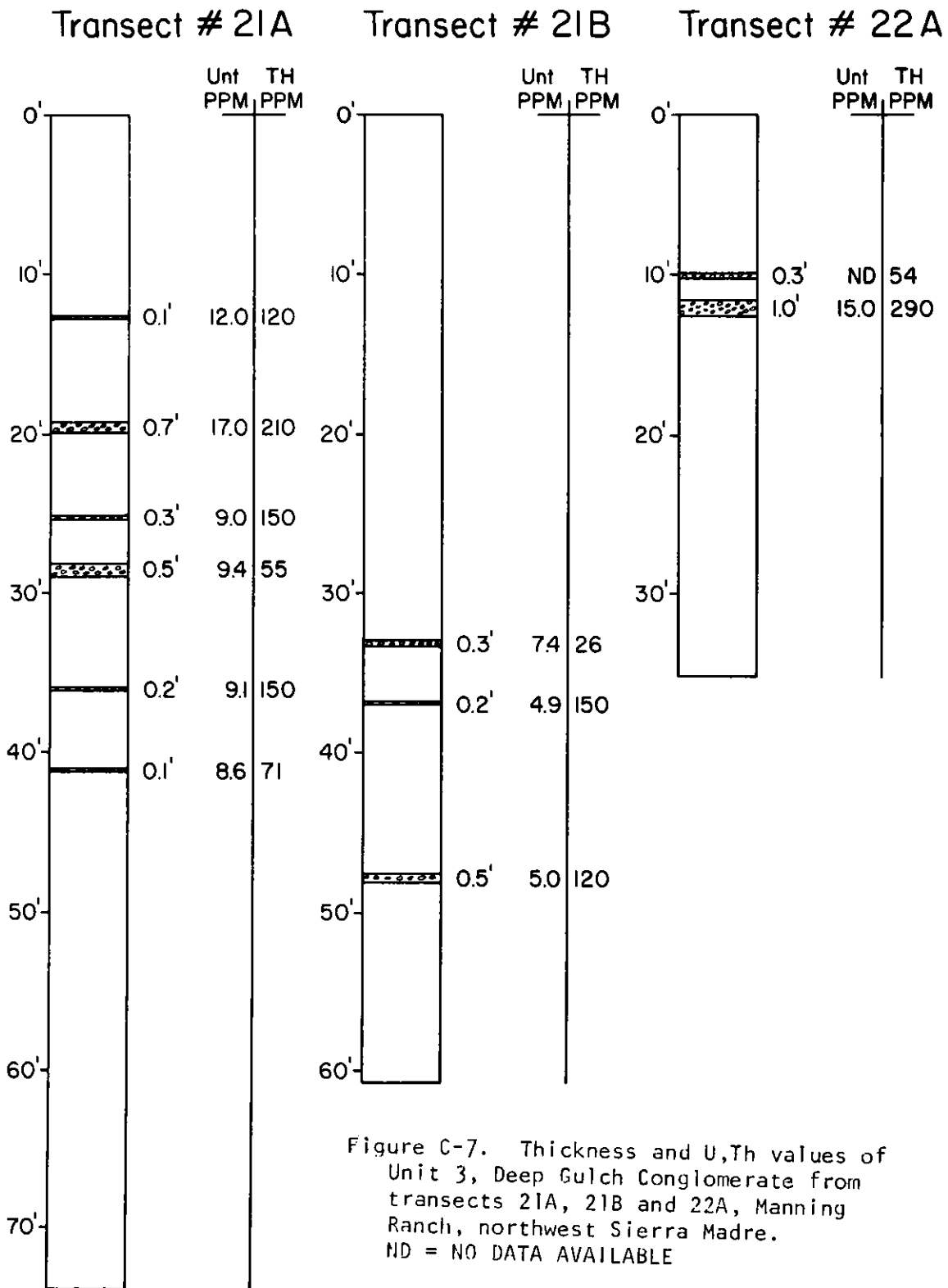
Figure C-7. Thickness and U,Th values of Unit 3, Deep Gulch Conglomerate from transects 21A, 21B and 22A, Manning Ranch, northwest Sierra Madre. ND = NO DATA AVAILABLE

134

Transect #22B   Transect #23   Transect #24

	Unt PPM	TH PPM
0.1'	10.0	35
0.3'	3.5	15
0.3'	12.0	15
0.1'	13.0	47
0.8'	15.0	200
0.1'	2.8	200

	Unt PPM	TH PPM
0.5'	19.0	370
0.4'	9.1	190
0.2'	7.4	48

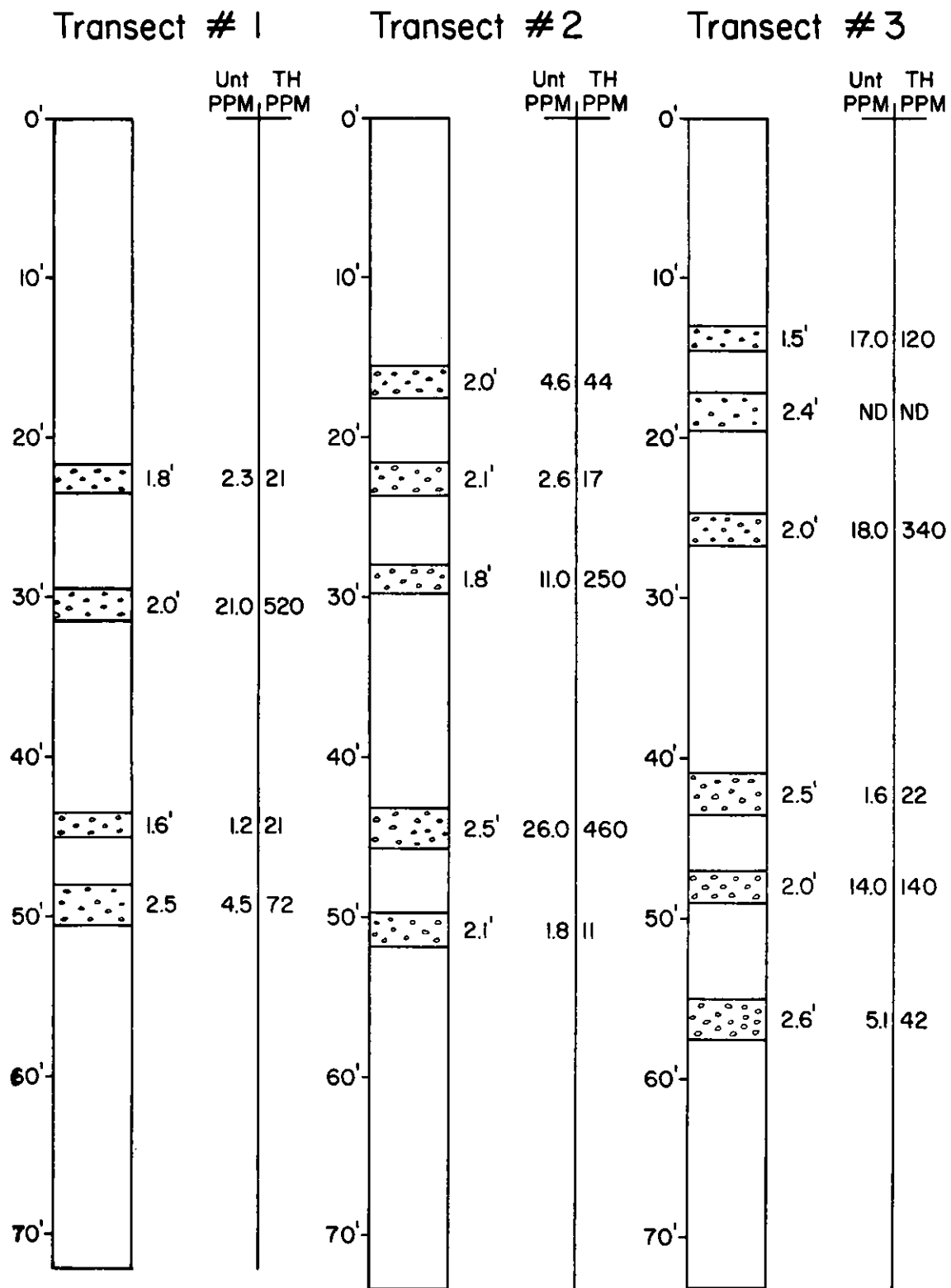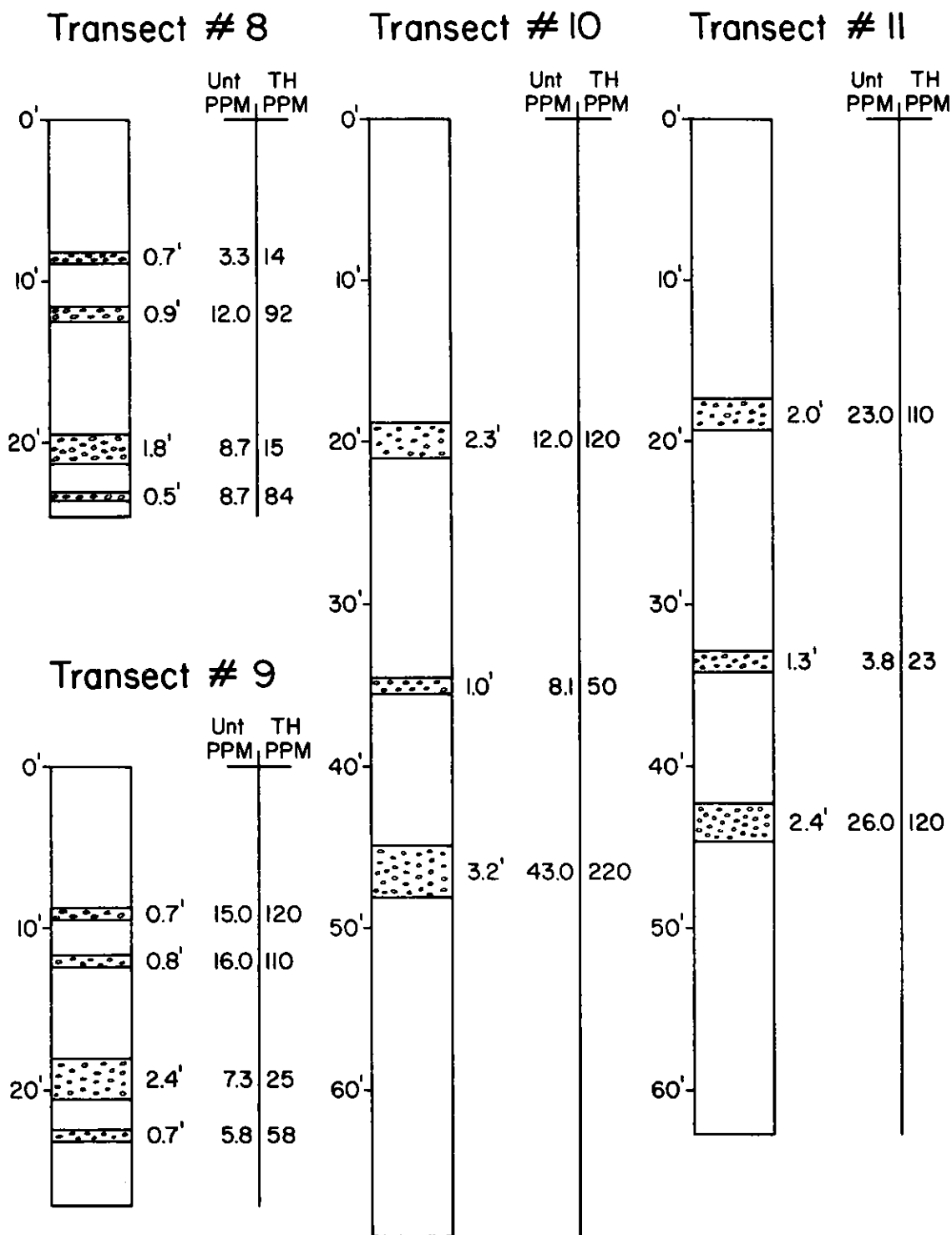|	Unt PPM	TH PPM
0.5'	11.0	81
0.2'	2.5	9
0.1'	12.0	61
0.6'	21.0	410
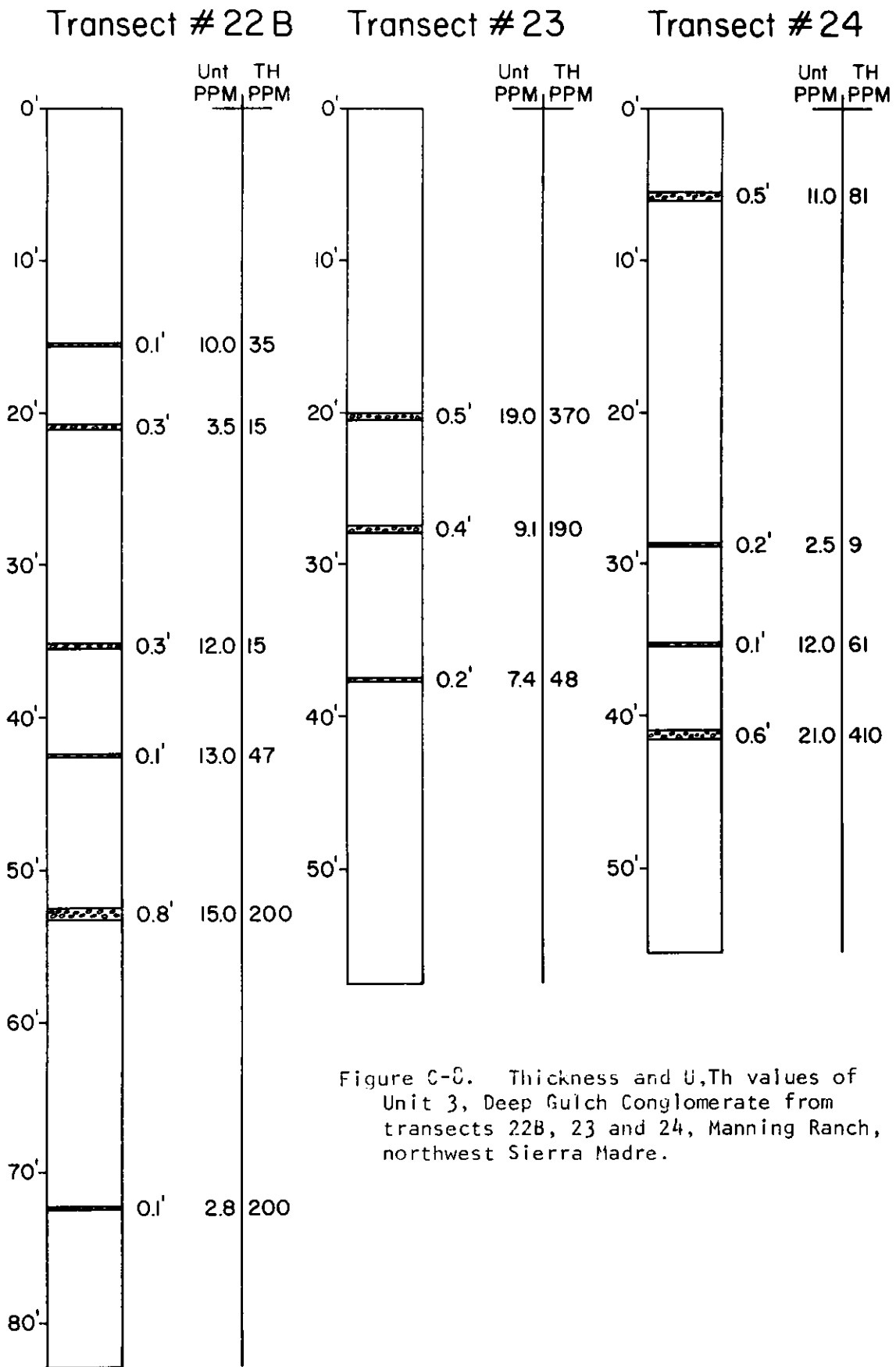
Figure C-8.   Thickness and U,Th values of
Unit 3, Deep Gulch Conglomerate from
transects 22B, 23 and 24, Manning Ranch,
northwest Sierra Madre.

SM-1 Core

	Unt PPM	TH PPM
0.73'	2.9	4
0.73'	6.2	9
0.73'	6.1	25
0.73'	5.2	12
0.73'	8.6	32
0.73'	3.5	5
0.73'	4.6	8
0.73'	3.8	7
0.73'	2.5	3
0.73'	6.1	10
0.73'	6.8	22
0.73'	84	22
0.73'	5.4	13
0.73'	14.0	31
0.73'	30.0	66
0.73'	15.0	31
0.73'	4.6	6
0.73'	4.4	10
0.73'	4.7	8
0.73'	3.6	15
0.73'	2.0	4
0.73'	3.5	13
0.73'	25.0	97
0.73'	18.0	53
0.73'	16.0	35
0.73'	11.0	29
0.73'	37.0	79
0.73'	92.0	300
0.73'	6.9	33
0.73'	3.4	8
1.5'	2.9	10

SM-2 Core

	Unt PPM	TH PPM
0.64'	12.0	47
0.64'	9.0	51
0.64'	7.9	40
0.64'	10.0	62
0.64'	4.8	22
0.64'	2.7	16
0.64'	1.6	10
0.64'	5.8	7
0.64'	2.9	8
0.64'	3.0	7
0.64'	2.1	6
0.64'	8.7	30
0.64'	15.0	150
0.64'	6.4	23
0.64'	5.1	19
0.64'	23.0	65
0.64'	58.0	150
0.64'	110.0	160
0.64'	270.0	670
0.64'	98.0	390
0.64'	28.0	260
0.64'	18.0	100
0.64'	39.0	440
0.64'	22.0	130
0.64'	23.0	160
0.64'	17.0	52
0.64'	46.0	97
0.64'	170.0	63
0.64'	78.0	180
0.64'	100.0	130
0.64'	49.0	26
0.64'	100.0	290
0.64'	120.0	330
0.64'	27.0	40
0.64'	15.0	14
0.64'	23.0	23
0.64'	46.0	12
MISSING		
0.96'	8.1	41
SS	11.0	43

JP-1 Core

	Unt PPM	TH PPM
0.4'	5.7	ND
0.4	5.7	ND

Sierra Madre Unit # 3
Figure C-9

ND = NO DATA AVAILABLE
SS = SPOT SAMPLE

JP-2 Core

	Unt PPM	TH PPM
SS	29.0	82
0.9'	5.8	ND
0.7'	5.8	ND

JP-4 Core

	Unt PPM	TH PPM
SS	4.2	42
0.5'	5.8	ND
0.5'	5.8	ND
SS	5.8	ND

JP-4 Core, cont.

	Unt PPM	TH PPM
SS	1.2	5
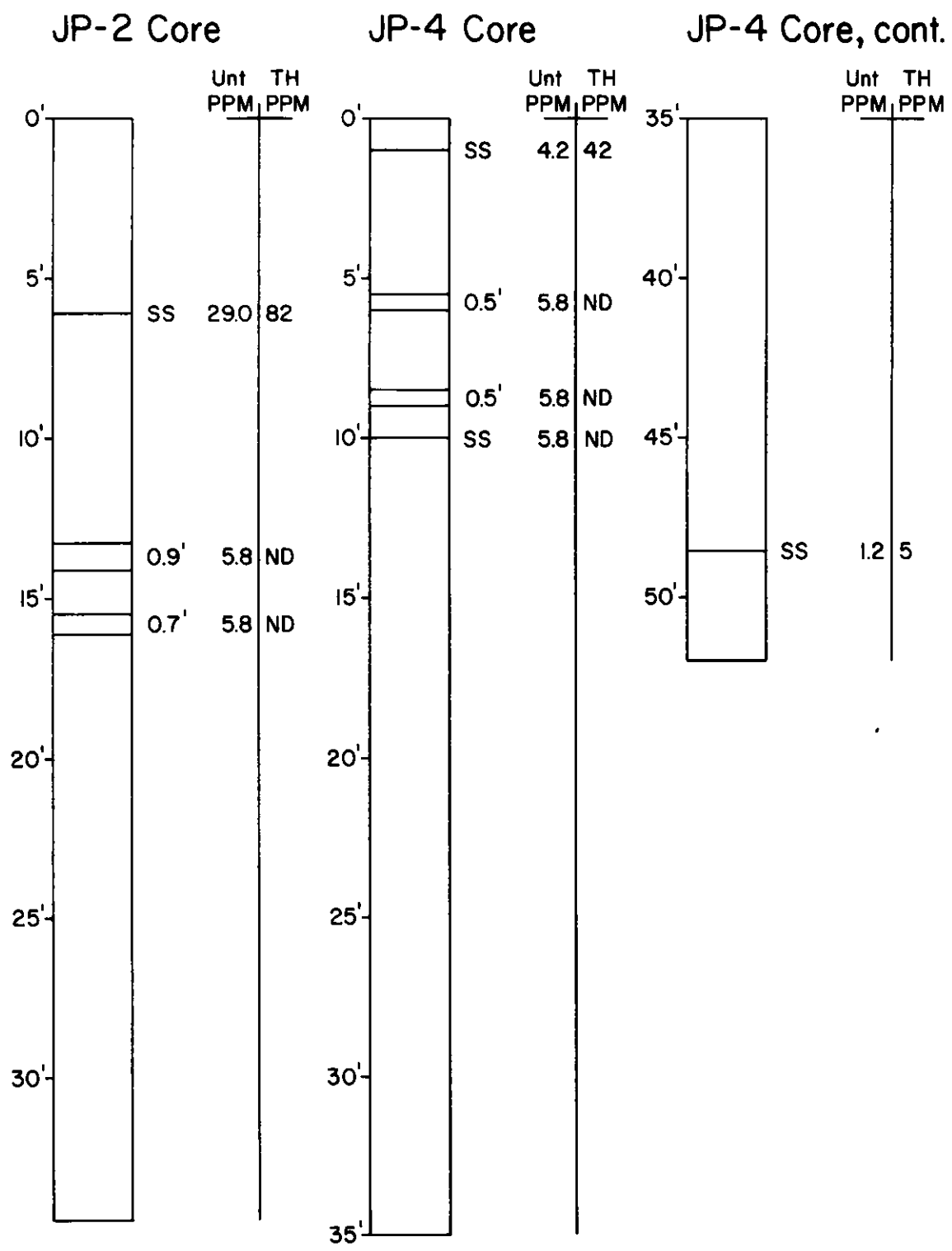
Sierra Madre Unit # 3
Figure C-10

ND = NO DATA AVAILABLE
SS = SPOT SAMPLE

Scale
(ft)

0

40

80

SS-spot sample
ND-no data available

U Th
(ppm)(ppm)

T1A

0.4' 11.0 20.0

0.5' 61.0 13.0

0.7' 49.0 120.0
2.7' 16.0 190.0

top of 1
0.9' 33.0 190.0
2.5' 10.0 10.0
0.4' 7.2 8.0

0.8' 14.0 30.0
1.2' 26.0 230.0
0.6' 29.0 16.0
0.6' 9.4 15.0
2.3' 18.0 34.0

T1B

0.7' 5.4 19.0

0.3' 26.0 210.0

0.3' ND ND

0.3' 2.9 7.0
0.2' 2.9 8.0
0.2' 13.0 18.0

2.7' 28.0 40.0

0.3' 9.3 89.0

0.2' 29.0 43.0

0.3' 32.0 140.0

14' ND ND

top of 1
0.2' 31.0 71.0

0.4' 5.8 5.0
0.7' 22.0 65.0

0.3' 8.6 13.0
0.1' 4.3 3.0
0.4' 43.0 270.0

0.4' 6.0 23.0
0.1' 3.3 17.0

0.4' 24.0 63.0
0.1' 14.0 19.0
0.7' 51.0 93.0

0.8' 53.0 34.0
0.4' 48.0 17.0
1.0' 22.0 34.0
2.0' 7.9 20.0
SS 100.0 110.0
bottom of 1

T1C

0.9' 55.0 33.0

SS 55.0 230.0

3.7' 9.6 12.0
1.2' 180.0 370.0

top of 2
0.5' 9.4 32.0
SS 11.0 9.0
2.8' 33.0 28.0
0.9' 36.0 25.0
0.3' 34.0 33.0
0.7' 21.0 59.0

0.9' 43.0 26.0
0.7' 60.0 100.0

SS 46.0 3.5
bottom of 1

Figure C-II. Thickness and U, Th values of radioactive conglomerates from surface transects, T1A, T1B, and T1C, Onemile Creek area, Medicine Bow Mtns.

Figure C-I2. Thickness and U, Th values of radioactive conglomerates from surface transect T2, Onemile Creek area, Medicine Bow Mtns.

139
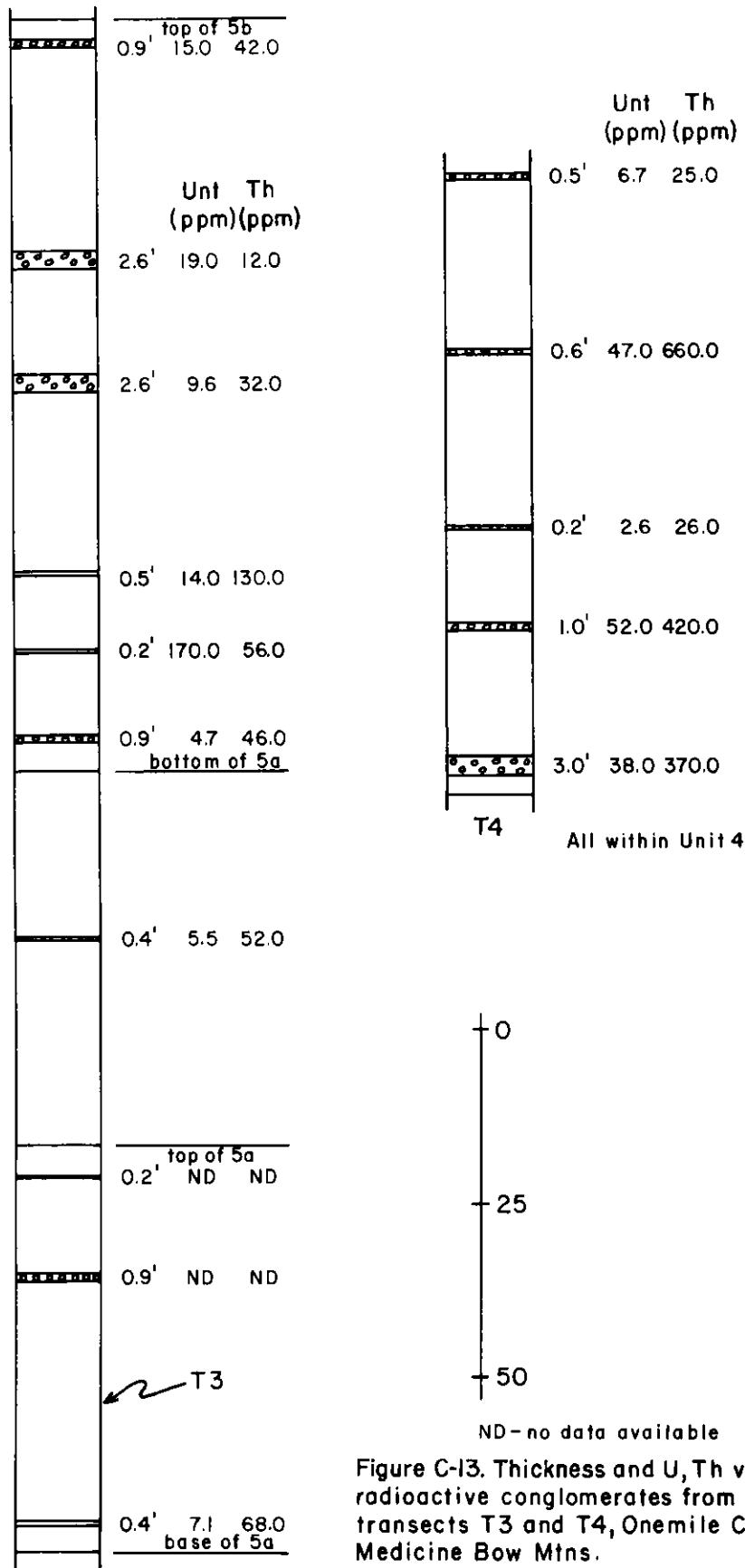
Figure C-13. Thickness and U, Th values of
radioactive conglomerates from surface
transects T3 and T4, Onemile Creek area,
Medicine Bow Mtns.

top of 5b

	U (ppm)	Th (ppm)
0.9'	15.0	42.0
2.6'	19.0	12.0
2.6'	9.6	32.0
0.5'	14.0	130.0
0.2'	170.0	56.0
0.9'	4.7	46.0

bottom of 5a

0.4'	5.5	52.0

top of 5a

0.2'	ND	ND
0.9'	ND	ND

T3

0.4'	7.1	68.0

base of 5a

	U (ppm)	Th (ppm)
0.5'	6.7	25.0
0.6'	47.0	660.0
0.2'	2.6	26.0
1.0'	52.0	420.0
3.0'	38.0	370.0

T4   All within Unit 4

0

25

50

ND - no data available

140

Column 1 (left):

	Unt (ppm)	Th (ppm)
		top of 5b
0.6'	8.2	39.0
0.6'	79.0	480.0
1.8'	9.4	70.0
1.2'	ND	ND
1.2'	ND	ND
SS	12.0	130.0
		bottom of 5b
0.9'	2.0	11.0
0.9'	5.0	58.0
0.9'	5.2	39.0
		top of 5a
1.5'	14.0	170.0
1.8'	1.9	12.0
1.8'	5.7	36.0
1.2'	15.0	150.0

1

Column I (middle):

SS	8.1	47.0
SS	14.0	120.0
SS	5.6	47.0
1.8'	12.0	.0
		bottom of 5a

Scale (ft)

+ 0
+ 25
+ 50

Unit 5

2

Column 2 (right):

Unit 4

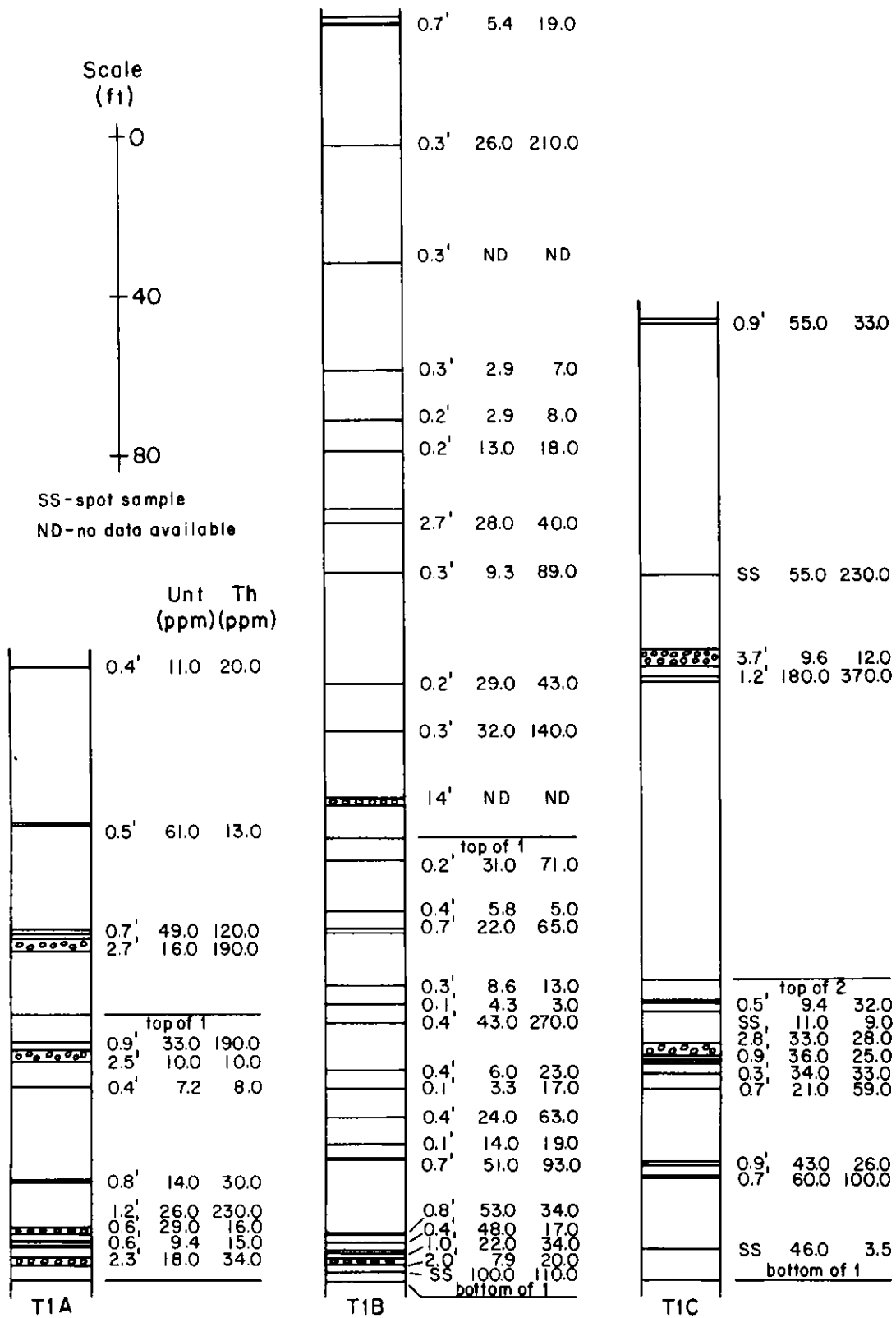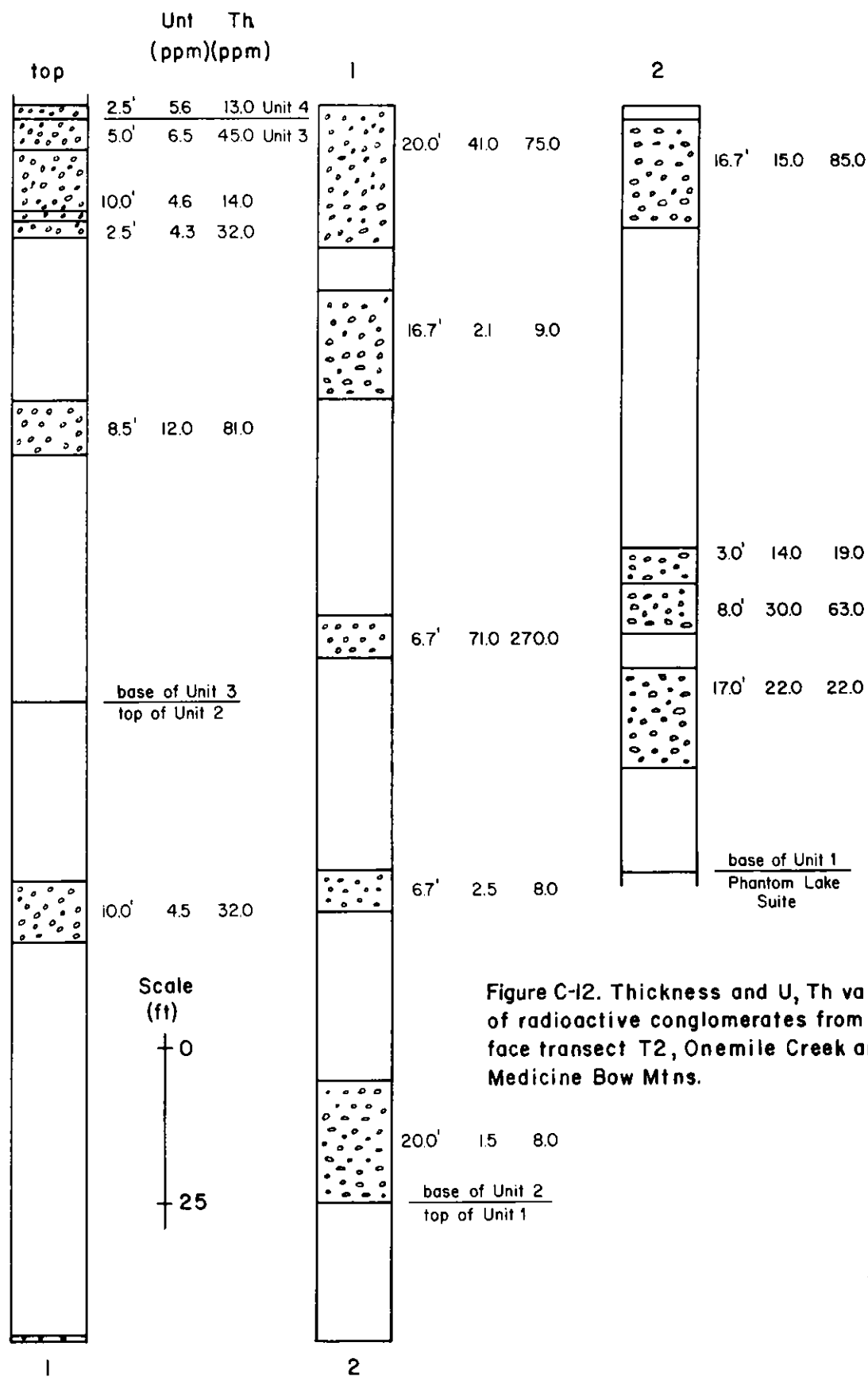| 3.3'	56.0	180.0
4.3'	57.0	24.0
1.8'	5.6	32.0
3.0'	100.0	210.0

SS – spot sample
ND – no data available

Figure C-14. Thickness and U, Th values of radioactive conglomerates from surface transect T5, Onemile Creek area, Medicine Bow Mtns.

141
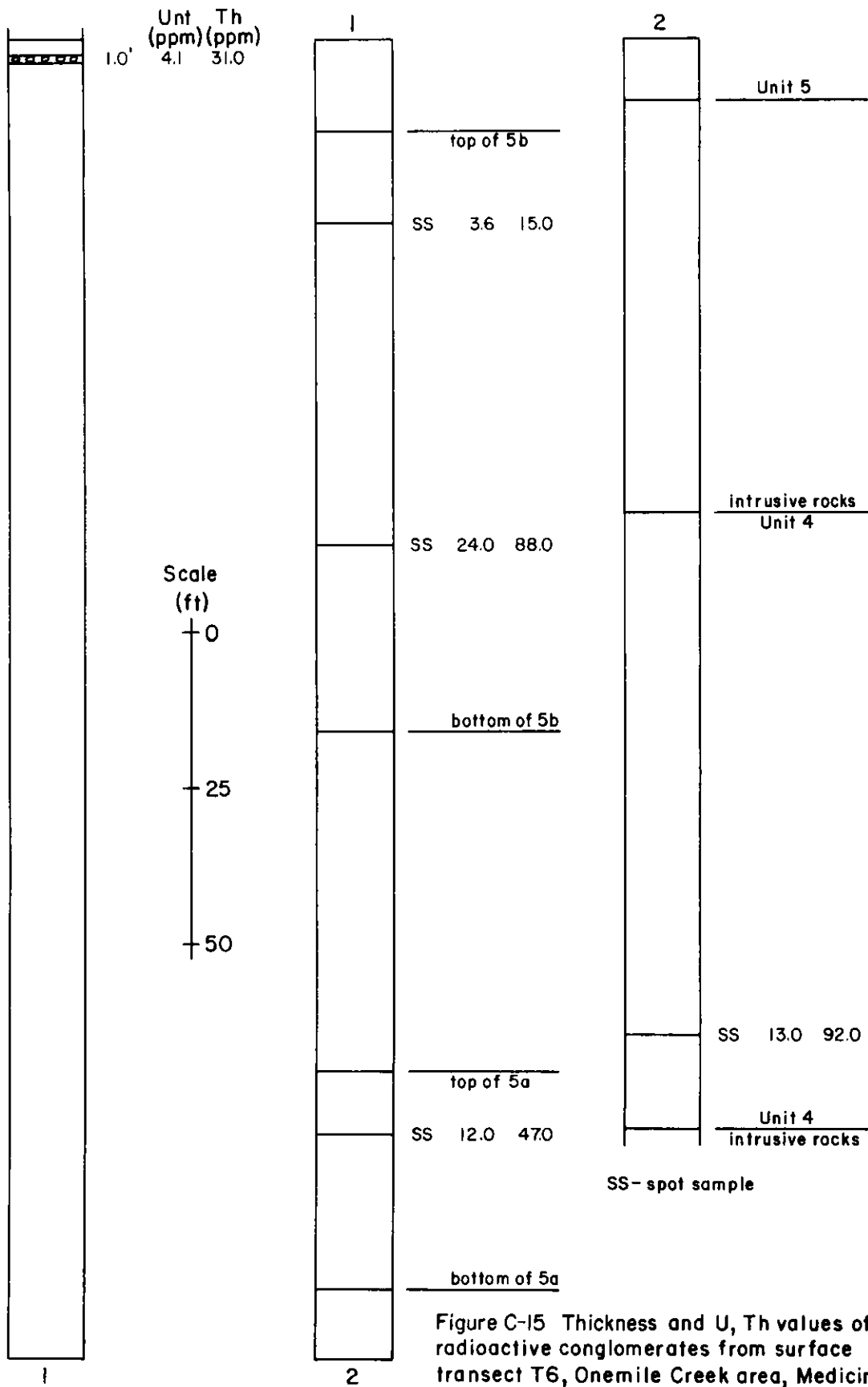
Figure C-15 Thickness and U, Th values of radioactive conglomerates from surface transect T6, Onemile Creek area, Medicine Bow Mtns.
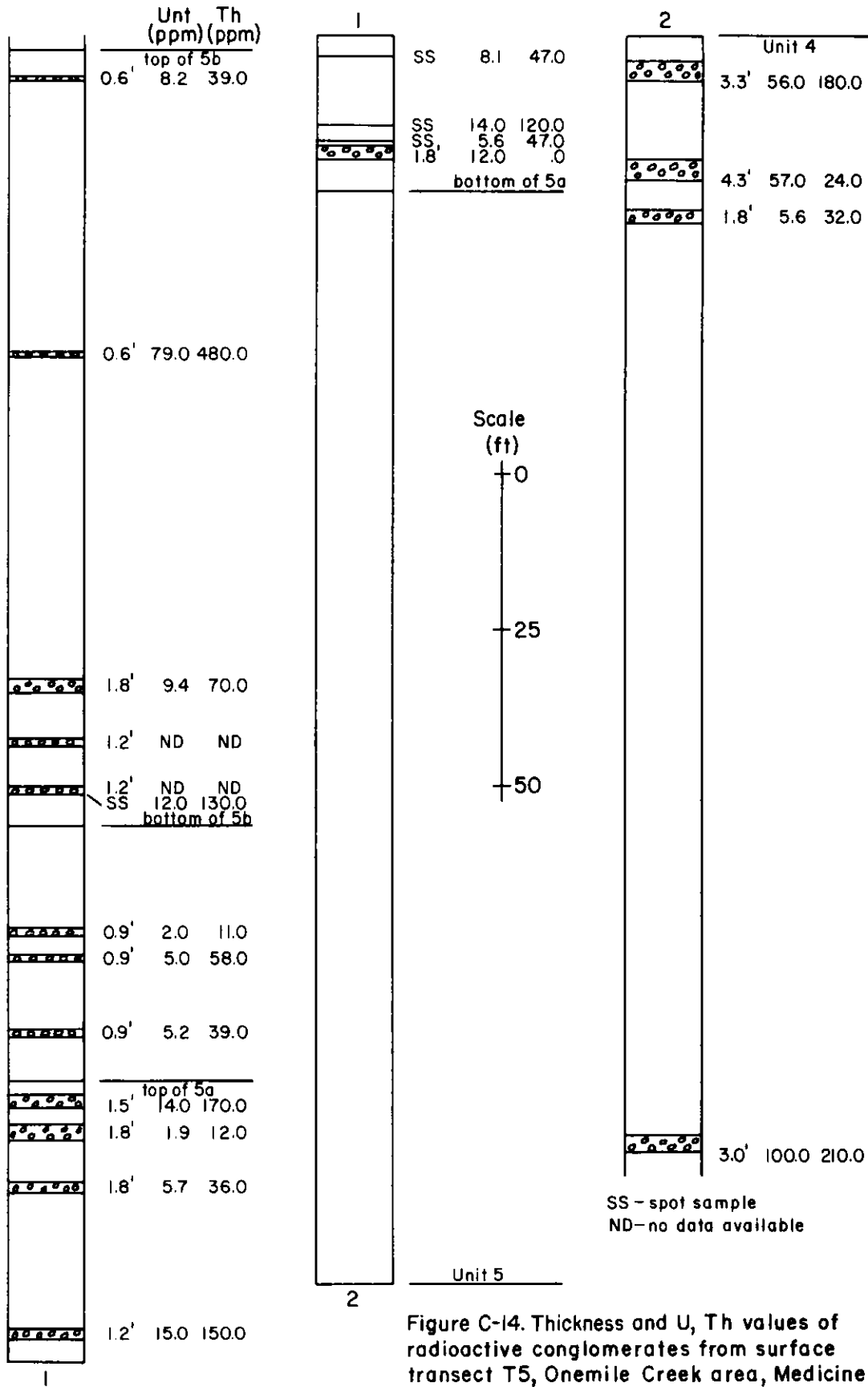
Unt   Th
(ppm)(ppm)
1.0'   4.1   31.0

Scale
(ft)

+ 0

+ 25

+ 50

SS   3.6   15.0

top of 5b

SS   24.0   88.0

bottom of 5b

top of 5a

SS   12.0   47.0

bottom of 5a

Unit 5

intrusive rocks
Unit 4

SS   13.0   92.0

Unit 4
intrusive rocks

SS- spot sample

142

Unt   Th
(ppm)(ppm)

intrusive rocks
Unit 5

Scale
(ft)

0

top of 5b
16.0'   6.8   46.0

25

8.0'   6.4   18.0

50

8.0'   64.0   320.0
base of 5b

Unit 5
intrusive rocks

Figure C-16. Thickness and U, Th values of
radioactive conglomerates from surface
transect T7, Onemile Creek area, Medicine
Bow Mtns.

143

Unt   Th
(ppm)(ppm)

1

Scale
(ft)

2

9.6' 14.0 35.0

4.0' 37.0 650.0

0

25

top of 5b

50

12.0' 28.0 230.0

5.0' 3.5 8.0

20.0' 33.0 170.0

top of 5a

12.0' 100.0 920.0

base of 5b

25.0' 15.0 240.0
7.0' 4.5 38.0

15.0' 14.0 110.0

65.0' 23.0 290.0

4.0' 10.0 83.0
base of 5a

10.0' 11.0 120.0
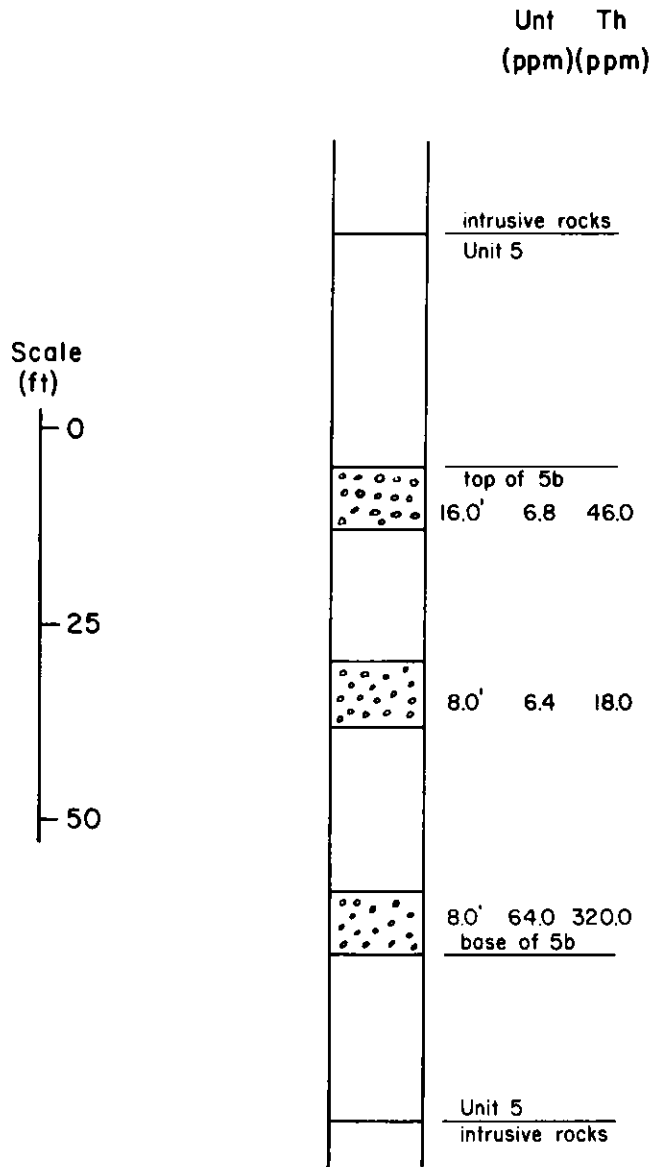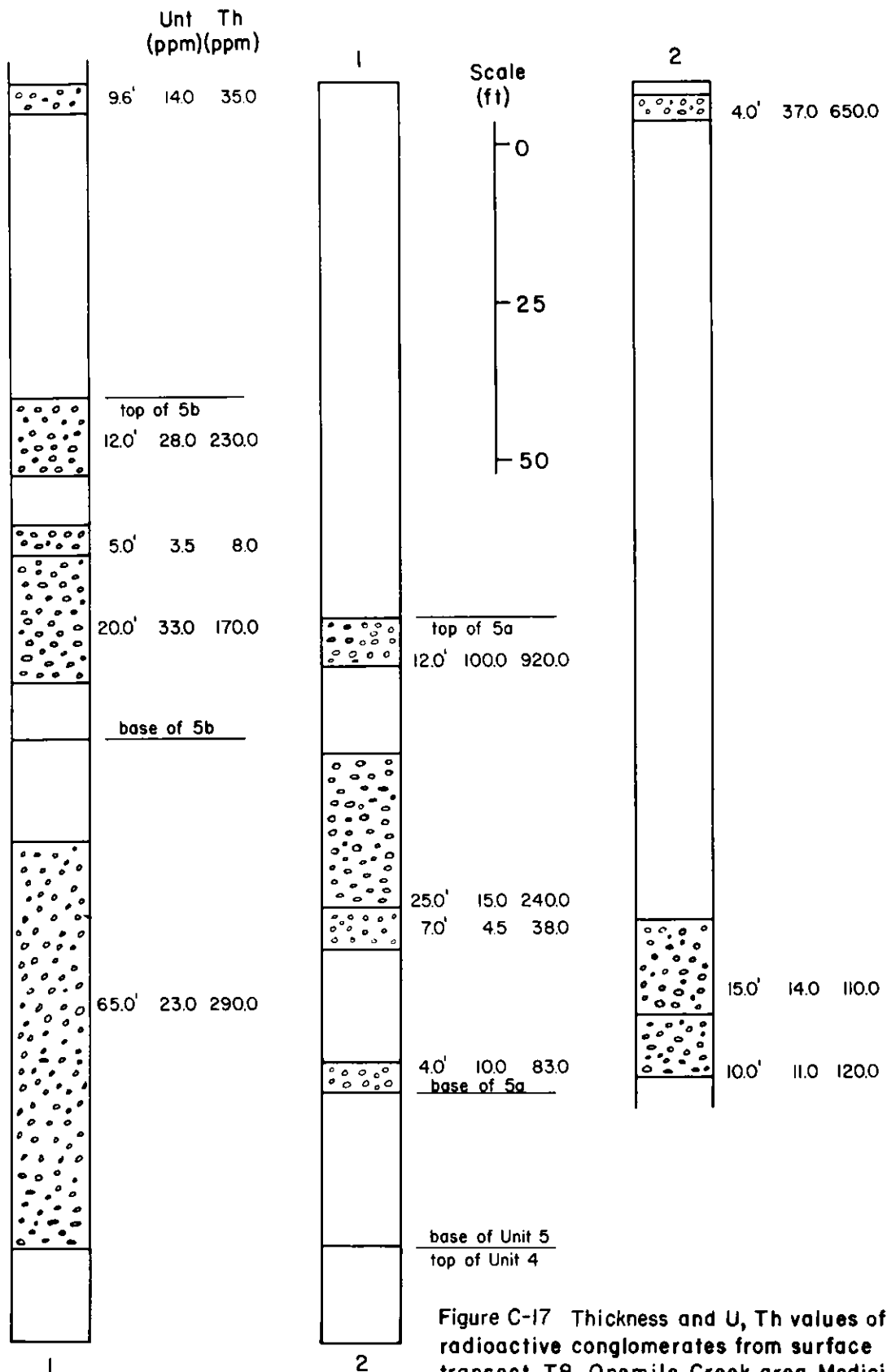
base of Unit 5
top of Unit 4

1

2

Figure C-17   Thickness and U, Th values of
radioactive conglomerates from surface
transect T8, Onemile Creek area, Medicine
Bow Mtns.

Figure C-18.
Thickness and analysis for beds exceeding 100 ppm U₃O₈ from drillhole EMB-I, Onemile Creek area, Medicine Bow Mountains.

145

Figure C-19.
Thickness and analysis for beds
exceeding 100 ppm U_3O_8 in core
from drillhole EMB-6, Onemile
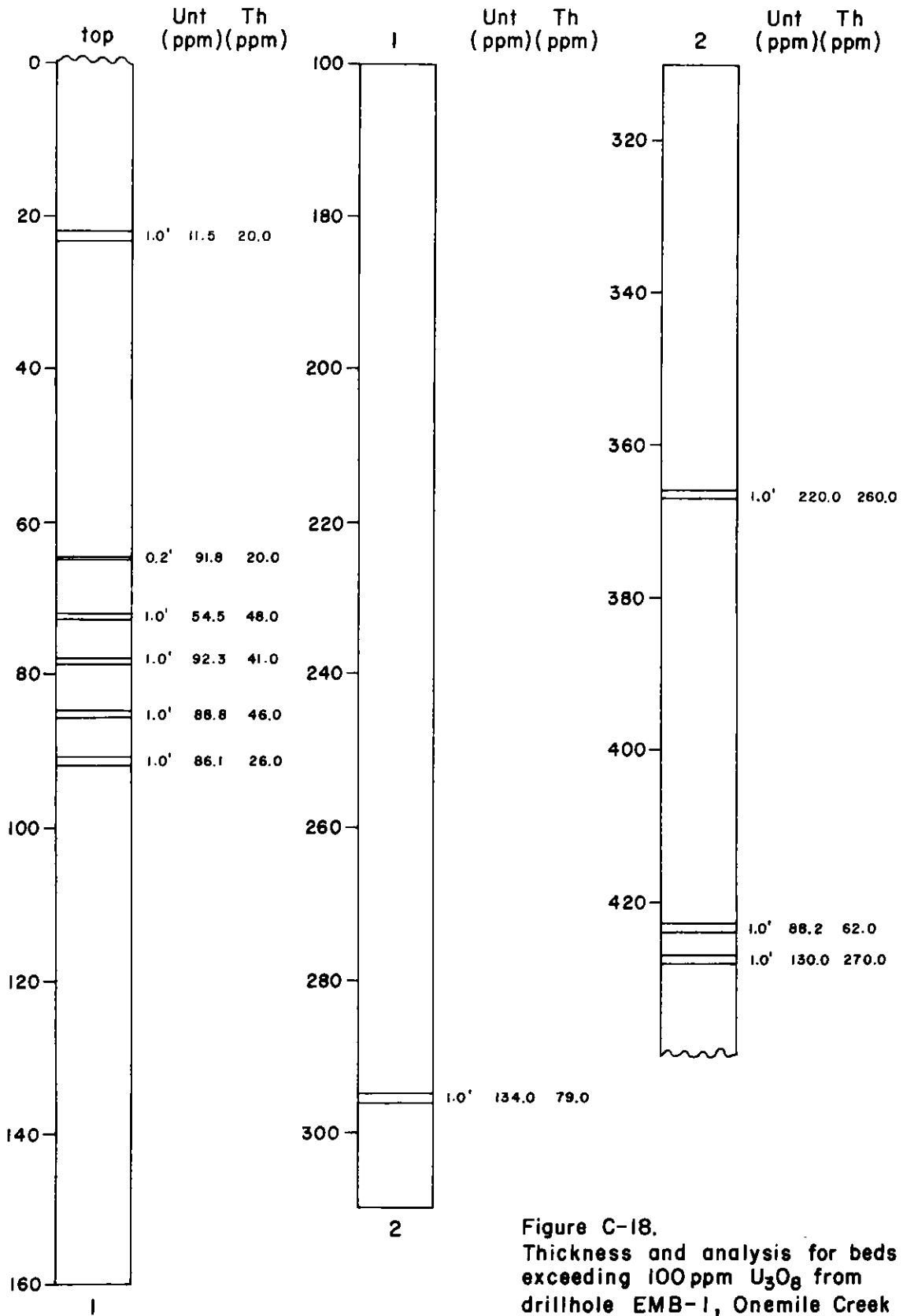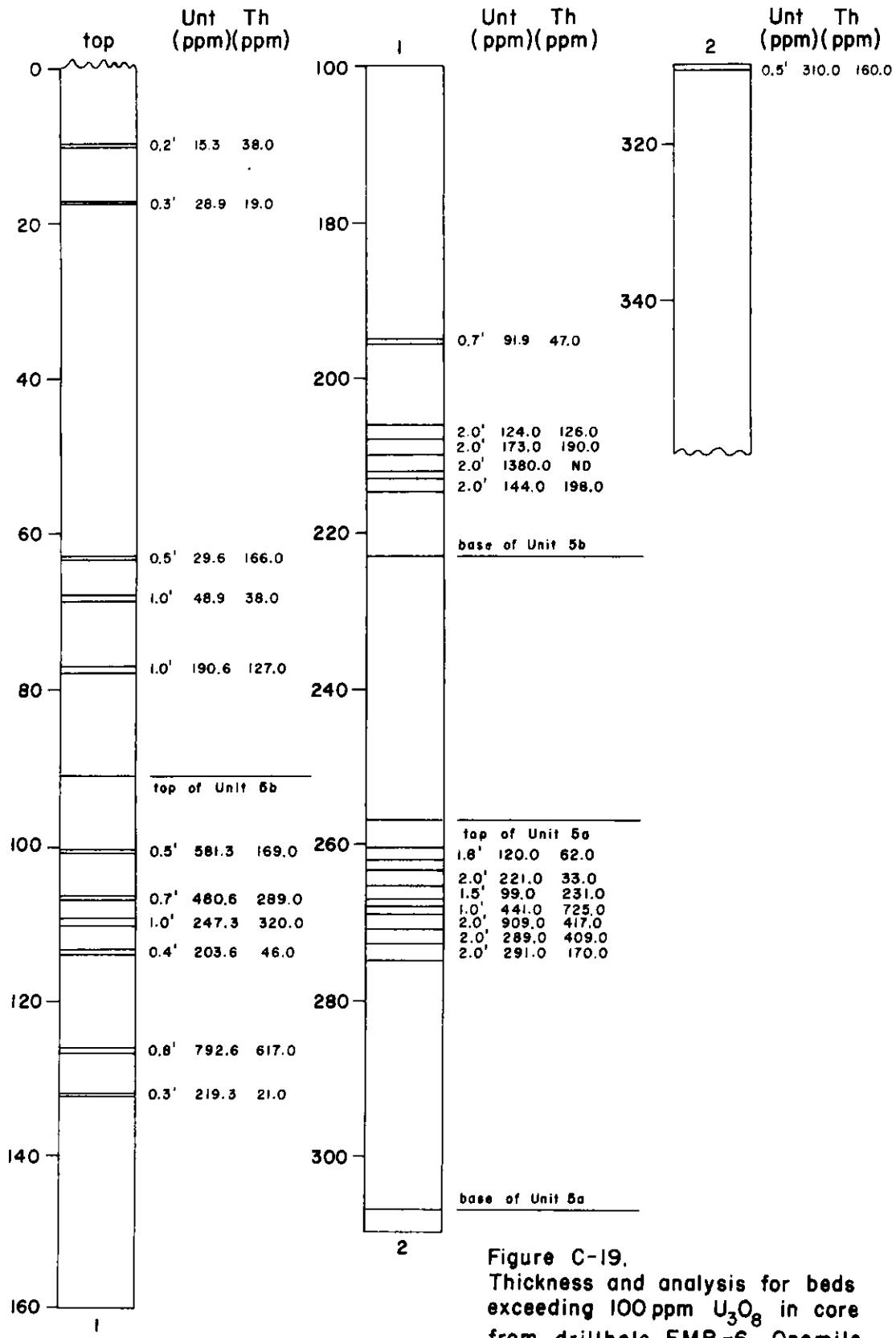Creek area, Medicine Bow Mountains.

Figure C-20.
Thickness and analysis for beds exceeding 100 ppm U_3O_8 in core from drillhole EMB-7, Onemile Creek area, Medicine Bow Mountains.

Figure C-21.
Thickness and analysis for
beds exceeding 100ppm U_3O_8
in core from drill hole EMB-8,
Onemile Creek area, Medicine
Bow Mtns.

Figure C-22.
Thickness and analysis for beds
exceeding 100 ppm U_3O_8 in core
from drill holes EMB-9 and EMB-10,
Onemile Creek area, Medicine Bow
Mtns.

Column 1 (left):

Unt (ppm)	Th (ppm)	
top of Unit 1		
1.0'	93.6	17.0
1.0'	144.1	23.0
1.0'	60.2	10.0
1.0'	89.0	10.0
1.0'	51.5	41.0
1.0'	236.0	104.0
1.0'	76.1	54.0
1.0'	84.3	212.0
1.0'	241.0	65.0
1.0'	99.0	30.0

Depth scale column 1: 0, 20, 40, 60, 80, 100, 120, 140, 160

Column 2 (middle):

Unt (ppm)	Th (ppm)	
base of Unit 1		
intrusive rocks		
Intrusive rocks		
top of Unit 2		
1.0'	273.0	212.0
1.0'	868.0	112.0
1.0'	95.9	10.0

Depth scale column 2: 160, 180, 200, 220, 240, 260, 280, 300

Column 3 (right):

Unt (ppm)	Th (ppm)	
1.0'	110.3	45.0
0.4'	220.7	40.0
0.8'	940.0	79.2
base of Unit 2		
intrusive rocks		

Depth scale column 3: 320, 340, 360

Figure C-23.
Thickness and analysis of beds exceeding 100 ppm U_3O_8 in core from drillhole MB-16, Onemile Creek area, Medicine Bow Mountains.
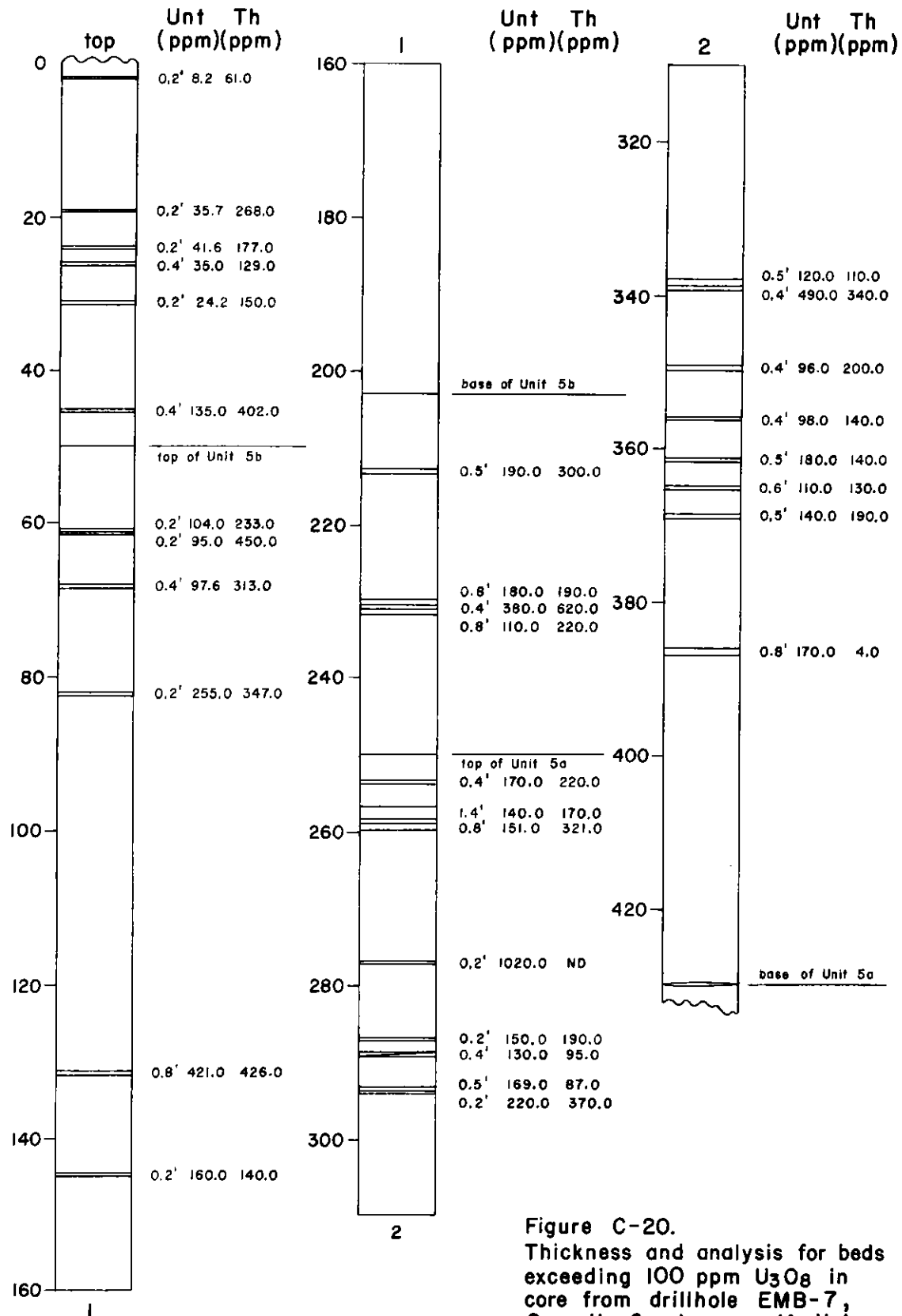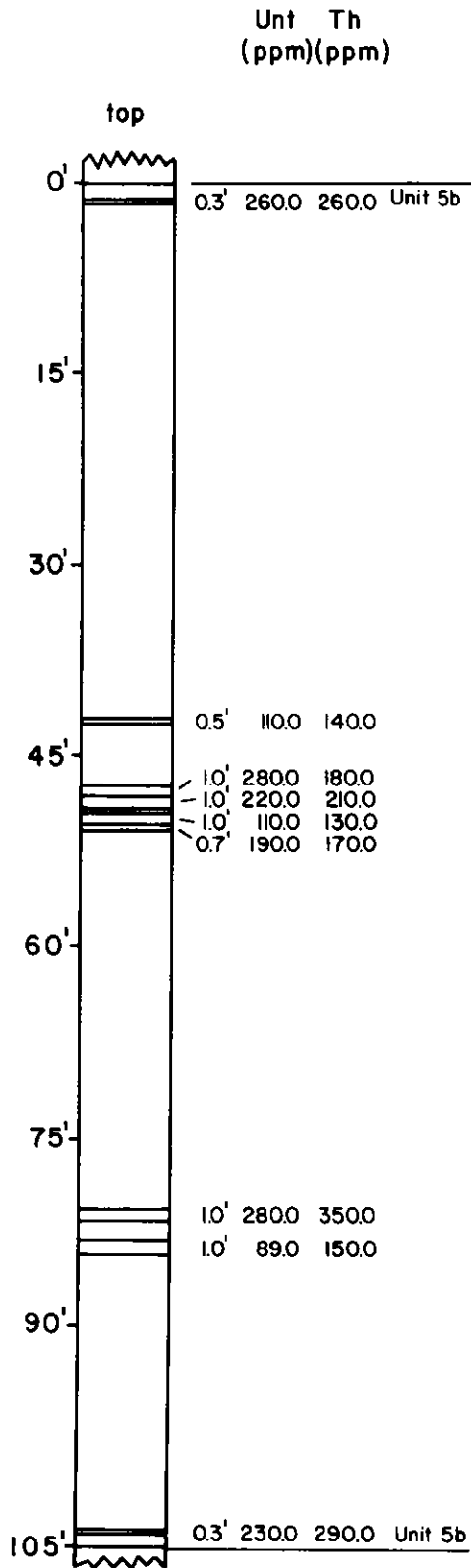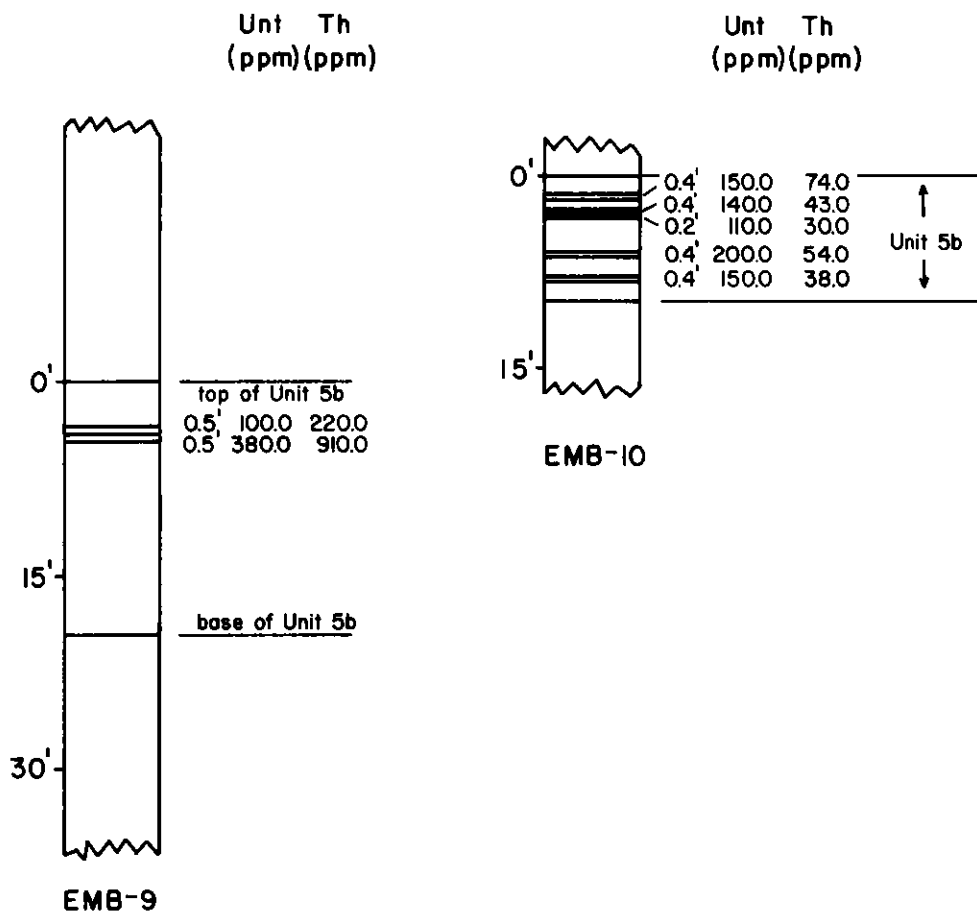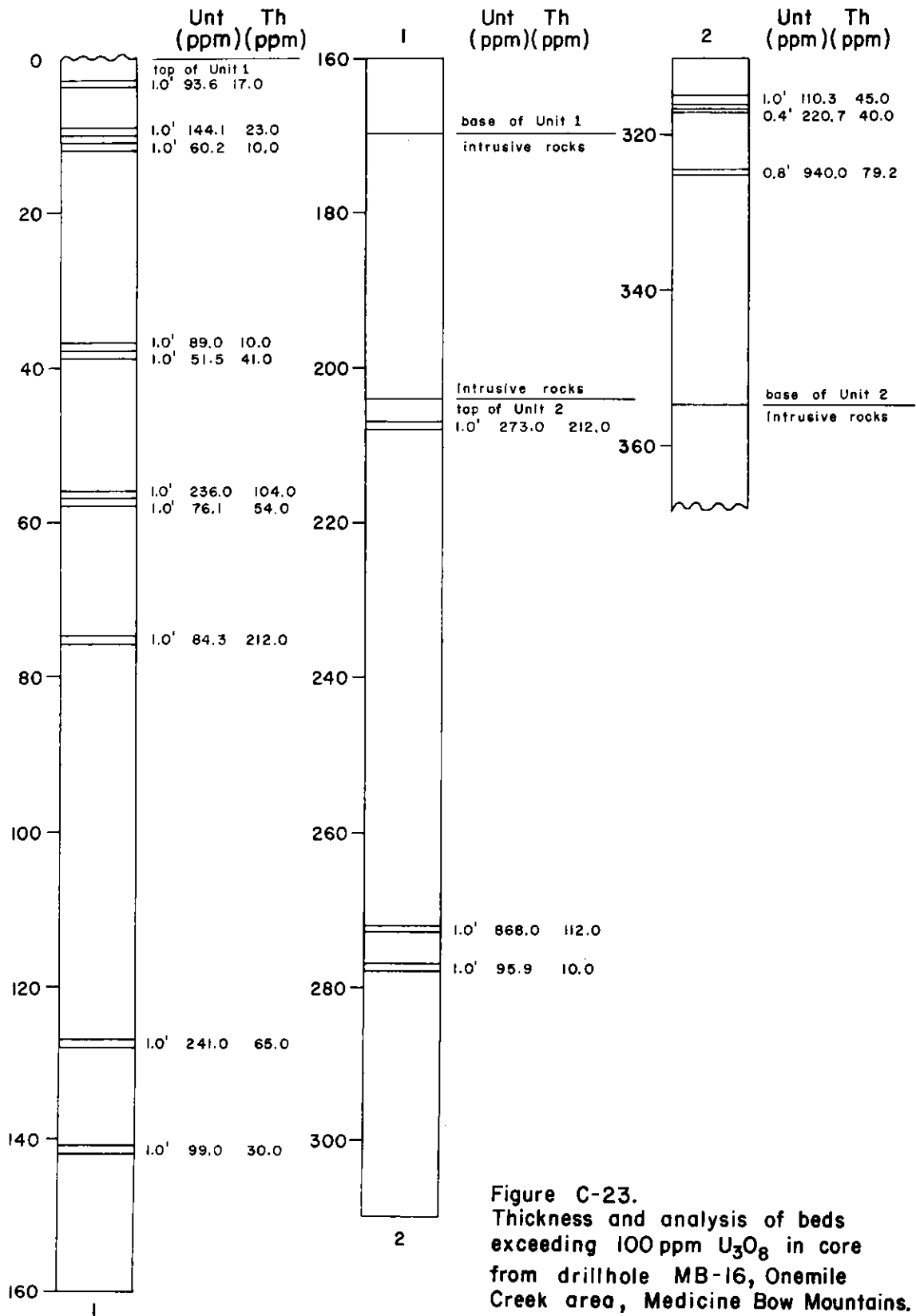
150
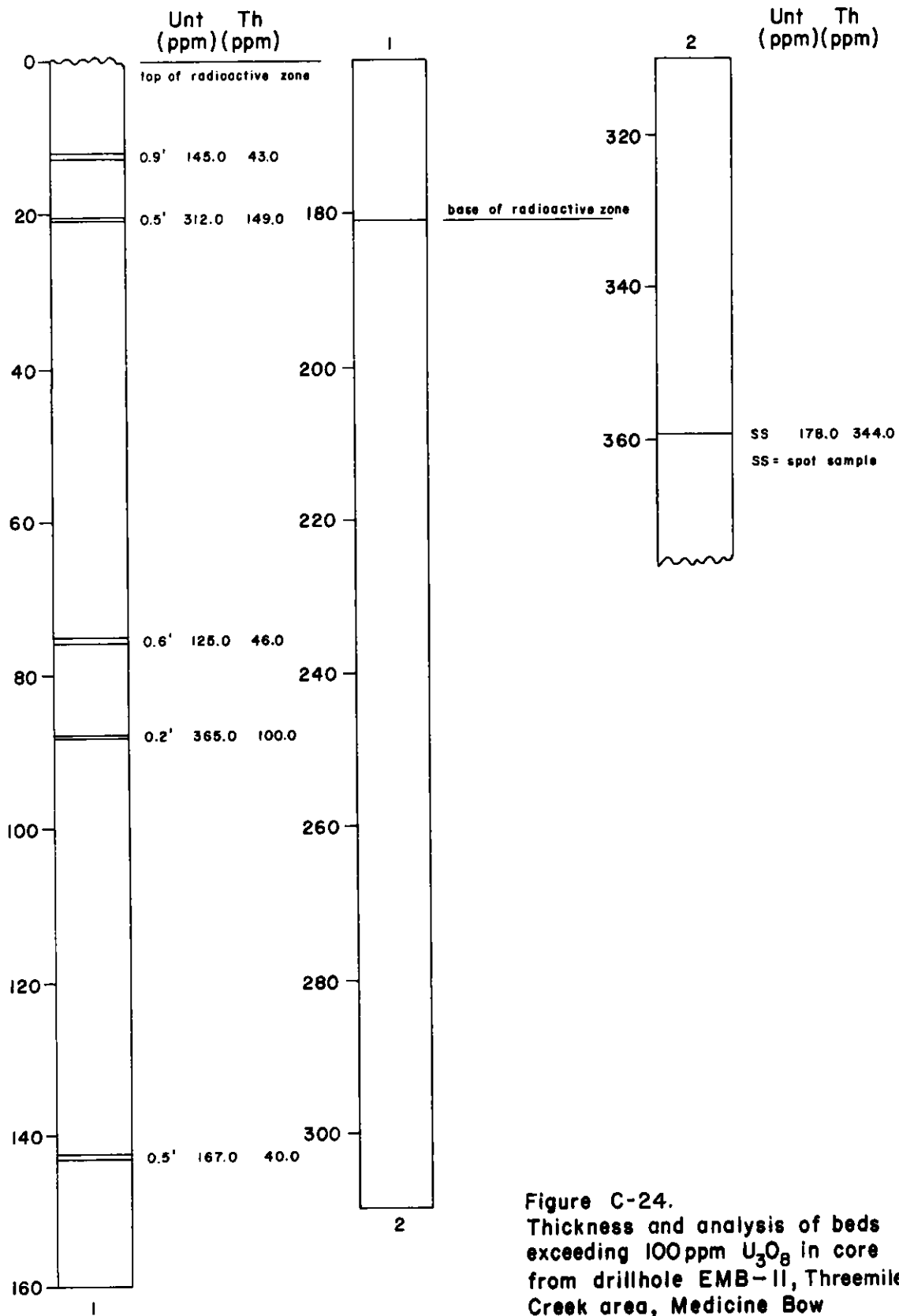
Figure C-24.
Thickness and analysis of beds
exceeding 100 ppm U_3O_8 in core
from drillhole EMB-II, Threemile
Creek area, Medicine Bow
Mountains.

151

Appendix D

Average Grade and Total Bed Thickness
for Outcrop Transects and Drill Holes

Table D-1

Sierra Madre Accumulations of U_3O_8 in exceedance of 100 ppm

Unit #3

Transect or Drill Hole	Average U_3O_8	Average $(U_3O_8)^2$	Average ln U_3O_8	Total Thickness	Average Thickness
Transect #5	109.9	12077	4.70	.7	.7
Transect #16	116.03	13464	4176	.5	.5
SM-1 Core	110.6	12232	4.71	.7	.7
SM-2 Core	184.29	43423	5.12	4.2	.60

Table D-2

Medicine Bow Accumulations of U_3O_8 in exceedance of 100 ppm

Transect or Drill Hole	Average U_3O_8	Average $(U_3O_8)^2$	Average lnU_3O_8	Total Thickness	Average Bed Thickness
Unit 1:					
Transect T1A	164.04	34145	4.99	8.4	1.20
Transect T1B	207.20	48501	5.27	8.4	0.65
Transect T1C	403.02	327435	5.69	8.4	1.05
Transect T2	245.24	83880	5.32	5.0	1.00
EMB-1 Core	175.31	33142	5.12	9.2	0.92
MB16 Core	392.60	255433	5.66	15.2	0.95
Unit 5a:					
Transect T4	379.51	145567	5.93	1.9	0.63
Transect T5	369.23	151538	5.86	9.4	3.13
Transect T8	416.26	268186	5.71	3.0	1.00
EMB-6 Core	424.77	276813	5.82	11.8	1.48
EMB-7 Core	195.73	71319	5.10	8.3	0.52
Unit 5b:					
Transect T3	175.97	95542	4.82	2.8	1.40
Transect T5	527.94	278678	6.26	0.6	0.60
Transect T7	485.40	235613	6.18	1.0	1.00
Transect T8	204.80	42608	5.31	3.0	1.00
EMB-6 Core	508.19	538639	5.76	15.4	0.96
EMB-7 Core	259.86	82586	5.45	6.7	0.37
EMB-8 Core	218.73	53081	5.32	4.8	0.69
EMB-9 Core	269.30	97202	5.39	1.0	0.50
EMB-10 Core	170.68	30032	5.12	1.8	0.36
Threemile Creek Area:					
EMB-11 Core	226.2	60521	5.34	2.7	0.54

Table D-3

Sierra Madre Accumulations of ThO_2 in exceedance of 100 ppm

Unit #3

Transect or Drill Hole	Average ThO_2	Average $(ThO_2)^2$	Average $lnThO_2$	Total Thickness	Average Thickness
Transect #1	591.70	350118	6.38	2.0	2.0
Transect #2	423.40	193168	6.00	4.3	2.15
Transect #3	235.85	68743	5.35	5.5	1.83
Transect #4	162.24	27903	5.06	5.8	2.90
Transect #5	341.35	116533	5.82	.7	.7
Transect #6	216.20	46742	5.36	1.3	1.3
Transect #7	257.75	67550	5.54	2.3	1.15
Transect #9	130.47	17057	4.86	1.5	.75
Transect #10	202.75	44259	5.26	5.5	2.75
Transect #11	131.37	17291	4.87	4.4	2.20
Transect #13	156.20	26378	5.00	1.1	.37
Transect #14	125.16	16832	4.80	1.0	.33
Transect #16	217.07	49381	5.35	1.3	.43
Transect #18	286.74	95090	5.57	1.5	.50
Transect #19	294.33	87149	5.68	1.5	.75
Transect #21A	204.81	43386	5.30	1.3	.32
Transect #21B	146.3	21641	4.97	.7	.35
Transect #22A	329.99	108894	5.79	1.0	1.0
Transect #22B	227.57	51792	5.42	.9	.45
Transect #23	329.98	119252	5.74	.9	.45
Transect #24	466.53	217658	6.13	.6	.6
SM-1 Core	341.36	116532	5.82	.73	.73
SM-2 Core	287.72	113536	5.5	8.96	.64

Table D-4

Medicine Bow Accumulations of ThO_2 in exceedance of 100 ppm

Transect or Drill Hole	Average ThO_2	Average $(ThO_2)^2$	Average In ThO_2	Total Thickness	Average Bed Thickness
Unit 1:					
Transect T1A	215.70	49540	5.33	2.3	0.77
Transect T1B	170.09	34774	5.04	2.3	0.38
Transect T1C	307.83	116724	5.56	1.9	0.95
Transect T2	307.28	94392	5.72	1.0	1.00
EMB-1 Core	256.79	69967	5.51	3.0	1.00
MB-16 Core	182.06	36658	5.14	3.2	0.80
Unit 5a:					
Transect T4	555.17	326314	6.29	1.9	0.63
Transect T5	188.51	37128	5.21	6.7	1.12
Transect T8	464.26	315377	5.78	5.0	1.00
EMB-2 Core	159.30	25376	5.07	1.0	1.00
EMB-6 Core	387.81	191748	5.83	8.0	1.33
EMB-7 Core	270.97	88583	5.49	4.4	0.55
Unit 5b:					
Transect T3	147.92	21882	4.99	0.5	0.50
Transect T5	297.27	125548	5.48	1.6	0.80
Transect T6	100.13	100027	4.61	0.2	0.20
Transect T7	364.12	132589	5.89	1.0	1.00
Transect T8	261.72	71603	5.54	3.0	1.00
EMB-6 Core	255.64	86390	5.44	10.5	1.17
EMB-7 Core	300.54	117203	5.56	6.4	0.40
EMB-8 Core	256.85	78249	5.46	9.6	0.74
EMB-9 Core	642.90	567455	6.23	1.0	0.50
Threemile Creek Area:					
EMB-11 Core	165.26	31371	5.04	1.7	0.43

Table D-5

SUMMARY OF AVERAGE ACCUMULATIONS AND VARIANCES FOR U_3O_8

Unit	Average accumulation of U_3O_8 above 100 ppm (ppm x ft.)	Average of accumulations squared (ppm x ft.)^2	Accumulation variance (ppm x ft.)^2	Number of transects with encounters of > 100 ppm U_3O_8 (k)	Total number of transects (n)
Sierra Madre unit 3	246.60	153596	18806	4	31
Medicine Bow unit 1	2551.73	9350811	3304805	6	6
Medicine Bow unit 5a	2415.49	8377562	2960192	5	9
Medicine Bow unit 5b	1455.88	7389445	4585649	9	10
Medicine Bow units 1, 5a and 5b combined (Onemile Creek area)	2024.53	8224884	3901555	20	25
Medicine Bow Threemile Creek area	610.74	373003	57969	1	1
All Medicine Bow units	1957.21	7850985	3842177	21	26

Table D-6

SUMMARY OF AVERAGE ACCUMULATIONS AND VARIANCES FOR ThO_2

Unit	Average accumulation of ThO_2 above 100 ppm (ppm x ft.)	Average of accumulations squared (ppm x ft.)^2	Accumulation variance (ppm x ft.)^2	Number of transects with encounters of >100 ThO_2 (k)	Total number of transects (n)
Sierra Madre unit 3	608.79	739051	344310	23	31
Medicine Bow unit 1	522.07	294759	54267	6	6
Medicine Bow unit 5a	1515.53	3194760	1058781	6	9
Medicine Bow unit 5b	1048.37	2042130	941041	9	10
Medicine Bow units 1, 5a and 5b combined (Onemile Creek area)	1007.01	1847084	830330	21	25
Medicine Bow Threemile Creek area	280.94	78928	10275	1	1
All Medicine Bow units	974.01	1766713	815667	22	26